Endocytic trafficking and oligodendroglial exosome secretion in axon-glia communication and myelination

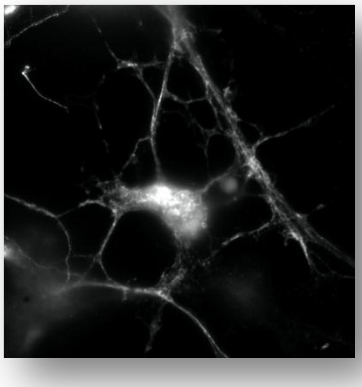

Dissertation zur Erlangung des Grades
Doktor der Naturwissenschaften
am Fachbereich Biologie
der Johannes Gutenberg - Universität in Mainz

Jesa Amphornrat

geb. am 10.05.1978 in Saraburi/Thailand

Mainz, 2011

Abstract

Oligodendrocytes form specialized plasma membrane extensions which in vertebrates spirally enwrap axons, thereby building up the myelin sheath. During myelination, oligodendrocytes produce large amounts of membrane components which are incorporated into the developing myelin sheath. Oligodendrocytes myelinate several axonal segments simultaneously and thus can be seen as a complex polarized cell type with two distinct membrane domains, i.e. the plasma membrane surrounding the cell body and the myelin membrane. SNARE proteins mediate the fusion of vesicular cargoes with their target membrane. The major myelin protein PLP was chosen as a representative to study the transport mechanisms contributing to myelin assembly and the involvement of the vesicle-associated R-SNAREs VAMP3 and VAMP7. A myelinating coculture system was established in which oligodendrocytes enwrap neuronal processes and build membrane domains sharing biochemical and biophysical characteristics with myelin *in vivo*. Functional inactivation of VAMP3 and VAMP7 in primary oligodendrocytes led to a significant decrease of relative surface PLP. In the cocultures, association of PLP with myelin-like membranes was decreased upon silencing of VAMP3 and VAMP7, confirming their involvement in myelination in *vitro*. Based on these studies, we propose a model in which PLP is transported by two different pathways. VAMP3 mediates the non-polarized transport of newly synthesized PLP via recycling endosomes to the plasma membrane, while transport of PLP from LE/Lys to myelin is controlled by VAMP7.

In the second part of the thesis, the role of exosome secretion in glia to axon signaling was studied. Functional inactivation of VAMP7 in primary oligodendrocytes had mixed effects on the release of exosomes. Further studies are required to clarify whether VAMP7 controls exosome secretion. In the recent years, it emerged that oligodendrocytes in addition to their function as myelin-producing cells also provide trophic support to axons to maintain longterm axonal integrity. Proteomic analyses of oligodendroglial exosomes revealed that in addition to canonical exosomal components they carry oligodendrocyte-specific proteins and proteins with putative functions in the relief of stress. We thus hypothesize that exosomes are involved in trophic support to axons. The cre-ERT2-loxP system was utilized to study the uptake of oligodendroglial exosomes by neurons. Cre as well as cre-ERT2 were shown to be present in oligodendroglial exosomes. Since activation of cre-ERT2 by tamoxifen has various side effects, further studies were performed utilizing cre. The thesis further focused on putative metabolic effects in the target neurons. Studies utilizing MTT assays showed no obvious influences of glial exosomes on neuronal metabolic activity. Analysis of the phosphorylation levels of the neurofilament heavy subunit revealed a decrease in presence of oligodendrocytes, indicating effects of oligodendroglial exosomes on the neuronal cytoskeleton. Candi-

dates for kinases which are possibly activated upon influence of oligodendroglial exosomes and could influence neuronal survival were identified by phospho-MAPK arrays.

Table of contents

1 Introduction

The nervous system is build up by neurons and glial cells. Glial cells of the CNS are astrocytes, microglia, ependymal cells and oligodendrocytes (Figure 1). Astrocytes induce and maintain the blood brain barrier and function in maintenance of brain homeostasis by controlling K^+ and H^+ levels, by the uptake of extracellular glutamate, GABA (γ-**A**mino**B**utyric **A**cid), glycine and taurine, by regulation of cerebral blood flow and by modulating synaptic activity. The uptake of glutamate is the best established property of astrocytes. After its uptake it is converted to glutamine by the astrocyte-specific enzyme glutamine synthetase. The amino acid is released and is taken up by neurons which use it to regenerate glutamate (Maragakis & Rothstein, 2006, Kimelberg, 2010, Lee & Pow, 2010).

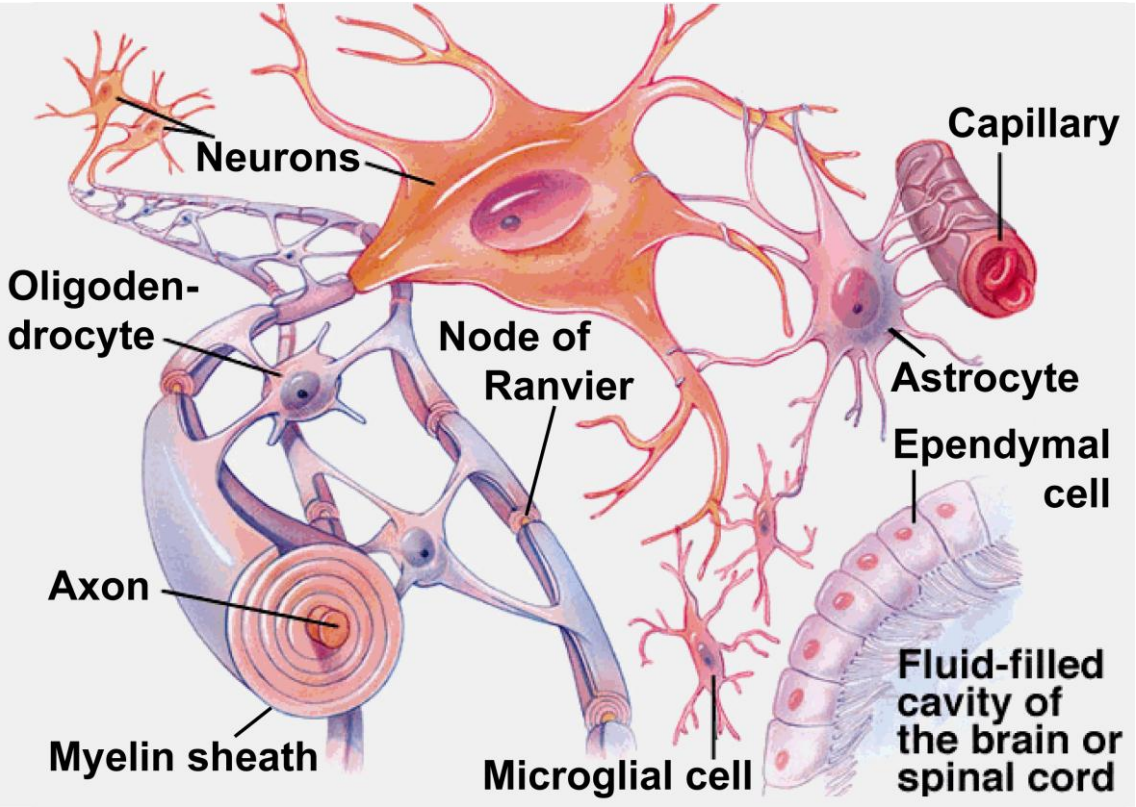

Figure 1: Schematic illustration of the neuroglial cells in the CNS. The CNS is composed of neurons and glial cells, which are astrocytes, ependymal cells, microglia and oligodendrocytes. The oligodendrocytes form plasma membrane extensions enwrapping axons, thereby building up the myelin sheath. Periodically, small parts of the axon remain unmyelinated. These unmyelinated regions between two myelin sheaths are called nodes of Ranvier. Action potentials are forwarded from one node to another, facilitating a speed-optimized conduction called “saltatory" (Human anatomy and physiology, 8th edition, 1999).

Microglia are thought to derive from myeloid precursors. They function as macrophages and antigen-presenting cells in the CNS and furthermore seem to play a role in initiation of neuropathic pain and maintenance of synaptic integrity (Ransohoff & Perry, 2009,

Schmitz, *et al.*, 2009, Graeber, 2010). Ependymal cells are ciliated cells lining the ventricular surface of the CNS. They play a role in embryonic brain development and filtration of the cerebrospinal fluid (CSF), thereby probably protecting the brain from potentially harmful substances from the CSF (Bruni, 1998, Del Bigio, 2010).

1.1 Axon-glia interaction between neurons and myelinating glia

In all complex nervous systems neurons coexist with myelinating glial cells. It was shown that myelin thickness directly correlates with axonal diameter (Friede, 1972). The ratio of the axonal diameter divided by the diameter of the axon and its myelin sheath was termed the g-ratio and is well preserved, with values between 0,6 and 0,7 (Sherman & Brophy, 2005). Myelination also depends on neuronal electrical activity. In myelinating cocultures, the increase of electrical activity enhanced myelination, whereas blocking of action potentials led to its inhibition (Demerens, *et al.*, 1996). Action potential firing of neurons has been shown to be associated with the non-synaptical co-release of several substances from the axon, including adenosine and ATP (Maire, *et al.*, 1982, Stevens & Fields, 2000, Fields & Burnstock, 2006). OPCs possess adenosine receptors which enable them to sense neuronal electrical activity. Adenosine was shown to inhibit their proliferation, stimulate differentiation and promote the formation of myelin (Stevens, *et al.*, 2002). Neuregulins are secreted or shed from axons and stimulate the proliferation of Schwann cells and oligodendrocytes by activation of the ErbB pathway. Later on, axon-bound neuregulin is required for their differentiation (Nave & Salzer, 2006). For Schwann cells, it was shown that myelin thickness is regulated and depends on the presentation of axonal neuregulins (Taveggia, *et al.*, 2005). Thus, the fact that axons modulate the myelinating glial cells they are associated with is known for a long time. But in the recent years it emerged that many neurological disorders are caused primarily by oligodendrocytes and Schwann cells, pointing to a strong dependence also of the axon on its myelinating glial cell. In *shiverer* mice, which carry a recessive mutation and therefore lack the myelin basic protein (MBP), the second most abundant CNS myelin protein, myelin is not compacted (Shine, *et al.*, 1992). These mice develop a severe tremor in early postnatal development and have a mean life span of 90-150 d (Readhead, *et al.*, 1987). Slow axonal transport rates and the number of neurofilaments were increased, and also microtubules were more abundant in *shiverer* axons. Because the mentioned alterations normally are characteristics of early postnatal axons before myelination, Brady et al. suggested that the formation of compact myelin is required for the maturation of the axonal cytoskeleton (Brady, *et al.*, 1999). *Trembler* mice carry a mutation in the peripheral myelin protein gene *PMP-22* and serve as a model for Charcot-Marie-Tooth type IA neuropathy in humans (CMT). These mice show severe hypomyelination. Neurofilament phosphorylation, slow axonal transport

rates and axonal diameter are decreased. On the other hand, neurofilament density is increased. Experiments, in which *trembler* nerves were grafted into wildtype mice, demonstrated that these changes are confined to axon segments without normal myelination, whereas adjacent regions of the same axon were not affected. These findings emphasize the importance of intercellular contact between neurons and myelinating glia (de Waegh & Brady, 1990, de Waegh, *et al.*, 1992, Suter, *et al.*, 1992). In summary, there is accumulating evidence that neurons and myelinating glia form a functional unit with strong interdependence, characterized by intimate cell-cell interactions and communication by ongoing mutual exchange of signals.

1.2 The myelin sheath and its microdomains

Oligodendrocytes are the myelinating cells in the CNS. They form specialized plasma membrane extensions which in vertebrates enwrap axons spirally and build up the myelin sheaths (Hartline & Colman, 2007, Simons & Trotter, 2007). These are periodically punctuated by small unmyelinated regions, the nodes of Ranvier, which allow "jumping" of action potentials from one node to another, thereby facilitating a very fast conduction called "saltatory". Myelin serves for electric insulation and speeds the conduction of nerve impulses by at least a factor of ten compared to unmyelinated fibers of the same diameter (Hartline & Colman, 2007). During its compaction the cytoplasm is almost entirely replaced. The typical ultrastructure of compact myelin is a result of association of the cytoplasmic (major dense lines) and extracellular membrane surfaces (intraperiod lines) of the lipid bilayers (Figure 2 A and B).

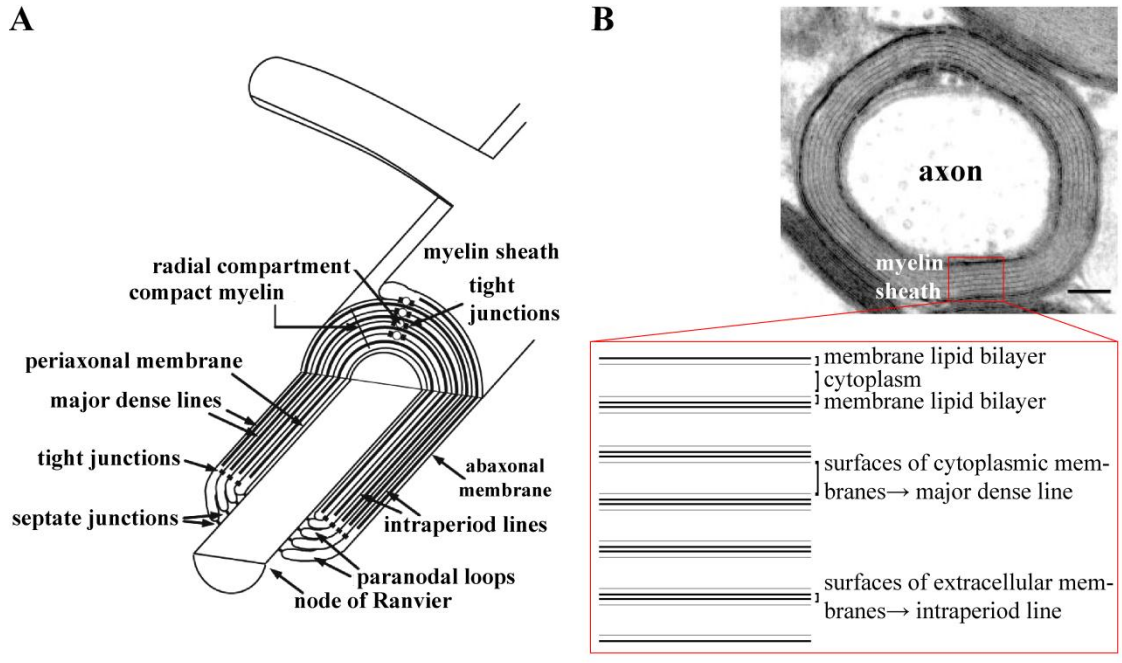

Figure 2: The membrane domains of the myelin sheath and compact myelin ultrastructure. A, Schematic representation of the myelin sheath and its microdomains. **B**, Electron micrograph showing a

cross section of a myelinated axon. Major dense lines and intraperiod lines are derived from the association of the cytoplasmic and extracellular surfaces of the lipid bilayers, respectively (red box). Scale bar, 0,1 µm. Adapted from (Rosenbluth, *et al.*, 2006, Debruin & Harauz, 2007).

Myelin formation requires an intimate cellular interaction between the axon and the myelinating oligodendroglial cell, leading to formation of compacted and noncompacted areas of myelin and microdomains with specific morphological and biochemical properties (Figure 2) (Arroyo & Scherer, 2000, Salzer, 2003, Debruin & Harauz, 2007). Proteins in compact myelin are PLP (**P**roteo**L**ipid **P**rotein), MBP (**M**yelin **B**asic **P**rotein), MOBP (**M**yelin-associated **O**ligodendrocytic **B**asic **P**rotein) and MAL (**M**yelin **A**nd **L**ymphocyte protein). MAL probably stabilizes the radial compartment and plays an important role in the maintenance of the paranodes, likely by controlling the trafficking of membrane components. Recent studies suggested that MAL has a functional role in axon-glia interaction (Schaeren-Wiemers, *et al.*, 2004, Buser, *et al.*, 2009). The noncompacted myelin consists of the paranodal loops, the inner and outer loop (built by the periaxonal and abaxonal membrane, respectively) and the radial compartment (Figure 2 A). The major proteins are CNP (**C**yclic **N**ucleotide **P**hosphodiesterase), MAG (**M**yelin-**A**ssociated **G**lycoprotein) and MOG (**M**yelin/**O**ligodendrocyte **G**lycoprotein). OSP/Claudin11 (**O**ligodendrocyte **S**pecific **P**rotein) is a constituent of tight junctions segregating compacted and noncompacted myelin areas. In the paranodal region they are thought to prevent current leakage into the interlamellar space and they are supposed to build up the radial compartment in compact myelin.

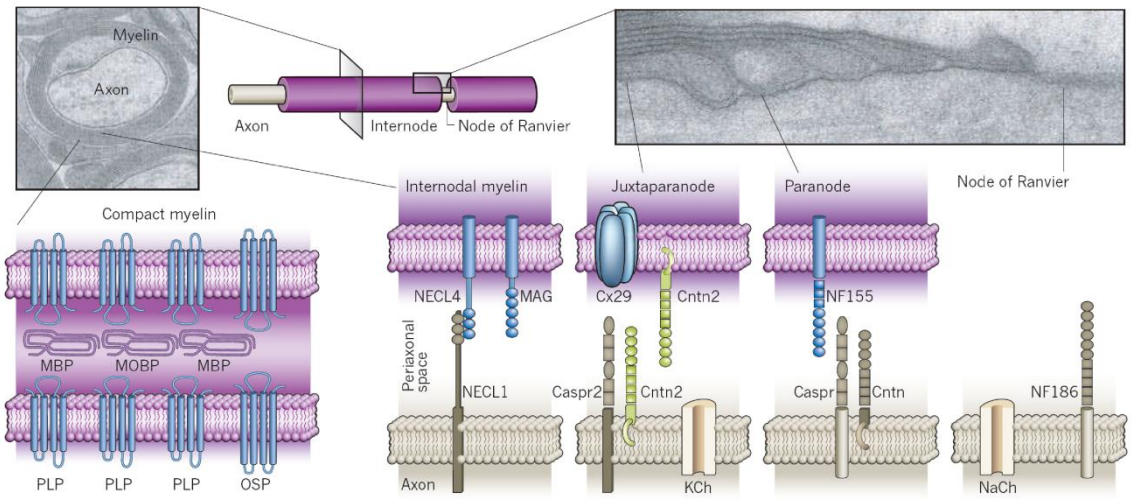

Figure 3: Proteins of the axon myelin unit. Compact myelin shows a typical ultrastructure in electron micrographs (inset on the left shows a myelinated optic nerve in cross section). The region around the node of Ranvier comprises a distinct molecular architecture (inset on the right shows a longitudinal section at the node of Ranvier). Na^+ channels are concentrated at the node of Ranvier where they are responsible for the generation of action potentials. At the paranodal region axoglial junctions separate the compact myelin from the outside milieu. K^+ channels are located at the juxtaparanode. Caspr, contactin-associated protein; Cntn, contactin; Cx29, connexin 29 kDa; KCh, fast potassium channels; MAG, myelin-associated glycoprotein; MBP, myelin basic protein; MOBP, myelin/oligodendrocyte basic protein; NaCh, voltage-gated sodium channels; NECL, nectin-like protein/synCAM; NF155/186, neurofascin 155 kDa/186 kDa; OSP, oligodendrocyte-specific protein, PLP, proteolipid protein (Nave, 2010).

Axoglial junctions at the contact sites between the axolemma and the glial membrane are composed of a battery of different adhesion molecules including NECL/synCAM, caspr/paranodin, F3/contactin in the axon and NECL/synCAM, F3/contactin and NF155 in the myelinating glia. Voltage-gated sodium channels are clustered at the node, potassium channels are located in the juxtaparanode (Figure 3) (Pedraza, *et al.*, 2001, Poliak & Peles, 2003, Maier, *et al.*, 2008, Susuki & Rasband, 2008, Nave, 2010).

1.3 The major myelin protein PLP

The X-linked proteolipid protein gene (*Plp*) encodes two isoforms, PLP with 276 amino acids and the minor DM20 (Figure 4). The latter is generated through alternative splicing within exon 3 and is identical to PLP, except for the deletion of 35 residues, which are predicted to be present on the cytoplasmic surface (Nave, *et al.*, 1987). PLP is a tetraspanin with the C- and N-terminus on the cytoplasmic surface. Due to the high content of apolar amino acids and a high number of palmitoylation sites, PLP is an extremely hydrophobic molecule. The second outer loop carries two disulfide bonds (Weimbs & Stoffel, 1992, McLaughlin, *et al.*, 2002). PLP and DM20 were thought to account for ~50% of total myelin protein (Karim, *et al.*, 2007) whereas recent studies showed that with a proportion of 17% their abundance was overestimated (Jahn, *et al.*, 2009).

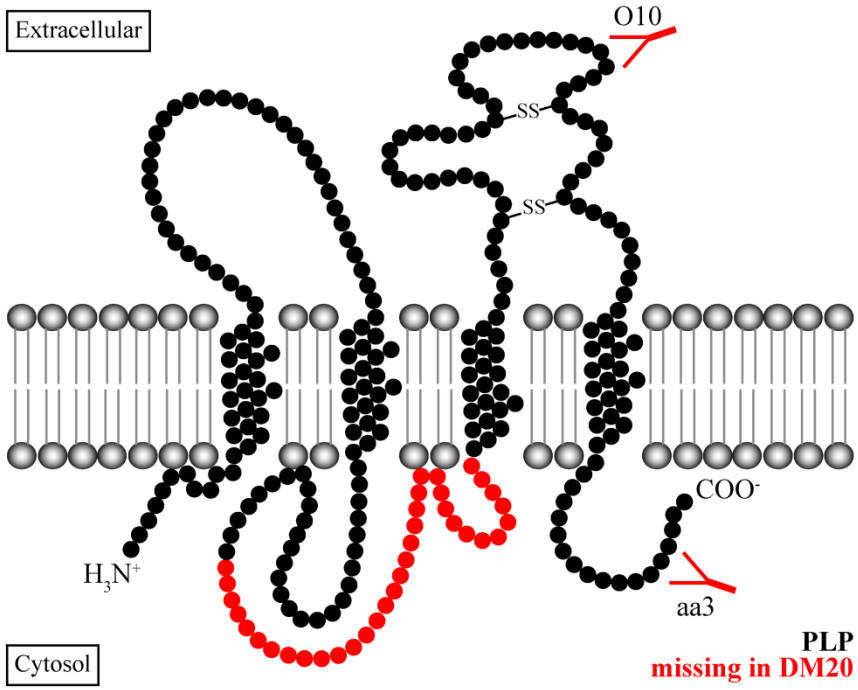

Figure 4: Illustration depicting PLP and its isoform DM20 and the epitopes recognized by the antibodies O10 and aa3. PLP consists of 276 amino acids of which 117 – 151 are missing in its splice isoform DM20. PLP is a tetraspanin with multiple palmitoylation sites anchoring the protein in the plasma membrane. The second outer loop carries two disulfide bonds. O10 recognizes an extracellular epitope in the second outer loop whereas aa3 binds to the C-terminus inside the cell. Adapted from (Weimbs & Stoffel, 1992).

DM20 is the more ancient isoform. During development it is prominent in a number of tissues and a role in compartmentalization and differentiation of the neural tube was suggested (Timsit, *et al.*, 1992, Tuason, *et al.*, 2008). In differentiated oligodendrocytes and in the postnatal brain, the ratio of PLP to DM20 transcripts is 3:1, accounting for the abundance of the PLP isoform (Wang, *et al.*, 2007). Mice, in which PLP was replaced by DM20, showed a similar phenotype as PLP knockout mice, indicating that DM20 is not able to functionally replace PLP (Stecca, *et al.*, 2000).

1.4 Mutations of PLP in human disease and related mouse models

In humans, *Plp1*-related disorders represent a broad clinical spectrum from the severe form of Pelizaeus-Merzbacher disease (PMD) to the milder spastic paraplegia type 2 (SPG-2). Distinct types of mutations, including point mutations and genomic duplications and deletions, have been identified as causes. The classic form of PMD is characterized by hypotonia, nystagmus and delay in motor development within the first year of life. Thereafter, the disease shows a slow progression and patients die in mid-adulthood. The connatal form is less frequent. Patients show severe neurological symptoms and die within the first decade of life. In general, the clinical course of SPG-2 is much milder. Patients display normal motor development in the first year of life. Progressive weakness and spasticity of the lower limbs evolve between 2 and 10 years. Some patients develop symptoms of PMD and therefore the borderline between both diseases becomes blurred. However, point mutations and duplications seem to predominate in PMD, whereas null mutations are suggested to be the major causes for SPG-2 (Inoue, 2005). Until now, three naturally occurring mouse mutants termed *jimpy*, *msd* (*myelin synthesis deficiency*) and *rsh* (*rumpshaker*) have been identified, which serve as models for PMD/SPG-2. In *jimpy*, a point mutation leads to the deletion of exon 5 and a concomitant shift in the reading frame (Griffiths, *et al.*, 1998). In *msd* mice, a missense mutation causes a conservative substitution of valin for alanine (Gow, *et al.*, 1998). *Jimpy* and *msd* mice both show severe apoptosis of oligodendrocytes when they have begun to express proteins that are characteristic to differentiated oligodendrocytes and severe hypomyelination occurs. A point mutation in the *rsh* mouse leads to an isoleucine to threonine change. *rsh* mice develop a generalized tremor, but have normal longevity and oligodendrocyte numbers are not decreased (Griffiths, *et al.*, 1990, Mitchell, *et al.*, 1992, Schneider, *et al.*, 1992). In contrast, PLP knockout mice develop normally and show none of the symptoms of *jimpy* or *msd* mice. Oligodendrocytes develop normally and there are no signs for demyelination. But surprisingly, these mice develop axonal swellings and degeneration (Griffiths, *et al.*, 1998). The fact that missense mutations cause more severe diseases than null mutations suggests that mutant PLP protein might be toxic to the cells. This assumption is supported by the fact that the complementation

of *jimpy* with a wildtype *Plp1* transgene was not able to increase survival (Schneider, *et al.*, 1995).

1.5 Myelin membrane trafficking

An oligodendrocyte can be seen as a very complex polarized cell type with two distinct membrane surfaces, i.e. the plasma membrane surrounding the cell body and the myelin membrane. During myelination, huge amounts of membranes have to be synthesized. For the rat, it has been estimated that the myelin membrane surface area expands at a rate of 5-50 x 10^3 μm^2/cell/day (Baron & Hoekstra, 2010). Since not all axons are myelinated simultaneously, the membrane transport has to be tightly regulated, temporally as well as spatially. In addition, the myelin sheath consists of several domains with compacted and noncompacted areas and differing protein and lipid compositions. While the myelin membrane is growing, donor membrane vesicles have to be targeted and fused to the correct sites. Where the new myelin membrane is added to the growing myelin sheath is not known. Also it remains elusive how compartmentalization of the myelin sheath is achieved. Four concepts of myelin membrane transport have been described which could contribute to myelin assembly (Kramer, *et al.*, 2001). The first is the directed transport of donor membrane vesicles from the *trans* Golgi network (TGN) to the growing myelin sheath. The second expects that the vesicles first all follow one general secretory pathway to the plasma membrane surrounding the cell body (bulk flow). The components are internalized again and enter the endosomal system. Here, a sorting process takes place and the required lipids and proteins are delivered to the myelin sheath. The concept of regulated exocytosis includes directed transport as well as transcytosis but emphasizes that a signal from the associated axon triggers the release of membrane components. The fourth concept suggests that myelin components are sorted utilizing lipid rafts. Lipid rafts are membrane domains which are enriched in cholesterol and glycosphingolipids. According to this model, the myelin components are already sorted in the TGN. The rafts then are transported to the plasma membrane where they merge and form the distinct myelin domains. Since myelin is enriched in cholesterol, sphingolipids and the glycosphingolipids galactosylceramide and its sulfatide, lipid rafts also could be involved in myelinogenesis. The listed models of membrane transport are not mutually exclusive. On the contrary, it is very likely that oligodendrocytes make use of several modes of transport.

1.6 SNARE proteins – key components of vesicle fusion

A typical transport reaction can be viewed as a four-step process that consists of the formation of a vesicle, movement of the vesicle towards its target compartment, tethering/docking with the acceptor membrane, and, ultimately, fusion of the lipid bilayers.

SNARE (**S**oluble **N**-ethylmaleimide-sensitive factor **A**ttachment protein **RE**ceptor) proteins form a superfamily of small proteins with 36 members in humans and are the key components of vesicle fusion. Their characteristic is an evolutionary conserved stretch of 60-70 amino acids that are arranged in heptad repeats, called SNARE motif (Jahn & Scheller, 2006, Maier, *et al.*, 2008).

1.6.1 The classification of SNAREs

Originally, SNARE proteins due to their location were classified as v-SNAREs (vesicle membrane SNAREs) and t-SNAREs (target membrane SNAREs), with at least one contributing v-SNARE and t-SNARE (called the SNARE hypothesis) (Sollner, *et al.*, 1993, Rothman, 1994). This terminology turned out to be not suitable if homotypic fusion reactions between two equal compartments need to be described. Furthermore, certain SNAREs function in several transport steps with varying partners and some are involved simultaneously in anterograde and retrograde transport between two compartments. Another classification is based on the composition of the SNARE core complex which is formed upon fusion. When appropriate sets of SNAREs come together, their SNARE motifs spontaneously associate to form core complexes of extraordinary stability (Figure 5).

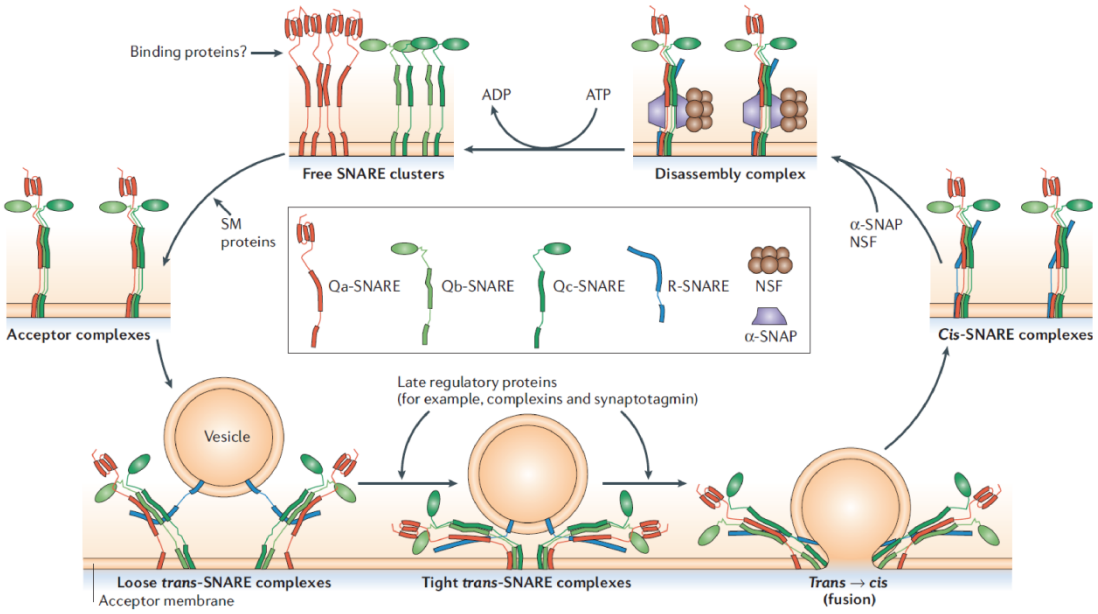

Figure 5: The SNARE conformational cycle during vesicle docking and fusion. The Q-SNAREs, which are organized in clusters, assemble into acceptor complexes. This assembly process might require SM (Sec1/Munc18-related) proteins. The acceptor complexes interact with the vesicular R-SNARE through the N-terminal end of the SNARE motifs and this nucleates the formation of a four-helical t*rans*-complex. *Trans*-complexes proceed from a loose state, in which only the N-terminal portion of the SNARE-complex is "zipped up", to the tight state, in which the zippering process is mostly completed. This is followed by the opening of the fusion pore. In regulated exocytosis, these transition states are controlled by late regulatory proteins. During fusion, the SNARE complex is transformed from a *trans*- to

a *cis*-configuration in which all of the SNAREs of a complex reside together in the resulting fused membrane. *Cis*-complexes are disassembled by the AAA+ (**A**TPases **A**ssociated with diverse cellular **A**ctivities) protein NSF (**N**-ethylmaleimide **S**ensitive **F**actor), together with SNAPs (**S**oluble **N**SF **A**ttachment **P**roteins), that function as cofactors. The R- and Q-SNAREs are then separated by sorting (Jahn & Scheller, 2006).

The SNARE core complex is a coiled coil of four intertwined parallel α-helices, with each helix being provided by a different SNARE motif. The center of the bundle contains 16 stacked layers of interacting side chains. The central "0"-layer contains three highly conserved glutamine (Q) residues and one highly conserved arginine (R) residue. Accordingly, the contributing SNARE motifs are classified into Q_a-, Q_b-, Q_c- and R-SNAREs. A functional SNARE complex requires one of each of the Q_a-, Q_b-, Q_c- and R-SNAREs. Usually, the R-SNARE is contributed by the vesicle, and the Q-SNAREs are contributed by the target membrane.

1.6.2 The SNARE cycle and accessory proteins

The Q-SNAREs are organized in clusters and assemble into so-called acceptor complexes in the target membrane (Figure 5). This assembly process might require sec1/munc18-related (SM) proteins. SM proteins are shaped like clasps and directly interact with SNARE proteins by binding to target SNAREs or to assembled SNARE complexes (Shen, *et al.*, 2007, Sudhof & Rothman, 2009, Bacaj, *et al.*, 2010). The initial contact between the vesicle and the target membrane is supported by several proteins which form a tethering complex (Yu & Hughson, 2010). Important factors are the Ras-related Rab GTPases. In the GTP-bound form, they recruit specific sets of effector proteins which are believed to differentially regulate various steps from budding over intracellular transport to membrane fusion (Stenmark & Olkkonen, 2001, Zerial & McBride, 2001, Jahn, *et al.*, 2003, Pfeffer & Aivazian, 2004, Lee, *et al.*, 2009, Ohya, *et al.*, 2009). During formation of the SNARE complex, free energy is released which is used to overcome the repulsive forces between the two membranes and drives fusion. To what extent SNAREs contribute to fusion specificity is still under debate. In many cases the deletion of an individual SNARE can result in surprisingly mild phenotypes. This indicates that SNAREs can functionally replace each other. Recent studies also have shown that three SNARE complexes or even perhaps only one SNARE complex is sufficient for membrane fusion (Hua & Scheller, 2001, Mohrmann, *et al.*, 2010, van den Bogaart, *et al.*, 2010). It is suggested that specificity is achieved by regulation of the acceptor complexes or regulation of tethering which might operate at a distance of up to 50 nm between the membranes (Pelham, 2001, Jahn & Scheller, 2006, Sudhof & Rothman, 2009). During fusion, the SNARE complex is transformed from a *trans*- to a *cis*-configuration in which all of the SNAREs of a complex are associated with the resulting fused membrane. The disassembly of the complex depends on the action of the ATP-bound AAA+ (**A**TPases **A**ssociated with diverse cellular **A**ctivities) protein NSF

(**N**-ethylmaleimide **S**ensitive **F**actor) and the adaptor protein α-SNAP (**S**oluble **N**SF **A**ttachment **P**rotein). The latter interacts directly with the SNARE complex and led to their naming as SNAP receptors (**S**oluble **N**SF **A**ttachment **P**rotein **RE**ceptors, SNAREs). α-SNAP stimulates the activity of ATP-bound NSF. The energy of ATP hydrolysis is used to disassemble the complex and the individual SNARE proteins can be recycled (Glick & Rothman, 1987, May, *et al.*, 2001).

1.7 The role of SNAREs in oligodendroglial membrane trafficking

A single oligodendrocyte can wrap up to 40 axonal segments simultaneously (Baumann & Pham-Dinh, 2001) and thus oligodendrocytes can be considered as a very complex polarized cell type. Oligodendrocytes probably utilize a modified version of the same transport machinery of other polarized cell types, such as epithelial cells. It is likely that the SNARE proteins are utilized to control the specificity of targeted fusion by selective pairing. Feldmann et al. characterized the oligodendroglial SNAREs by analyzing their expression depending on differentiation, their subcellular localization and by identification of putative interacting SNAREs. These studies allowed the assignment of SNAREs to trafficking pathways (Figure 6) (Feldmann, *et al.*, 2009).

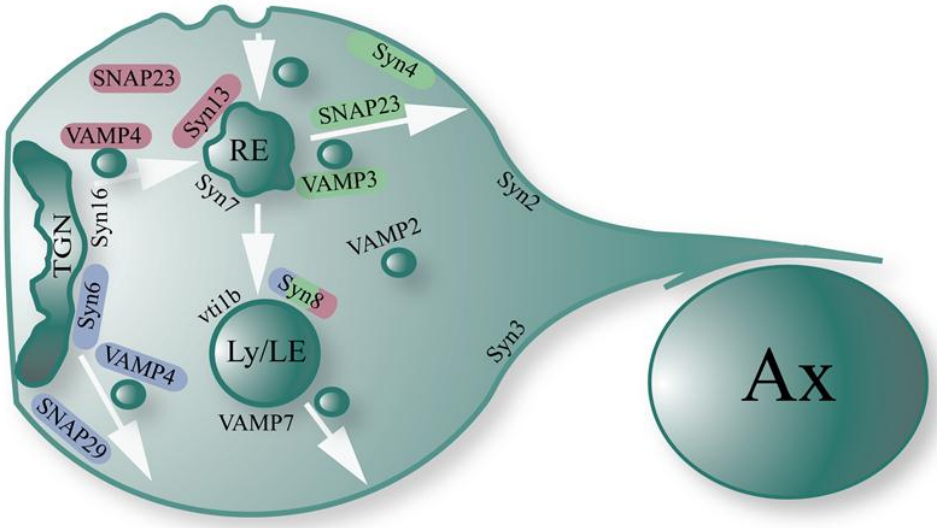

Figure 6: Assignment of SNAREs to trafficking pathways. The assignment is based on subcellular localization and putative SNARE complex formation. SNAREs interacting with each other are highlighted in the same color. Ax, axon; Ly/LE, lysosome/late endosome; RE, recycling endosome; TGN, *trans*-Golgi network; Syn, Syntaxin (Feldmann, *et al.*, 2009).

The major myelin protein PLP was chosen as a model to study the trafficking of myelin components in oligodendrocytes. The R-SNARE VAMP3 was found to be associated with recycling endosomes (REs), whereas another R-SNARE called VAMP7 was found in lysosomes/late endosomes (Ly/LEs). For both R-SNAREs colocalization with PLP

could be confirmed and furthermore, expression of VAMP3 increases with maturation and VAMP7 is accumulated in myelin during development. Thus, these two R-SNAREs were identified as the most promising candidates mediating the fusion of myelin membrane vesicles (Feldmann, *et al.*, 2011). Studies concerning the myelin proteins MAG, MOG and PLP revealed that they undergo endocytic sorting and recycling. Endocytic recycling may assist morphogenesis and microdomain formation of the myelin sheath by sorting and redirecting myelin components and furthermore may facilitate a fast adaptation to changing conditions (Winterstein, *et al.*, 2008). PLP was shown to be internalized at the plasma membrane and thereafter stored in Lys/LEs, mediated by a cholesterol-dependent and clathrin-independent endocytosis pathway. A neuronal cAMP-dependent signal was demonstrated to trigger the transport of PLP from Lys/LEs to the plasma membrane (Trajkovic, *et al.*, 2006).

1.8 The biogenesis of exosomes

Trafficking of PLP also involves the accumulation in LEs of multivesicular appearance, called multivesicular bodies (MVBs). MVBs are generated by inward budding of the limiting membrane resulting in the formation of small vesicles in the lumen of the MVB called intraluminal vesicles (ILVs). MVBs can have distinct fates. Degradative MVBs evolve into degradative lysosomes, whereas exocytic MVBs fuse with the plasma membrane and release the ILVs into the extracellular space. Once released, the ILVs are called exosomes (Figure 7) (Stoorvogel, *et al.*, 2002, Fevrier & Raposo, 2004, Cocucci, *et al.*, 2009).

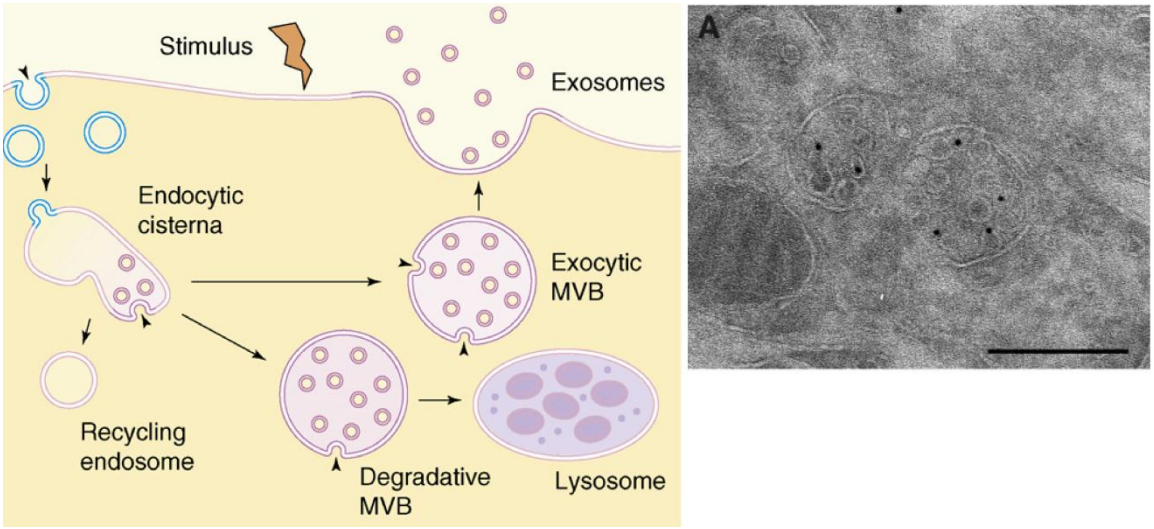

Figure 7: The generation of exosomes. Left, endosomes generated at the plasma membrane fuse to build endocytic cisternae. Three types of compartments can emerge from these: recycling endosomes, degradative MVBs and exocytic MVBs. Degradative MVBs evolve into degradative lysosomes, whereas exocytic MVBs fuse with the plasma membrane upon stimulation (thunderbolt) to release exosomes into the extracellular space. The arrows indicate the direction of membrane traffic; the arrowheads indicate the directions of vesicle fusion and generation (Cocucci, *et al.*, 2009). **Right**, electron micrograph of immu-

no-labeled primary cultured oligodendrocytes using antibodies recognizing PLP. PLP is associated with the ILVs of MVBs. Scale bar, 250 nm (Kramer-Albers, *et al.*, 2007).

Exosomes are released by a variety of cell types and thus can be found in various body fluids like blood, urine, bronchial lavage fluid, semen, saliva, breast milk, amniotic and CSF (Simpson, *et al.*, 2009). They carry canonical exosomal proteins and in addition cell type-specific cargo (van Niel, *et al.*, 2006, Simpson, *et al.*, 2008).

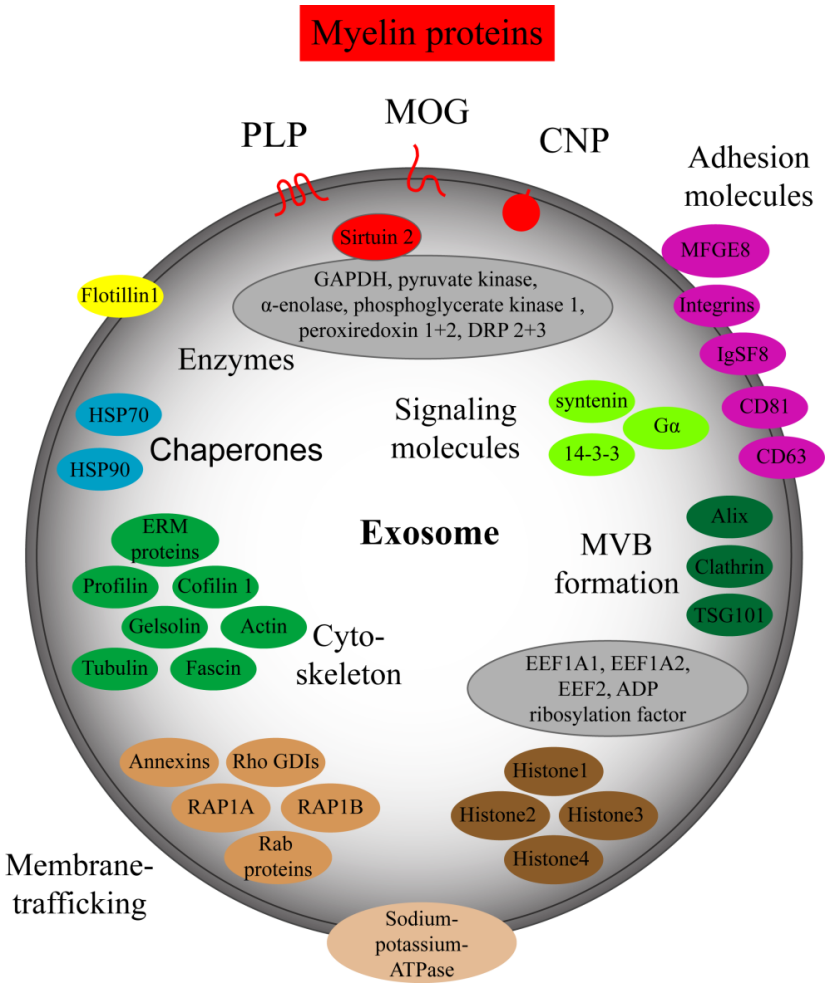

Figure 8: The oligodendroglial exosome proteome. Illustration depicting the proteins that can be found in oligodendroglial exosomes using mass spectrometry (Kramer-Albers, *et al.*, 2007). Oligodendroglial exosomes carry the canonical exosomal proteins belonging to versatile groups such as cell adhesion and signaling molecules, enzymes, histones, chaperones, etc., and beside the cell type-specific myelin proteins PLP, MOG, CNP and Sirtuin 2. Particularly to emphasize are also the proteins Flotillin 1, Alix and TSG101, which play a role in the generation of exosomes and therefore can be used as exosomal markers. Modified after (Schorey & Bhatnagar, 2008, Thery, *et al.*, 2009).

In oligodendroglial exosomes these are PLP, MOG, CNP and Sirtuin 2 (Figure 8) (Kramer-Albers, *et al.*, 2007). Due to their endosomal origin the orientation of the present proteins mimics that in the plasma membrane. Hence, exosomes are often described as miniatures of cells. They carry proteins of versatile groups, such as cell adhesion and signaling molecules, enzymes, histones and chaperones, many of them with putative protective functions (Kramer-Albers, *et al.*, 2007). Exosomes can be characterized by their size, their specific density and by the presence of protein markers. With only 50-

100 nm in diameter they are very small and display a cup-shaped structure in electron micrographs (Thery, *et al.*, 2009). Exosomes are enriched in cholesterol and ceramide, which play a critical role in the formation of membrane rafts. Due to the enrichment in lipids they display a specific density which facilitates their isolation by density gradient centrifugation. The transformation of the lipid sphingomyelin to ceramide requires action of the neutral sphingomyelinase. Its inhibition leads to a reduction of exosome release, indicating the necessity of ceramide in ILV budding. Membrane rafts could play a role in the lateral segregation of cargo within the endosomal membrane before budding (Stoorvogel, *et al.*, 2002, Trajkovic, *et al.*, 2008). Moreover, exosomes carry flotillin which is a lipid-binding protein able to bind and recruit cholesterol. In the lysosomal storage disorder Niemann-Pick type C1 disease, accumulating cholesterol is released via exosomes, pointing to a function of exosomes in cholesterol homeostasis (Kokubo, *et al.*, 2003, Roitbak, *et al.*, 2005, Strauss, *et al.*, 2010). TSG101 (**T**umor **S**usceptibility **G**ene 101 protein) and Alix (**AL**G-2 (**A**poptosis-**L**inked-**G**ene 2) -**I**nteracting protein **X**) are involved in MVB biogenesis. They are also present in exosomes and thus can serve as exosomal markers. Four complexes called ESCRT 0-III (**E**ndosomal **S**orting **C**omplex **R**equired for **T**ransport) are necessary for the sorting of proteins into ILVs and their budding and scission. TSG101 is part of the ESCRT-I complex, whereas Alix is thought to be a regulator of the ESCRT machinery by linking different ESCRT complexes (Trioulier, *et al.*, 2004, Hurley, 2008, Lakkaraju & Rodriguez-Boulan, 2008).

1.9 The diverse functions of exosomes

Depending on their origin, exosomes can be involved in many biological processes. They were first discovered in conjunction with maturing reticulocytes which use exosomes to externalize obsolete membranes and proteins, such as the transferrin receptor. Here, exosome biogenesis and secretion seem to be an important mechanism in red blood cell differentiation (Johnstone, *et al.*, 1987, Blanc, *et al.*, 2005). Exosomes also are able to modulate cellular signaling pathways. β-catenin was shown to be released via exosomes leading to a downregulation of the Wnt-signaling pathway in HEK293T (**H**uman **E**mbryonic **K**idney cell line) cells (Chairoungdua, *et al.*, 2010). It was demonstrated that exosomes of infected cells contain microbial components. These exosomes were able to promote antigen presentation and macrophage activation and thus could function as biomarkers or vaccines (Schorey & Bhatnagar, 2008). Exosomes produced by dendritic cells (DCs) can spread MHC (**M**ajor **H**istocompatibility **C**omplex) -peptide complexes between DCs and stimulate T-cell responses (Segura, *et al.*, 2005). They also were suggested to be involved in the establishment and maintenance of cell polarity (Lakkaraju & Rodriguez-Boulan, 2008). Pathogens like prion proteins might be passed on from one cell to another by exosomes, thereby increasing pathogen infectivity (Leblanc, *et al.*, 2006). In addition, exosomes can facilitate genetic exchange between

cells by mediating the transfer of mRNAs and miRNAs (Valadi, *et al.*, 2007, Hunter, *et al.*, 2008, Pegtel, *et al.*, 2010, Mittelbrunn, *et al.*, 2011). Tumor-derived exosomes carry mRNAs and miRNAs which change conditions in favor of tumor growth (Skog, *et al.*, 2008). It appeared that exosomes, the surface properties of which have been modified, allow efficient, tissue-specific and nonimmunogenic delivery of siRNAs, making them a valuable therapeutic tool (Alvarez-Erviti, *et al.*, 2011).

1.10 The exocytosis of oligodendroglial exosomes

The molecular mechanisms regulating the biogenesis and exocytosis of exosomes are poorly understood. Rab27a and Rab27b were found to function in targeting the MVBs to the cell periphery and their docking at the plasma membrane (Ostrowski, *et al.*, 2009). Another Rab protein that was shown to be involved in docking and tethering is Rab35. Rab35 and its GAPs (**G**TPase-**A**ctivating **P**roteins) TBC1D10A-C regulate exosome release in Oli-*neu* cells (Hsu, *et al.*, 2010). In K562 cells (a myelogenous leukemia cell line), Rab11 seems to be involved in homotypic fusion reactions of MVBs. Time lapse confocal microscopy revealed that many Rab11-positive MVBs were docked and ready to fuse in presence of a calcium chelator indicating that the final fusion reaction requires calcium (Savina, *et al.*, 2005). In neurons, the release of exosomes can be triggered by depolarization. It seems to be regulated by synaptic glutamatergic activity and is modulated by AMPA- and NMDA-receptors (Faure, *et al.*, 2006, Lachenal, *et al.*, 2011). Treatment of oligodendrocytes with the calcium-ionophore ionomycin enhances exosome release, demonstrating its calcium-dependence also in oligodendrocytes (Kramer-Albers, *et al.*, 2007). The mechanisms controlling the calcium-dependent release of oligodendroglial exosomes are still unknown. The question arises whether oligodendroglial exosomes could be involved in intercellular signaling. Recipient cells have not been identified yet, but a function in trophic support of axons has been proposed (Kramer-Albers, *et al.*, 2007). The nature of putative signaling pathways and their influence on neuronal metabolism are topics which have to be clarified in the future.

1.11 The neurofilaments are intermediate filaments of the neuronal cytoskeleton

The cytoskeleton provides cell shape and stability and facilitates the transport of particles and organelles within its cytoplasm. Based on differences in diameter, cytoskeletal proteins are classified into three groups, which are MTs (**M**icro**T**ubules, ~24 nm), MFs (**M**icro**F**ilaments, ~6-8 nm) and Ifs (**I**ntermediate **F**ilaments, ~10 nm). MTs are predominantly composed of tubulin and are responsible for maintaining cell shape, organelle and vesicle movement, and the formation of spindle fibers during mitosis. MFs are pre-

dominantly composed of actin and are necessary for cellular movement, muscle contraction and cytokinesis. IFs are a very versatile group and differ in different tissues and cells. Based on molecular structural homology, five types of IFs have been defined. The first are acid keratins, the second basic keratins, the third contains desmin, GFAP (**G**lial **F**ibrillary **A**cidic **P**rotein) and peripherin/vimentin, the fourth are the NFs (**N**euro**F**ilaments), α-internexin and nestin (Figure 9 A), and type V IFs comprise nuclear lamins. Type IV IFs share common sequence structures. They have an α-helical rod domain of about 310 amino acids flanked by a globular N-terminal region (head domain) and a non- α-helical carboxy-terminal side-arm (tail) domain. The central rod domain contains highly conserved motifs. Every seventh residue is hydrophobic which facilitates the formation of α-helical coiled-coil dimers (Liu, *et al.*, 2004).

1.11.1 Composition

NFs are composed of three subunits which are defined by their molecular weight: the light (NF-L), the medium (NF-M), and the heavy subunit (NF-H) with 60 kDa, 100 kDa and 110 kDa, respectively. These subunits exhibit greater molecular weights on SDS-PAGE (**S**odium **D**odecyl **S**ulfate **P**oly**A**crylamide **G**el **E**lectrophoresis) of 70 kDa, 160 kDa and 200 kDa, respectively, because of their enrichment in negatively charged amino acids (glutamic acids) and post-translational modifications such as phosphorylation and glycosylation. *In vivo*, rodent NFs are obligate heteropolymers requiring NF-L plus either NF-M or NF-H to form a filamentous network. Neurofilament assembly is believed to start with the dimerization of NF-L with either NF-M or NF-H (Figure 9 B). The rod domains form a coiled-coil in a head-to-tail fashion. Two coiled dimers overlap with each other in an anti-parallel, half-staggered manner, forming the tetramers. Finally, eight tetramers are packed laterally and longitudinally together in a helical array, forming a rope-like 10 nm filament. The C-termini of NF-M and NF-H are not in the coils, they form the side arms of the neurofilaments. These form cross-bridges to other neurofilaments or cytoskeletal elements (Hisanaga & Hirokawa, 1990, Gotow, *et al.*, 1994, Wagner, *et al.*, 2003, Stevens & Hoh, 2011). There are hints that also the typeIV IF α-internexin and the typeIII IF peripherin could contribute to NF-formation (Ching & Liem, 1993, Beaulieu, *et al.*, 1999).

1.11.2 Transport

The NF proteins are synthesized at free ribosomes in the neuronal cell body and thereafter need to be transported along the axon to their final destination. Depending on speed the axonal transport is divided in two major categories: the fast axonal transport (~250-400 mm/day) conveys mitochondria, neurotransmitters, channel proteins, lysosomes and endosomes and the slow axonal transport (~0,1-4 mm/day) conveys axonal cytoskeleton and cytosolic proteins. The slow axonal transport can be further subdivided in two com-

ponents: the slow component a (SCa, 0,1-1 mm/day), containing NFs and microtubules, and the slow component b (SCb, 2-4 mm/day), containing actin, spectrin and other cytosolic proteins (Brady, 1993, Perrot, *et al.*, 2008). The slow transport rate of NFs is supposed to arise because periods of fast movement are interrupted by prolonged pauses (Roy, *et al.*, 2000, Wang, *et al.*, 2000, Wang & Brown, 2001).

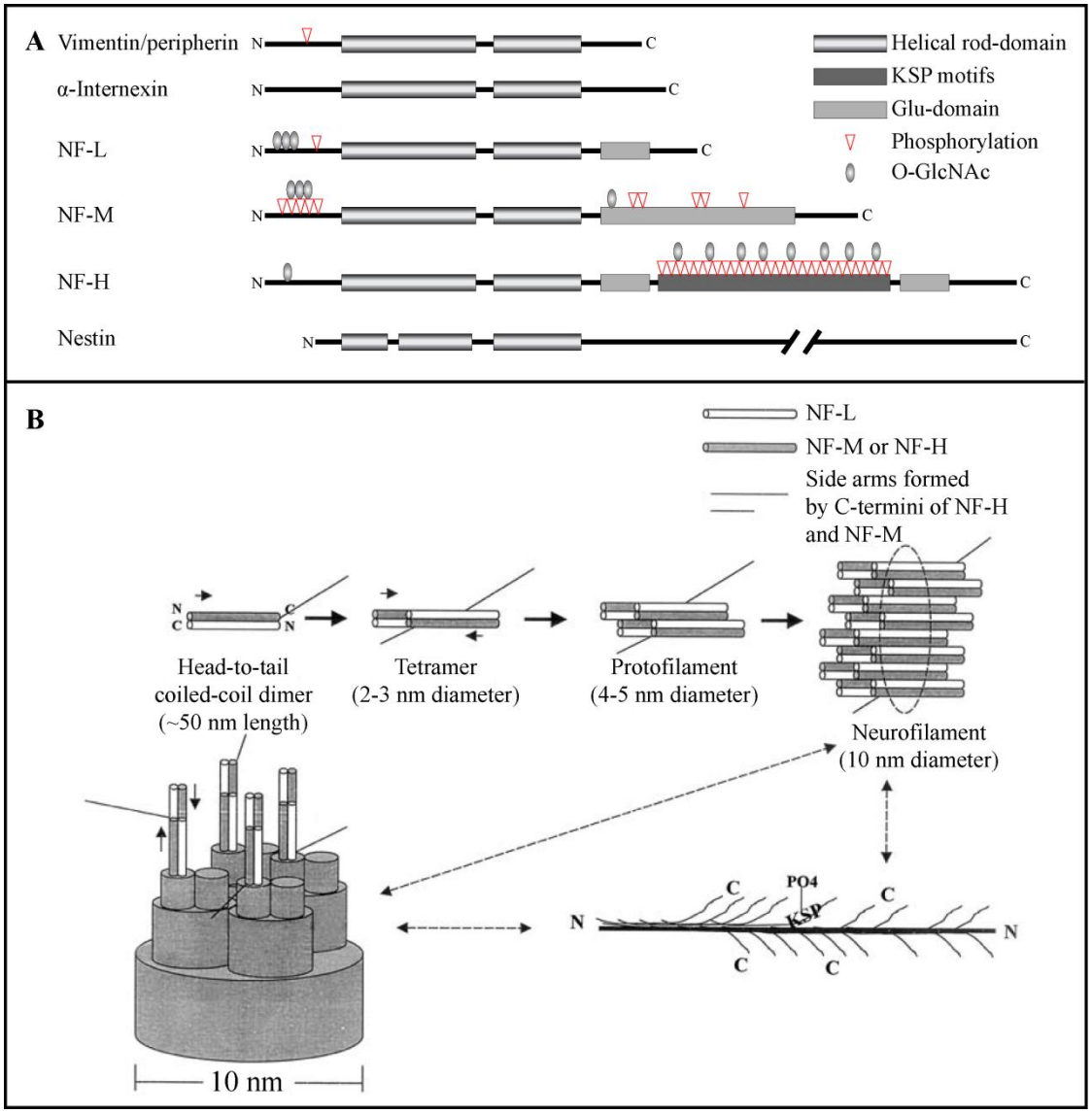

Figure 9: Type IV intermediate filaments and neurofilament assembly. A, Structure of the neurofilament subunits in comparison to the other type IV intermediate filaments vimentin/peripherin, α-internexin, and nestin. All type IV intermediate filaments have central helical rod domains in common, containing highly conserved motifs. Every seventh residue is hydrophobic, which facilitates the formation of α-helical coiled-coil dimers. Especially the C-termini of NF-M and NF-H carry post-translational modifications such as glycosylation and phosphorylation. KSP motif, lysine-serine-proline (KSP) repeat domain containing motif; Glu-domain, glutamic acid rich domain; O-GlcNAc, O-linked glycosylation site. **B**, Schematic model of NF assembly. For dimerization, the rod domains of NF-L and either NF-M or NF-H form a coiled-coil in a head-to-tail fashion. Two dimers overlap with each other to form the tetramer. Eight tetramers are helically arranged to form the 10 nm neurofilament. The C-termini of NF-M and NF-H build the side arms of the neurofilaments. Modified after (Liu, *et al.*, 2004, Perrot, *et al.*, 2008).

This mode of transport also confounded the interpretation of studies on this subject in the past. Also not known is where the assembly of the NF subunits actually takes place. The polymer hypothesis suggests that NF subunits are transported already as polymeric structures whereas the subunit hypothesis argues that the NFs are transported as individual subunits or small oligomers. Until now, none of these two hypotheses could be clearly confirmed or disproved (Brady, 2000). Also not clearly solved is the question which motor proteins mediate transport of NFs. It was suggested that the transport occurs along MTs and is mediated by kinesin and dynein/dynactin (Shah, *et al.*, 2000, Yabe, *et al.*, 2000). Studies using cytochalasin B which inhibits actin polymerization showed that actin and myosin are involved in transport of NFs, too (Jung, *et al.*, 2004).

1.11.3 Post-translational modifications

The head and tail domains of NFs are sites of post-translational modification which is essential for the assembly and axonal transport of NFs.

1.11.3.1 Glycosylation

NFs can be modified by O-linked glycosylation (O-GlcNAc) to individual serine and threonine residues. The function of these modifications is still unclear although a role in NF assembly is suggested. The glycosylation sites in the head domains are located in regions that have been shown to be essential for *in vivo* assembly, and are close to the phosphorylation sites involved in this process. This also indicates that glycosylation and phosphorylation sites can influence each other.

1.11.3.2 Phosphorylation

Phosphorylation sites are located at the N- and C-termini of the NF subunits. NFs are synthesized in the cell bodies and subsequently transported into the axon. Almost all of the NFs in myelinated axonal regions are known to be phosphorylated at the tail domains of NF-M and NF-H. In contrast, they are less phosphorylated in neurites, at nodes of Ranvier and in cell bodies. Thus, the tail domains of NFs are phosphorylated after their entry into the axon. The phosphorylation of the head domains of NF-L and NF-M inhibits axonal transport and neurofilament assembly and their dephosphorylation was shown to be a prerequisite for the phosphorylation of the tail domains (Zheng, *et al.*, 2003, Yates, *et al.*, 2009). It is hypothesized that this prevents abnormal NF assembly in the soma. Aberrant NF phosphorylation associated with accumulation of filamentous aggregates in cell bodies was observed in many neurodegenerative diseases, such as Alzheimer disease, Pick disease, dementia, Parkinson disease and amyotrophic lateral sclerosis (Grant & Pant, 2000, De Vos, *et al.*, 2008). Phosphorylation of the tail domains of NF-M and NF-H was long suspected to control the spacing between the neurofilaments and thus axonal caliber. It was suggested that the negative charges of the

phosphate groups lead to mutual repulsion of the side arms and their lateral expansion, thereby increasing interfilament spacing (de Waegh, *et al.*, 1992). The phosphorylation of NF-M and NF-H side arms also was shown to correlate with the speed of transport. There are hints that phosphorylation of NF-H and NF-M influences attachment of NFs to motor proteins (Shah, *et al.*, 2000, Yabe, *et al.*, 2000, Miller, *et al.*, 2002). This is in contrast to the analysis of mice expressing a truncated form of NF-H without the tail domain and its phosphorylation sites which showed no changes in interfilament spacing, axonal diameter or neurofilament transport rate. However, there was a compensatory increase in phosphorylation of NF-M which confounds interpretation and indicates that NF-M can functionally replace NF-H (Rao, *et al.*, 2002, Yuan, *et al.*, 2006, Shea & Chan, 2008).

1.11.4 Effects of myelination on neurofilament phosphorylation

In normal axons, only the initial segments, the nodes of Ranvier (approximately 1 µm) and the terminals are not covered by myelin. Almost all (> 99%) of the NFs in myelinated internodal regions of an axon are known to be phosphorylated (Hsieh, *et al.*, 1994). In comparison, NFs are less phosphorylated at nodes of Ranvier. At this distinct area, axon diameter is reduced and NFs show increased density (Mata, *et al.*, 1992). In *trembler* mice, which carry a missense mutation in the peripheral myelin protein *PMP-22* gene leading to severe hypomyelination in the PNS, average axonal caliber is reduced, whereas the density of axonal cytoskeletal elements is increased. Analysis of NF phosphorylation levels showed that dephosphorylated NF-H was increased, with a concomitant reduction of phosphorylated NF-H. Furthermore, graft studies demonstrated that these alterations were restricted to axon segments without normal myelination (Aguayo, *et al.*, 1977, de Waegh & Brady, 1991, de Waegh, *et al.*, 1992). A deletion in the *MBP* gene causes severe hypomyelination in the CNS of *shiverer* mice, although MBP is present in CNS and PNS. It was suggested that other proteins, such as P_0, are sufficient to compensate for the lack of MBP in the PNS. Furthermore, these findings suggest that different mechanisms might operate in CNS and PNS myelination. In *shiverer* mice, axon caliber is slightly decreased, whereas NF packing density is increased. Expression levels and phosphorylation of NF-H were shown to be reduced, but MT density was strongly increased (Popko, *et al.*, 1987, Readhead & Hood, 1990, Readhead, *et al.*, 1990, Brady, *et al.*, 1999). In MAG-deficient mice, myelin shows normal compaction. Also in these mice, nerve caliber is decreased, whereas NF density is increased. NF phosphorylation is decreased, with a concomitant increase of dephosphorylated NF-H. No changes were found in unmyelinated fibers of MAG-deficient mice (Yin, *et al.*, 1998). In addition, MAG initially is found exclusively in the adaxonal space. Its expression starts with myelination and is maintained during compaction. Therefore, it is a candidate for axon-glia signaling (Trapp, *et al.*, 1984, de Waegh, *et al.*, 1992). The identity

of the axonal ligand remains unknown as do downstream effectors of the signaling cascade. In summary, these studies suggest that alterations of the neuronal cytoskeleton appear whenever the relationship between the myelinating glia and the axon is missing or disrupted. The disruption of normal interaction can be due to either altered compaction or changes in myelin protein expression, such as adhesion molecules. In general, it leads to a decrease of axonal caliber and NF phosphorylation and increases of NF density. Thus, most of the studies on demyelinated regions in different genetic backgrounds suggest that the dephosphorylation of NF-H has negative effects on the axon. But Brady et al. mentioned that many of the cytoskeletal alterations observed in *shiverer* axons also are features of wildtype axons before myelination (Brady, *et al.*, 1999). Witt et al. supposed a model in which NF phosphorylation results from a balance of kinase and phosphatase activities. In a myelinated axon segment, kinase activities dominate, caused by an increase of kinase activities and/or a decrease of phosphatase activities (Witt & Brady, 2000). Thus, the opposite would be case for unmyelinated regions, including axonal segments before myelination. The regulators of such a kinase/phosphatase cycle are still unknown.

1.12 The trophic support of neurons by oligodendrocytes

Nave et al. proposed a model in which myelination imposes a burden for insulated axons, by isolating them from external nutrients (Nave & Trapp, 2008). They refer to the dimensions of the myelin sheath. Myelin segments assume a length of between 100 and 1700 µm and are separated by the nodes of Ranvier which are approximately 1 µm in length. Thus, the surface of the axon is largely isolated from the external milieu. They suppose that the oligodendrocyte provides trophic support for the axonal segments it has myelinated and that mutant oligodendrocytes fail to deliver this support (Nave & Trapp, 2008, Edgar & Nave, 2009). Mice with deletions of the *PLP1* gene, serving as a model for SPG-2 and mild forms of PMD in humans, as well as CNP knockout mice develop late onset axonal degeneration. In PLP knockout mice, membranous organelles accumulate preferentially at the distal juxtaparanode, leading to large axonal swellings with first appearance between P20 and P40 (Griffiths, *et al.*, 1998, Edgar, *et al.*, 2004) (Figure 10). Analysis of $PLP^{+/-}$ heterozygotes revealed that all accumulations were associated with PLP-deficient myelin. To unequivocally demonstrate that the observed axonopathy results only from the absence of PLP in the overlying oligodendrocyte, neurospheres from wildtype or PLP null mice were transplanted into the myelin-deficient *shiverer* mutant. The transplant sites were analyzed approximately 4 months later. None of the mice myelinated by wildtype cells developed any axonal abnormalities, whereas all of axonal segments myelinated by the PLP null mice showed the characteristic changes described previously. The accumulation of membranous organelles at the distal paranode suggests a defect in retrograde axonal transport. Indeed, an impairment of retro-

grade and anterograde fast axonal transport could be confirmed. The motor proteins dynein and dynactin, both acting in retrograde transport, and the regulatory proteins for dynein were elevated in the absence of PLP. Complementation of the null phenotype with a wildtype *PLP* genomic transgene restored wildtype levels. Analysis of myelin ultrastructure in PLP knockout mice revealed no differences in the proportion of myelinated axons, myelin sheath thickness or size range of myelinated fibers between PLP knockout and wildtype mice. However, alterations in myelin periodicity were observed. The difference between major dense lines and intraperiod lines was less distinct than in wildtype, with the intraperiod line being a single condensed structure. This condensed intraperiod line later on has been related to an increased interlamellar space, indicating a role of PLP in intraperiod line formation (Boison & Stoffel, 1994, Klugmann, *et al.*, 1997, Griffiths, *et al.*, 1998, Yool, *et al.*, 2002, Rosenbluth, *et al.*, 2006).

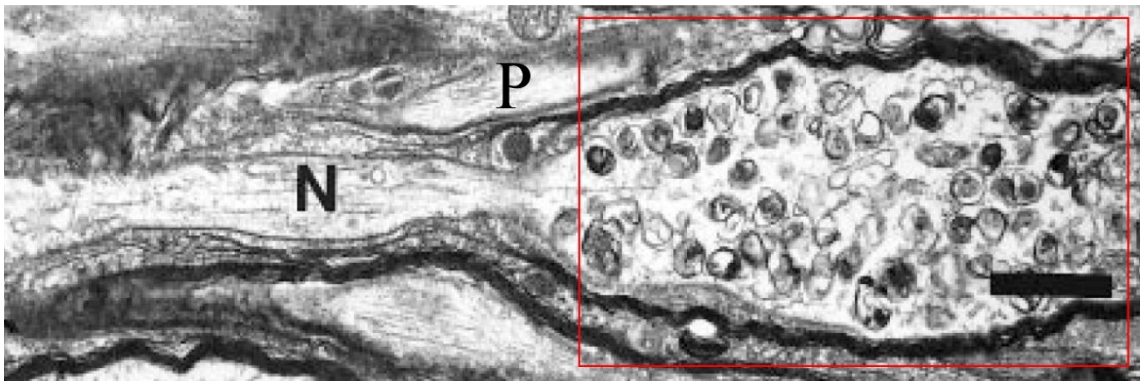

Figure 10: Longitudinal section of the optic nerve from a 4-month-old *PLP-/Y* mouse. Electron micrograph showing an axonal swelling in the optic nerve from a 4-month-old PLP-/Y mouse. The area of the swelling is characterized by accumulation of membranous organelles (encircled in red). N, node of Ranvier; P, paranode; scale bar, 1 µm. Adapted from (Griffiths, *et al.*, 1998).

CNP knockout mice showed a much more severe phenotype than PLP knockout mice. They had decreased motor performance at earlier ages and their lifespans were drastically reduced, with less than 20% of the homozygous mutants reaching the age of 13 months. The myelin sheaths showed regular thickness and seemed to be structurally intact. In addition, no changes in periodicity could be found. The only structural abnormality was the enlargement of the inner adaxonal loop. Edgar et al. used the same approach as described previously and transplanted neurospheres from CNP knockout mice into the *shiverer* mutant. The transplanted cells generated compact myelin sheaths around the *shiverer* axons and the CNP null phenotype was reproduced at the transplantation sites (Edgar, *et al.*, 2009). In CNP knockout mice axonal swellings similar to those in PLP knockout mice could be detected, but with first appearance as early as at P5 they developed much earlier (Lappe-Siefke, *et al.*, 2003, Edgar, *et al.*, 2009). PLP and CNP knockout mice both have normally compacted myelin sheaths and show only subtle alterations on the ultrastructural level. This is in contrast to MPB knockout mice, in which the compaction of myelin fails and axons are nonmyelinated or only loosely

ensheathed, but no axonal swellings are detected (Kirkpatrick, *et al.*, 2001). Thus, a primary oligodendroglial defect leads to secondary axonal degeneration despite apparent myelin formation. Oligodendrocytes seem to have a function independent of myelination, namely to provide support for longterm axonal integrity (Griffiths, *et al.*, 1998, Lappe-Siefke, *et al.*, 2003, Yin, *et al.*, 2006, Kramer-Albers, *et al.*, 2007, Nave & Trapp, 2008, Edgar, *et al.*, 2009). Oligodendrocytes were shown to release exosomes which carry PLP, CNP, MOG, Sirtuin 2, and several proteins with proposed functions in the relief of stress. Therefore, oligodendroglial exosomes could be involved in glia-mediated trophic support to axons (Kramer-Albers, *et al.*, 2007).

1.13 Aim of the study

The study is divided in two parts. The first part is dedicated to the question how oligodendrocytes establish the myelin membrane and which trafficking mechanisms are utilized to achieve a temporally and spatially controlled delivery of myelin membrane components. The role of the R-SNAREs VAMP3 and VAMP7 in cell surface transport of the major myelin protein PLP in primary cultured oligodendrocytes has been analyzed. A myelinating coculture system of cortical neurons and oligodendrocytes has been established to study myelin assembly *in vitro*. In the second part, the specific role of oligodendroglial exosomes in glia to axon signaling has been examined. One goal was to visualize the transfer of oligodendroglial exosomes to neurons. Hereafter, possible effects on recipient neurons were studied. Three aspects of neuronal metabolism, including metabolic activity, phosphorylation of the neurofilament heavy subunit and the activation of kinases, were analyzed.

2 Materials and methods

2.1 Materials

2.1.1 Centrifuges and accessory

	Manufacturer
3K20	Sigma-Aldrich, München
Biofuge 17RS	Heraeus Sepatech, Osterode
Megafuge 1.0R	Heraeus, Hanau
Optima L-90 K Ultracentrifuge	Beckman Coulter, München
Optima Ultracentrifuge Max-E	Beckman Coulter, München
Optima XL-100 K Ultracentrifuge	Beckman
Rotors: TLS-55, TLA-55, SW28-Ti, SW40-Ti, SW41-Ti	Beckman
Z383K	Hermle, Wehingen

Table 1: Centrifuges and accessory

2.1.2 Microscopes

	Manufacturer
AF 6000 LX	Leica, Wetzlar
DMIL	Leica, Wetzlar
DMLB	Leica Wetzlar

TCS SP5	Leica, Wetzlar

Table 2: Microscopes

2.1.3 Other equipment

	Manufacturer
Amersham Hyperfilm ECL, High performance chemiluminescence film	GE Healthcare
Biotrak II Plate reader	Amersham Biosciences
C200 Incubator	Labotect, Göttingen
Electrophoresis chamber	Bio-Rad, München
Electrophoresis chamber NuPAGE	Invitrogen, Karlsruhe
GenePulser Xcell	Bio-Rad, München
NanoDrop 1000 Spectrophotometer	Peqlab, Erlangen
Nucleofector II	AMAXA, Köln
Odyssey Imager	LI-COR
Optimax Type TR X-Ray Film Processor	PROTEC, Oberstenfeld
SterilGARD III Advance Class II Biological Safety Cabinet	The Baker Company

Table 3: Other equipment

2.1.4 Software

	Manufacturer
ApE plasmid editor	M. Wayne Davis
CLC Free Workbench	CLC bio, Aarhus, Denmark
Clone Manager 9, Professional Edition	Scientific & Educational Software
Endnote X4	Wintertree Software Inc., Canada
Excel 2010	Microsoft
Illustrator CS2	Adobe, München

ImageJ	NIH, Bethesda, Maryland
Photoshop CS2	Adobe, München
Word 2010	Microsoft

Table 4: Software

2.1.5 Chemicals

	Manufacturer
4-OHT (4-Hydroxytamoxifen)	Sigma-Aldrich, München
DiButyryl-cyclic-adenosine mono-phosphate (DBcAMP)	Sigma-Aldrich, München
Dye reagent concentrate (Bradford protein assay)	Bio-Rad, München
GW4869	Sigma-Aldrich, München
Hydrogen peroxide	Roth, Karlruhe
L-Glutamic acid monosodium salt hydrate	Sigma-Aldrich, München
N,N-Dimethylformamide (DMF)	Sigma-Aldrich, München
Sodiumbutyrate	Sigma-Aldrich, München
Trypan Blue	Matheson Coleman and Bell
Other chemicals	Merck, Darmstadt Roth, Karlsruhe Sigma-Aldrich, München

Table 5: Chemicals

2.1.6 Kits

	Manufacturer
AMAXA Basic Nucleofector Kit for Primary Neurons	Lonza
Proteome Profiler Arrays, Human Phospho - MAPK Array	R&D Systems, Minneapolis, USA

PureLink HiPure Plasmid Maxi Kit	Qiagen, Hilden
PureLink HiPure Plasmid Miniprep Kit	Qiagen, Hilden

Table 6: Kits

2.1.7 Protein markers

	Manufacturer
Precision Plus Protein Standards Dual Color	Bio-Rad, München
SeeBlue Plus2 Pre-Stained Standard	Invitrogen, Karlsruhe

Table 7: Protein markers

2.1.8 DNA markers

	Manufacturer
Lambda/HindIII Marker, 2, ready-to-use	Fermentas
O´GeneRuler 1kb DNA Ladder, ready-to-use	Fermentas
PhiX 174 DNA/BsuRI (HaeIII) Marker, 9, ready-to-use	Fermentas

Table 8: DNA markers

2.2 Buffers and media

2.2.1 Cell culture

	Composition
Cryoprotective medium	RPMI 1640 70%, FCS 20%, DMSO 10%
HBSS	KCl 5,33 mM, KH_2PO_4 0,441 mM, $NaHCO_3$ 4,17 mM, NaCl 137,93 mM, Na_2HPO_4 0,338 mM, D-glucose 5,56 mM, Phenol Red 0,0266
HBSS$^+$	HBSS, 0,15% $MgSO_4$
Laminin	2-10 µg/ml

Neurobasal feeding medium	Neurobasal, B27 supplement 20 ml/l, L-glutamine 0,5 mM, Pen-Strep (penicillin G K-salt 63,2 µg/l, streptomycin sulfate 135 µg/l)
Neurobasal plating medium	Neurobasal, B27 supplement 20 ml/l, L-glutamine 0,5 mM, Pen-Strep (penicillin G K-salt 63,2 µg/l, streptomycin sulfate 135 µg/l), glutamate 12,5 µM
Poly-L-lysine	Poly-L-lysine hydrobromide (chain length 70.000-150.000) 0,1 g/l
SATO/B27 (pOL)	DMEM 13,4 g/l, $NaHCO_3$ 2 g/l, B27 supplement 20 ml/l, sodium pyruvate 1 mM, TIT 500 nM, L-thyroxine 500 mM, gentamycin, horse serum 1%
SATO/B27, –Phenol Red (MTT assay)	DMEM –Phenol Red, B27 supplement 20 ml/l, sodium pyruvate 1 mM, TIT 500 nM, L-Thyroxine 500 mM, L-glutamine 4 mM, gentamycin, horse serum 1%
SATO (Oli-*neu* cells)	DMEM 13,4 g/l, $NaHCO_3$ 2 g/l, 0,01 g/l transferrin, insulin 100 µg/l, putrescine 100 µM, progesterone 200 nM, TIT 500 nM, sodium selenite 220 nM, L-thyroxine 520 mM, horse serum 1%
Trypsin/EDTA	HBSS, 0,01% trypsin, 0,02% EDTA

Table 9: Cell culture

2.2.2 Protein biochemistry

	Composition
4 x sample buffer	Tris-HCl (pH 6,8) 200 mM, SDS (sodium dodecylsulfate) 8%, bromphenolblue 0,4%, glycerol 40%, DTT 400 mM
5 x electrophoresis buffer (tris-glycine)	Tris 125 mM, glycine 1,25 M, SDS 0,5% (pH 8,3)
20 x electrophoresis buffer (NuPage MES)	MES 50 mM, Tris 50 mM, SDS 0,1%, EDTA 1 mM (pH 7,3)
20 x electrophoresis buffer (NuPage MOPS)	MOPS 50 mM, Tris 50 mM, SDS 0,1%, EDTA 1 mM (pH 7,7)

Blocking solution (IC)	PBS, horse serum 10%
Blocking solution (WB)	PBST, milk powder 4%
ECL homemade	Solution A: Tris-HCl 0,1 M (pH 8,6), luminol 0,25 g/l Solution B: Para hydroxyl coumaric acid 1,1 g/l Use: 1 ml solution A + 0,1 ml solution B + 0,3 µl H_2O_2
Fixation solution (IC)	PBS, paraformaldehyde 4%
Homogenization buffer (membrane fractionation)	Tris 10 mM (pH 7,5), EDTA 5 mM
Mowiol	Mowiol 4-88 2,4 g, glycerol 6 g, H_2O bidest 6 ml, Tris 0,2 M (pH 8,5) 12 ml
MTT stock solution	PBS, 5 mg/ml
PBS	NaCl 150 mM, Na_2HPO_4 8 mM, NaH_2PO_4, 1,74 mM
PBST	PBS, Tween 20 0,1%
Permeabilization solution	PBS, Triton X-100 0,1%
Protease inhibitors	PMSF 1 mM (Sigma), aprotinin 1 µg/ml (Boegringer), leupeptin 5 µg/ml (Sigma), pepstatin 1 µg/ml (Sigma)
Protease- and phosphatase inhibitor cocktail	Aprotinin, bestatin, E-64, leupeptin, sodium fluoride, sodium orthovanadate, sodium pyrophosphate, β-glycerophosphate (Pierce)
RIPA buffer (membrane fractionation)	Tris/HCl (pH 7,5) 10 mM, NaCl 150 mM, Nonident P40 1%, SDS 0,1%, EDTA 2 mM, sodium deoxychelate 0,5%
RIPA buffer (neurofilament phosphorylation assay)	Tris/HCl (pH 7,5) 50 mM, NaCl 150 mM, Nonident P40 1%, SDS 0,1%, EDTA 1 mM, sodium deoxychelate 0,5%
Solubilization solution (MTT assay)	H_2O, DMF 40%, SDS 10%, acetic acid (conc.) 2%

Separation gel buffer	Tris 1,5 M (pH 8,8)
Stacking gel buffer	Tris 1 M (pH 6,8)
TBS (pH 7,2)	Tris 50 mM, NaCl 150 mM
Transfer buffer (WB)	Tris 24 mM, glycine 192 mM, ethanol 20%
Triton lysis buffer	Tris/HCl 50 mM (pH 7,2), NaCl 150 mM, Triton X-100 1%

Table 10: Protein biochemistry

2.2.3 Molecular biology

	Composition
LB agar	LB medium, agar 15 g/l
LB medium	NaCl 10 g/l, trypton 10 g/l, yeast extract 5 g/l
Sample buffer (agarose gels)	EDTA 1 mM, bromphenolblue 1%, sucrose 0,5%, xylencyanol 2%
TAE	EDTA 1 mM, Tris 0,04 M, adjusted to pH 8,0 with acetic acid

Table 11: Molecular biology

2.2.4 Enzymes

Restriction enzymes and phosphatases were obtained from New England BioLabs, Fermentas and Promega, and were used according to the manufacturer´s instructions.

2.2.5 Antibodies

2.2.5.1 Primary antibodies

epitope	**Clone**	**Species**	**Dilution**	**origin**
AIP-1/Alix		mouse	WB 1:250	BD
AKT1		rabbit	WB 1:1000	Cell signaling
AKT phosph.		mouse	WB 1: 1400	Cell signaling
Calnexin		rabbit	WB 1:2000	Stressgen, Hamburg
Calreticulin			WB 1:4000	Stressgen, Hamburg

Cre recombinase		rabbit	IF 1:1000, WB 1:5000	Covance
Enolase γ		mouse	WB 1:500	Santa Cruz
ERK1		rabbit	WB 1:5000	Cell signaling
ERK phosph.		mouse	WB 1:1000	Cell signaling
GFAP		rabbit	1:5000	Dako
GFP		rabbit	1:1000	
L1	324	rat	IF 1:10	Hybridoma
L1	555	rat	WB 1:50	Hybridoma
MAP-2		Guinea pig	1:1000	Boehringer, Mannheim
MBP	12	rat	1:500	Serotec
NeuN		mouse	IF 1:500	Chemicon
NF-H phosph.	SMI31R	mouse	IF 1:10.000, WB 1:1000	Covance
NF-M	RMO44	mouse	WB 1:1000	Zymed
PLP	Aa3	Rat	IF undiluted, IC-MDA 1:10, WB 1:10	Hybridoma, M. B. Lees, Waltham, USA
PLP	O10	mouse	IF undiluted	Hybridoma, M. Schachner, Hamburg
TSG 101	4A10	mouse	WB 1:250	Genetex
Tubulin α	DM1A	mouse	WB 1:5000	Sigma-Aldrich, München
Tubulin β class III	TUJ1	rabbit	IF 1:1000	Covance
VAMP3		rabbit	WB 1:1000	Synaptic Systems, Göttingen
VAMP7		rabbit	WB 1:1000	Synaptic Systems, Göttingen

Table 12: Primary antibodies

2.2.5.2 Antibodies directed against PLP

In the present work two antibodies called O10 and aa3 were used. O10 recognizes an extracellular epitope of PLP/DM20 at the second outer loop, whose presence depends on the protein conformation of PLP/DM20. Therefore, the antibody O10 selectively stains PLP/DM20 localized in the plasma membrane of live cells (Jung, *et al.*, 1996). Aa3 recognizes an epitope at the C-terminus of PLP and thus all intracellular PLP/DM20 molecules in addition (Figure 4) (M.B. Lees, Waltham) (Kramer-Albers, *et al.*, 2006).

2.2.5.3 Secondary antibodies

species	anti	conjugation	dilution	origin
goat	mouse	Cy2	1:100	Dianova, Hamburg
goat	mouse (c.-ads.)	Cy2	1:100	Dianova, Hamburg
goat	rabbit	Cy2	1:100	Dianova, Hamburg
goat	rat	Cy2	1:100	Dianova, Hamburg
goat	rat (c.-ads.)	Cy2	1:100	Dianova, Hamburg
goat	mouse	Cy3	1:1000	Dianova, Hamburg
goat	mouse (c.-ads.)	Cy3	1:1000	Dianova, Hamburg
goat	rabbit	Cy3	1:1000	Dianova, Hamburg
goat	rat	Cy3	1:1000	Dianova, Hamburg
goat	rat (c.-ads.)	Cy3	1:1000	Dianova, Hamburg
goat	mouse	Cy5	1:100	Dianova, Hamburg
goat	Mouse (c.-ads.)	Cy5	1:100	Dianova, Hamburg
goat	rabbit	Cy5	1:100	Dianova, Hamburg
goat	rat	Cy5	1:100	Dianova, Hamburg
goat	mouse	HRP	1:10.000	Dianova, Hamburg
goat	rabbit	HRP	1:10.000	Dianova, Hamburg
goat	rat	HRP	1:10.000	Dianova, Hamburg
goat	rat	Alexa-488	1:400	Invitrogen, Karls-ruhe
goat	rat (c.-ads.)	Alexa-488	1:400	Invitrogen, Karls-

				ruhe
donkey	mouse	IRDye 800CW	1:800	LI-COR
goat	rat	Alexa Fluor 680	1:1500	Invitrogen, Karls-ruhe

Table 13: Secondary antibodies

c.-ads., cross-adsorbed.

2.2.6 Small interfering RNAs (siRNAs)

siRNA (QIAGEN, Hilden)	**Target sequence**
Control	**AATTCTCCGAACGTGTCACGT** Sense: UUCUCCGAACGUGUCACGUTT Antisense: ACGUGACACGUUCGGAGAATT
VAMP3	**AAGATTATTCTCCGTTTGTAA** Sense: GAUUAUUCUCCGUUUGUAATT Antisense: UUACAAACGGAGAAUAAUCTT
VAMP7	**CTCCTTGTAAATGATACACAA** Sense: CCUUGUAAAUGAUACACAATT Antisense: UUGUGUAUCAUUUACAAGGAG

Table 14: siRNAs

2.2.7 Plasmids

2.2.7.1 pRK5/CMV-Cre-ERT2 plasmid

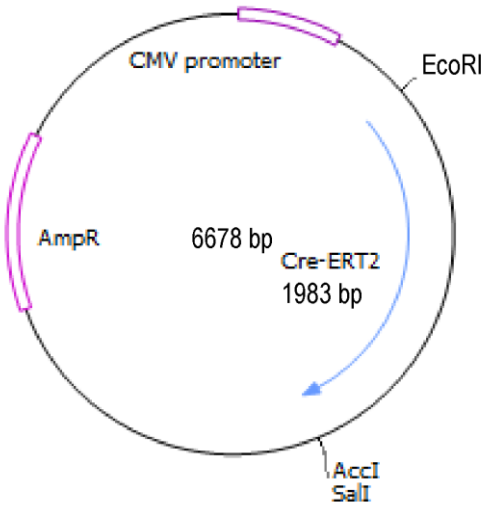

Figure 11: pRK5/CMV-Cre-ERT2 plasmid. The Cre-ERT2 sequence was isolated by PCR from a GFAP-Cre-ERT2 plasmid which was kindly provided by K.-A. Nave (Göttingen, Germany). Concomitantly, EcoRI and SalI restriction sites for the subsequent insertion into the pRK5 vector were added. AmpR, ampicillin resistance gene; CMV, cytomegalovirus.

2.2.7.2 pAM/CBA-Cre-ERT2 plasmid

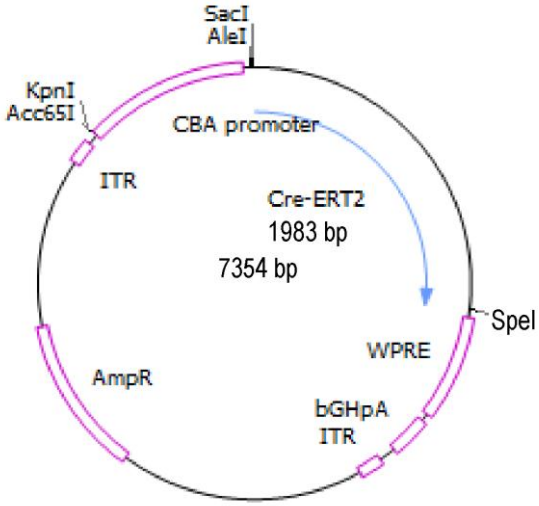

Figure 12: pAM/CBA-Cre-ERT2 plasmid. The Cre-ERT2 sequence was isolated by PCR from a GFAP-Cre-ERT2 plasmid which was kindly provided by K.-A. Nave (Göttingen, Germany). Concomitantly, SacI and SpeI restriction sites for the subsequent insertion into the pAM vector were added. AmpR, ampicillin resistance gene; CBA, chicken β actin; ITR, inverted terminal repeats; bGHpA, bovine growth hormone polyadenylation signal; WPRE, woodchuck hepatitis virus (WHP) posttranscriptional regulatory element.

2.2.7.3 pAM/MBP-Cre-ERT2 plasmid

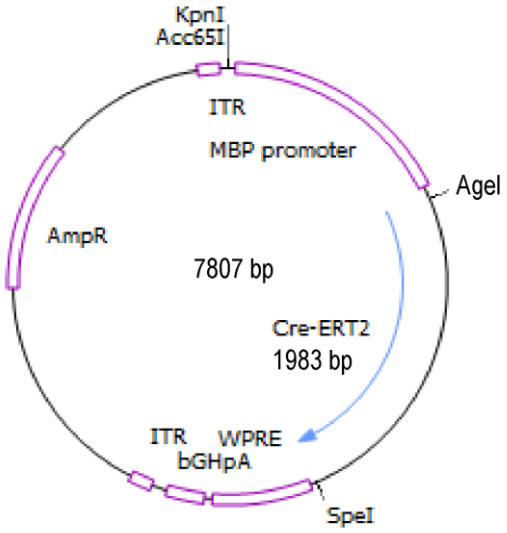

Figure 13: pAM/MBP-Cre-ERT2 plasmid. To obtain the MBP-Cre-ERT2 plasmid, first the CBA promoter was excised from the generated pAM/CBA-Cre-ERT2 plasmid using the restriction sites for KpnI and AleI. The MBP promoter sequence was excised from its original vector using the restriction sites for KpnI and AgeI. For proper ligation, the 5´ overhang was filled up using a Klenow fragment the 3´→5´ exonuclease activity of which has been inactivated. Finally, the MBP promoter sequence was inserted into the promoter-depleted pAM/CBA-Cre-ERT2 plasmid. AmpR, ampicillin resistance gene; MBP, myelin basic protein; ITR, inverted terminal repeats; bGHpA, bovine growth hormone polyadenylation signal; WPRE, woodchuck hepatitis virus (WHP) posttranscriptional regulatory element.

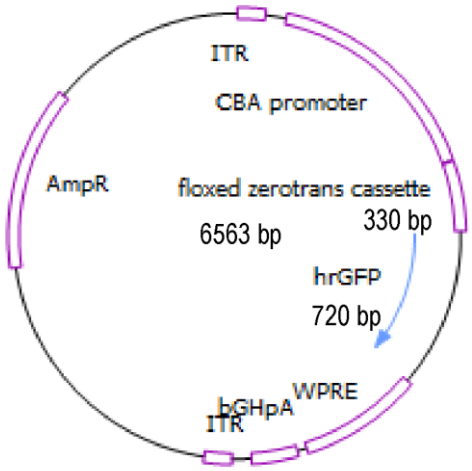

Figure 14: pAM/CBA-floxstop-hrGFP plasmid. This plasmid carries the coding sequence for hrGFP (**h**umanized **r**enilla **GFP**), preceded by a floxed zerotrans cassette which allows expression of hrGFP only in the presence of cre. HrGFP has been humanized by using codons preferred in highly expressed human genes. The plasmid kindly was provided by Beat Lutz (Mainz, Germany). AmpR, ampicillin resistance gene; CBA, chicken β actin; ITR, inverted terminal repeats; bGHpA, bovine growth hormone polyadenylation signal; WPRE, woodchuck hepatitis virus (WHP) posttranscriptional regulatory element.

2.3 Immunocytochemistry and imaging

Cells were washed twice in PBS and fixed in 4% PFA for 15 min. After washing in PBS cells were permeabilized for 2 min in 0,1% Triton X-100 in PBS and after another washing step in PBS they were blocked in PBS/10% HS for 30 min. First antibodies were diluted in blocking buffer and incubated for 45 min. After washing in PBS fluorophore-conjugated secondary antibodies diluted in PBS/10% HS were applied and incubated for 35 min. Finally, the cells were washed in PBS and mounted. Images were acquired with a fluorescence microscope or a confocal laser scanning microscope and were processed using the Photoshop and Illustrator software (Adobe).

2.4 Statistics

Statistical analysis was performed by application of the paired, two-tailed student´s t-test using the Excel software. Values were expressed in relation to control which was set to 100%.

2.5 Protein biochemistry

2.5.1 Cell lysates

Cells were washed twice in PBS and scraped into lysis buffer. After incubation for 30 min on a rotor the lysate was centrifuged at 350 g for 10 min to spin down the nuclei and the supernatant was collected. All steps were carried out at 4° C.

2.5.2 Bradford protein assay

The Bradford protein assay is a colorimetric method to determine the protein content of solutions. The dye Coomassie Brilliant Blue G-250 under acidic conditions forms complexes with aromatic and basic amino acids leading to a shift of the absorption maximum from 470 nm to 595 nm. Thus, the increase of absorption at 595 nm can be utilized as a measure for the protein content. For this purpose the photometer first has to be calibrated using protein solutions of known concentration. The samples were diluted and protein content was determined by means of the calibration curve. Samples and calibration solutions were incubated with the Bradford dye reagent concentrate for 10 min at RT before measurement. If the protein content of samples of small volumes had to be determined, a small scale Bradford protein assay was performed (mini Bradford protein assay). Therefore, calibration solutions of 25 µg/ml, 50 µg/ml, 100 µg/ml, 200 µg/ml, and 300 µg/ml BSA diluted in TBS were prepared and 10 µl of each calibration solution was mixed with 10 µl of 2 x dye reagent concentrate. 2 µl of the samples were

diluted with 8 µl TBS and mixed with 10 µl of 2 x dye reagent concentrate. Protein concentration was measured after an incubation time of 7 min at RT.

Concentration	BSA solution (0,5 mg/ml)	0,01% Triton-X 100	Dye reagent concentrate 5 x
0 µg/ml	0 µl	800 µl	200 µl
1 µg/ml	2 µl	798 µl	200 µl
5 µg/ml	10 µl	790 µl	200 µl
10 µg/ml	20 µl	780 µl	200 µl
15 µg/ml	30 µl	770 µl	200 µl
20 µg/ml	40 µl	760 µl	200 µl
25 µg/ml	50 µl	750 µl	200 µl

Table 15: Composition of calibration solutions

2.5.3 SDS-PAGE and western blotting

SDS-PAGE (**S**odium **D**odecyl **S**ulfate **P**oly**A**crylamide **G**el **E**lectrophoresis) is a technique to separate proteins according to their electrophoretic mobility, a function of molecular weight. Samples were prepared by adding 4 x sample buffer and cooked for 5 min at 95° C, if applicable. The anionic detergent SDS denatures secondary and tertiary structures and applies a negative charge to each protein in proportion to its mass, allowing a fractionation by size. Additionally, DTT (**D**i**T**hio**T**hreitol) reduces disulfide bonds and thus helps to further unfold the polypeptides. Electrophoresis was performed using 4%-12% Bis-Tris-gradient gels (NuPAGE, Invitrogen, Karlsruhe) or discontinuous gels according to the Lämmli-system. 6%-12% separation gels (tris-glycine buffer, pH 8,8) were covered over with 4% stacking gels (tris-glycine buffer, pH 6,8).

	Stacking gel 5 ml	separation gel (10 ml)			
	4%	6%	8%	10%	12%
H_2O	3,4 ml	5,3 ml	4,6 ml	4,0 ml	3,3 ml
acrylamide mix 30%	0,83 ml	2,0 ml	2,7 ml	3,3 ml	4,0 ml
Tris 1 M	0,63 ml	-------	-------	-------	-------
Tris 1,5 M	----------	2,5 ml	2,5 ml	2,5 ml	2,5 ml

SDS 10%	0,05 ml	0,1 ml	0,1 ml	0,1 ml	0,1 ml
ammonium persulfate 10%	0,05 ml	0,1 ml	0,1 ml	0,1 ml	0,1 ml
TEMED	5 µl	8 µl	6 µl	4 µl	4 µl

Table 16: Composition of stacking gel and separation gels

2.5.4 Immunoblotting

Separation of the protein solutions was followed by western blotting. Hereto an electrical field is applied and the proteins are transferred from the gel to a PVDF (**P**oly**V**inyl-i**D**ene **F**luoride) membrane in a wet blot chamber (Bio-Rad). The transfer required 2 h 10 min with a current of 300 mA.

To detect a specific protein, the PVDF membrane (Immobilon-P transfer membrane, 0,45 µm pore size, Millipore) first was blocked in 4% milk powder in PBST for 20 min at RT. The first antibody was incubated for 1 h at RT or at 4° C overnight. After washing three times for 15 min in PBST the secondary antibody coupled to HRP (**H**orse **R**adish **P**eroxidase) was applied and incubated for 45 min. After another washing step in PBST (3 x 15 min) the labeled proteins were detected using a self-made luminol-containing solution. HRP transforms the luminol which leads to light emission and is used for illumination of a radiographic film. The strength of the signal is proportional to the amount of detected protein and was quantified using the ImageJ software.

2.6 Molecular biology

2.6.1 Polymerase chain reaction

For the amplification of DNA sequences from plasmids the plasmid was mixed with the appropriate oligonucleotides (Sigma-Aldrich), Pfu polymerase, dNTPs and the corresponding buffer according to the manufacturer´s instructions. The DNA sequence was amplified in multiple rounds of melting, annealing and elongation of the DNA. The PCR product was loaded on an agarose gel (agarose 1% in TAE) to separate the different fragments of DNA.

2.6.2 Isolation of the PCR product

The band corresponding to the desired DNA sequence was excised and the DNA was isolated from the gel using the QIAquick PCR Purification Kit (QIAGEN) according to the manufacturer´s instructions.

2.6.3 Restriction enzyme digestion

The DNA was digested with the appropriate digestion enzymes and buffers according to the manufacturer´s instructions within 1-1½ h at 37° C. Thereafter, the enzymes were heat inactivated for 20 min at 65° C. The digested DNA was loaded on an agarose gel and the DNA fragment of interest was isolated. The plasmid, into which the DNA fragment should be inserted, was digested simultaneously with the same restriction enzymes and digestion was verified by separation on an agarose gel. In this connection, also the DNA quantity of both the plasmid and the eventual insert was determined.

2.6.4 Dephosphorylation of the plasmid

To prevent self-ligation of the digested plasmid the plasmid was dephosphorylated prior to ligation. The plasmid was mixed with phosphatase and the corresponding buffer according to the manufacturer´s instructions and incubated for 15 min at 37° C. The phosphatase was heat inactivated for 5 min at 65°C.

2.6.5 Ligation

The digested plasmid and the DNA fragment to be inserted were mixed, and the ligase and the corresponding buffer were added according to the manufacturer´s instructions. The DNA fragment was added in excess to increase the probability of its insertion. Ligation took place overnight at 4° C.

2.6.6 Transformation

The ligation product was used to transform chemical competent E. coli (TOP10F). Hereto, the bacteria were mixed with the DNA and kept on ice for ½ h. After giving a heat shock for 1 min at 42° C, 1 ml LB medium was added to the suspension and incubated for ½ h at 37° C. Transformed bacteria were selected by plating them on LB-agar containing the appropriate antibiotic. The next day multiple colonies were used to inoculate LB medium. After reproduction overnight, the bacteria were pelleted and DNA was isolated using a Miniprep Kit (QIAGEN). The DNA was analyzed by restriction enzyme digestion. DNA with the appropriate restriction patterns was sequenced to exclude point mutations.

The bacteria carrying the desired plasmid were used to inoculate LB medium for isolation of plasmid DNA on a large scale. After reproduction overnight, bacteria were pelleted and plasmid DNA was isolated using a Maxiprep Kit (QIAGEN). A small amount of the cell suspension was mixed with glycerol at a ratio of 4:1 and stored at -80° C for later applications.

2.7 Cell culture and transfections

2.7.1 Preparation of primary cortical neurons

Primary cortical neurons were obtained from E15 C57/Bl6-N mouse brains according to a modified protocol by (Hoogenraad, *et al.*, 2010). Brains were extracted from the skull and after removal of the meninges the cortices were incubated in HBSS/1% trypsin for 4-6 min. After washing in $HBSS^+$, the brains were dissociated in HBSS/0,05% DNase using fire polished Pasteur pipettes to obtain a single-cell suspension. After two washing steps in $HBSS^+$, cells were seeded on PLL-coated dishes in Neurobasal plating medium at a density of 35-55 x 10^3 cells/cm^2. The glutamate contained in the medium was shown to promote the survival of neurons and the proliferation of neuronal precursor cells (Suzuki, *et al.*, 2006). Primary cortical neurons could be cultured up to 3 weeks. Half of the medium was renewed every 3-4 days with Neurobasal feeding medium without glutamate. Cells were kept at 37° C, 95% humidity and 8 % CO_2.

2.7.2 Preparation of oligodendroglial precursor cells

2.7.2.1 Preparation of mouse brains

Primary mouse cultures of oligodendrocytes were prepared as described previously (Kramer, *et al.*, 1997). Brains of E14-16 C57/Bl6-N mice were extracted from the skull and after removal of the meninges incubated in HBSS/1% trypsin for 4-6 min. After washing in $HBSS^+$, the brains were dissociated in HBSS/0,05% DNase using fire-polished Pasteur pipettes to obtain a single-cell suspension. After washing two times in $HBSS^+$ including two centrifugation steps at 130 g and 4° C, cells were seeded onto PLL-coated culture flasks in cold DMEM/10 % HS at a density of 3-3,5 x 10^6 cells/cm^2.

2.7.2.2 Neuron kill and removal of microglia

Five days after preparation, the neurons were removed from the mixed cultures by a complement-mediated immunocytolysis. Cells were incubated for 1 h at 37° C with the M5 antibody (diluted 1:15, clone 358) and guinea pig complement. The killed neurons were washed off in DMEM/10% HS at 37°C and cells were further cultivated in DMEM/10% HS containing 0,5 µg insulin/ml. Half of the medium was renewed at day 7. At day 11, microglial cells sitting on top were removed by gently swirling the flasks and changing the medium.

2.7.2.3 Oligodendrocyte shake off

Two weeks after preparation of the mixed culture a dense astrocyte monolayer has been formed. After removal of remaining microglial cells, OPCs (**O**ligodendroglial **P**recursor **C**ells) sitting on top of the monolayer could be shaken off. OPCs were centrifuged at

130 g and 4° C for 10 min and seeded onto PLL-coated culture dishes or coverslips in B27-supplemented SATO medium containing PDGF and FGF (**P**latelet-**D**erived **G**rowth **F**actor and **F**ibroblast **G**rowth **F**actor, 10 ng/ml and 5 ng/ml, respectively). Cells were cultured at 37° C, 95% humidity and 8% CO_2.

2.7.3 Preparation of neuron-oligodendrocyte cocultures

We prepared primary cortical neurons and cultured them for 6-8 days. The Neurobasal medium was removed and OPCs were added directly after shake-off from the astrocyte monolayer. The neurons were plated at a density of 35-55 x 10^3 cells/cm^2 and OPCs were added resulting in a ratio of 1:2 between neurons and OPCs. The OPCs were added in SATO/B27 medium which is suitable for coculturing neurons together with oligodendrocytes. Half of the medium was renewed every 3-4 d. The cocultures could be cultured for up to 3 weeks.

2.7.4 The oligodendroglial cell lines Oli-*neu* and Oli-*neu* PLP-eGFP

The cell line Oli-*neu* was obtained by immortalization of murine primary oligodendroglial precursor cells via transfer of the oncogene t-*neu* (Jung, *et al.*, 1995). The cell line Oli-*neu* PLP-eGFP stably expresses the fusion protein PLP-eGFP, in which eGFP is linked C-terminally to PLP. PLP-eGFP was brought into the peGFP-N1 expression vector using the restriction sites EcoRI and NotI. To receive a stable cell line, Oli-*neu* cells were cotransfected with the expression vectors pPLP-eGFP-N1 and pMSCV-hygro and selected for hygromycin resistance. The cell line Oli-*neu* PLP-eGFP was kindly provided by K.-A. Nave (Göttingen, Germany) (Trajkovic, *et al.*, 2006). Oli-*neu* and Oli-*neu* PLP-eGFP cells were cultured in SATO medium at 37° C, 95% humidity and 8% CO_2. Oli-*neu* cells can be treated with DBcAMP (**D**i**B**utyryl **c**yclic **A**denosine **M**ono**P**hosphate, 1 mM) to prevent further proliferation and induce differentiation.

2.7.5 Passaging, freezing and thawing

2.7.5.1 Thawing

Frozen cells were thawed and immediately resuspended in cold SATO medium to avoid cell damage caused by the DMSO which is present in the cryoprotective medium. They were pelleted by centrifuging at 130 g and 4°C for 10 min. After resuspending they were seeded onto culture dishes in warm (37°C) SATO medium.

2.7.5.2 Passaging

Cell lines regularly were passaged when reaching confluency. Cells were detached by incubating in trypsin/EDTA. Proteolysis was stopped by adding PBS/10% HS and cells

were centrifuged for 10 min at 130 g and 4°C. The cell pellet was resuspended in SATO medium, split, and fractions were seeded onto PLL-coated culture dishes.

2.7.5.3 Freezing

Cells were frozen in cryoprotective medium. Hereto, they were detached by incubating in trypsin/EDTA and proteolysis was stopped by adding PBS/10% HS. Cells were spun down at 130 g and 4°C for 10 min, resuspended in cryoprotective medium and after freezing at -80°C transferred to liquid nitrogen.

2.7.6 Transient transfection of plasmids

Plasmids were introduced into the cell line Oli-*neu* by electroporation. 1 x 10^6 Oli-*neu* cells were resuspended in SATO medium and mixed with 10-20 µg DNA in an electroporation cuvette. By omitting an electric shock (220V and 950 µF), the cell membranes are permeabilized and DNA is able to enter the cell. After incubation for 5 min at RT the Oli-*neu* cells were seeded onto culture dishes or coverslips in SATO medium. 3-4 h after transfection the medium was renewed and DBcAMP and sodium butyrate were added, if applicable.

2.7.7 AMAXA siRNA transfection of OPCs

OPCs were siRNA-transfected directly after shake-off from the astrocyte monolayer using the AMAXA Basic Nucleofector Kit for primary neurons (Lonza) according to the manufacturer´s instructions. 4 x 10^6 OPCs were resuspended in 100 µl nucleofector solution, mixed with 160 pmol of siRNA in an electroporation cuvette and nucleofected using the AMAXA nucleofector II (program O-005). The cells were seeded onto PLL-coated culture vessels in B27-supplemented SATO medium. 4 h after nucleofection the medium was exchanged for B27-supplemented SATO medium containing PDGF and FGF (10 ng/ml and 5 ng/ml, respectively).

2.8 In-cell multiplex detection assay

SiRNA-transfected OPCs were seeded onto PLL-coated 6 well-plates (4 x 10^6 transfected OPCs/well) and cultured for 3-4 days. Living cells were washed in PBS and incubated with undiluted antibody O10 (surface PLP, recognizing an extracellular epitope) for 45 min. After washing in PBS, the cells were fixed for 30 min in 4% PFA. Cells again were rinsed in PBS and permeabilized in 0,1% Triton X-100 for 2 min. After washing the wells in PBS, cells were blocked in PBS/10 % HS and the antibody aa3 (total PLP, recognizing an intracellular epitope) diluted 1:20 in blocking buffer was applied and incubated for 45 min. Afterwards cells were washed in 0,1 % Tween-20 in PBS. Secondary antibodies (anti-mouse IRDye 800 recognizing O10 and anti-rat Alexa Fluor-

488 recognizing aa3) were diluted in 0,2% Tween-20 in blocking buffer and incubated for 1 h. After washing in 0,1% Tween-20 in PBS, epifluorescence was scanned using the Odyssey Imager (LI-COR). All steps were carried out at RT. Background values obtained from cells only incubated with secondary antibodies were subtracted and relative surface levels of PLP were determined by normalizing epifluorescence of surface PLP to that of total PLP.

2.9 Membrane fractionation of neuron-oligodendrocyte cocultures

Primary cortical neurons were cultured for one week before seeding siRNA-transfected OPCs on top. In each case, 4 x 10^6 siRNA-transfected OPCs were added to 1 x 10^6 neurons. The medium was switched to SATO/B27 when the oligodendrocytes were added. Cells were cocultured for 5 days to allow axon-glia interaction and formation of myelin-like membranes (MLM). Membranes were isolated by scraping the cells into homogenizing buffer followed by traversing through a 22 g syringe. Nuclei were pelleted by two consecutive 10 min centrifugation steps at 1000 g and membranes were obtained from the resulting supernatant by centrifuging for 10 min at 20.000 g. The membrane pellet was resuspended in 200 µl 0,32 M sucrose in TBS/1 mM PMSF and subjected to a discontinuous gradient of 0,8 M and 0,62 M sucrose in TBS/1 mM PMSF. After centrifugation for 1 ½ h at 75.000 g, fractions of 0,5 ml were harvested from the top. Three fractions were obtained containing light (0,32 M/0,62 M interface), medium (0,62 M/0,8 M interface) and heavy membranes (pellet). The light fraction contains the myelinlike membranes (MLM), which are specifically enriched in myelin proteins and lipids, whereas the medium and the heavy fraction contain the higher density membranes of noncompacted myelin and axon-glia junctions (Figure 15) (Rios, *et al.*, 2000, Winterstein, *et al.*, 2008).

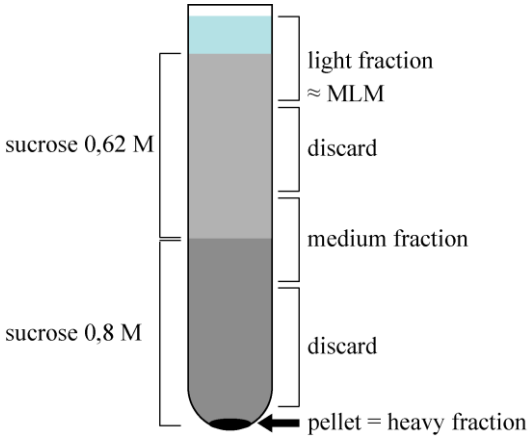

Figure 15: Membrane fractionation of neuron-oligodendrocyte cocultures. After centrifugation at 20.000 g the membrane pellet was resuspended in 0,32 M sucrose in TBS and subjected to a discontinuous gradient of 0,8/0,62 M sucrose in TBS. After centrifugation for 1½ h at 75.000 g, fractions of 0,5 ml

were harvested from the top. Three fractions were obtained containing light, medium and heavy membranes. The light fraction was collected at the 0,32 M/0,62 M interface, the medium fraction at the 0,62 M/0,8 M interface and the heavy fraction was represented by the pellet.

The fractions were pelleted by centrifuging for 1 h at 100.000 g and resuspended in equal amounts of RIPA buffer. All steps were carried out at 4°C. Equal volumes of the fractions were analyzed by SDS-PAGE and western blotting. Western blots of PLP were subjected to densitometric quantification using the ImageJ software and relative amounts of MLM in the cultures were calculated by assessing the ratio of the values obtained from the light fractions and the sum of medium and heavy fractions.

2.10 The Cre-loxP-system

The cre recombinase (shortly named cre) is a type I topoisomerase from the P1 bacteriophage (Abremski, *et al.*, 1986). It catalyzes site-specific recombination of DNA between two loxP (locus of crossover [x] in P1) sites. The loxP recognition element is a 34-base pair sequence composed of two 13 base pair repeats flanking an 8 base pair spacer region. The spacer region determines directionality. The type of recombination depends on the orientation of the loxP sites in relation to each other. If the loxP sites have an opposite orientation, the DNA inbetween will be inverted, which is a reversible process. If the loxP sites are in the same orientation, the DNA inbetween will be excised as a circular molecule, which is an irreversible reaction. Thus, cre can serve to delete a sequence of DNA which is flanked by loxP sites (floxed). The cell-specific expression of cre in cells carrying a reporter gene located downstream of a floxed stop cassette will result in cell-specific expression of the reporter, which can be β-galactosidase or a fluorescent protein. A modification of cre allows not only a cell-specific but also a temporally controlled expression of the reporter. Steroid receptors were shown to convey ligand-dependent regulation to proteins which they are fused to. Cre-ERT2 (**Cre** recombinase-**E**strogen **R**eceptor **T**amoxifen-inducible **2)** is a fusion protein of cre and the mutated form of the ligand-binding domain of the human estrogen receptor, called ERT2. ERT2 carries 3 mutations when compared to the human estrogen receptor α isoform 1. These result in exchange of 3 amino acids located in the ligand binding domain of the receptor (G400V, M543A and L544A). Due to the mutations, the synthetic estrogen-like agonist tamoxifen is able to bind to cre-ERT2 and activate cre, whereas binding of the natural ligand of the receptor, 17β-estradiol, is prevented. In cells, Cre-ERT2 is associated with a complex containing HSP90. Binding of tamoxifen causes a conformational change in the receptor and allows nuclear entry of cre-ERT2 by disrupting the interactions with the HSP90 complex (Figure 16) (Huang, *et al.*, 2010). Intraperitoneal injection of tamoxifen into mice or its application to cells thus allows a temporally controlled activation of cre. 4-OHT (4-hydroxytamoxifen) has been modified to facilitate access to cells (Feil, *et al.*, 1997, Metzger & Chambon, 2001, Zhao, *et al.*, 2006). In our studies,

we utilized a reporter strain in which the gene for RFP is under control of the ROSA26 promoter (Luche, *et al.*, 2007). The ROSA26 locus was shown to be expressed ubiquitously during embryonic development and in adult mice. It is believed to encode three transcripts of unknown function. Mice in which two of the three transcripts were disrupted showed no phenotype, making the ROSA26 locus a suitable site for reporter gene targeting (Friedrich & Soriano, 1991, Zambrowicz, *et al.*, 1997).

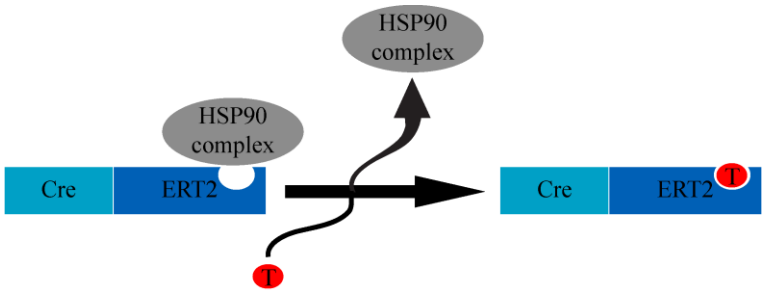

Figure 16: Ligand-dependent activation of cre-ERT2. Cre-ERT2 is a chimeric protein consisting of cre recombinase derived from the bacteriophage P1 and the mutated ligand-binding domain of the human estrogen receptor called ERT2. In absence of tamoxifen, cre-ERT2 is inactivated by binding of the HSP90 complex. Binding of tamoxifen (T) to ERT2 dissociates the HSP90 complex and allows nuclear entry of cre-ERT2.

2.11 Isolation of exosomes – fractionation of culture supernatants

To isolate exosomes, the supernatants of the cell lines Oli-*neu*, Oli-*neu* PLP-eGFP or of primary oligodendroglial cells were collected and subjected to several centrifugation steps (Figure 17). Exosomes can be isolated from cell culture supernatants by differential ultracentrifugation. In the first steps dead cells and cell debris are eliminated. Exosomes are pelleted from the resulting supernatant at 100.000 g and can be further purified by loading the pellet on a continuous sucrose gradient. Oligodendroglial exosomes can be found at a density of 1,10-1,14 g/ml. By comparison, vesicles from the endoplasmic reticulum float at 1,18-1,25 g/ml and those from the Golgi at 1,05-1,12 g/ml (Thery, *et al.*, 2006). First, the supernatants were centrifuged for 10 min at 130 g and for 20 min at 10.000 g to get rid of dead cells and cell debris, respectively. The supernatant was centrifuged for 1 h at 100.000 g. The pellet contains the exosomes (crude exosome preparation). Exosomes also can be further purified by an additional centrifugation step. Hereto, the exosomes are pelleted onto a sucrose pad (1,8 M in TBS) and the pellet is loaded onto a continuous sucrose gradient. The gradient was obtained by overlaying 1,8 M sucrose with 0,3 M sucrose and was built up within 1 h by diffusion. After centrifugation for 4 h or overnight at 100.000 g, 12 fractions were collected. The density of each fraction was determined using a refractometer. Finally, the membrane particles contained in the fractions were pelleted by centrifuging for 1 h at 100.000 g. Due to

their characteristic density (1,10-1,14 g/ml), oligodendroglial exosomes can be found in fractions 6-8. All steps were carried out at 4° C.

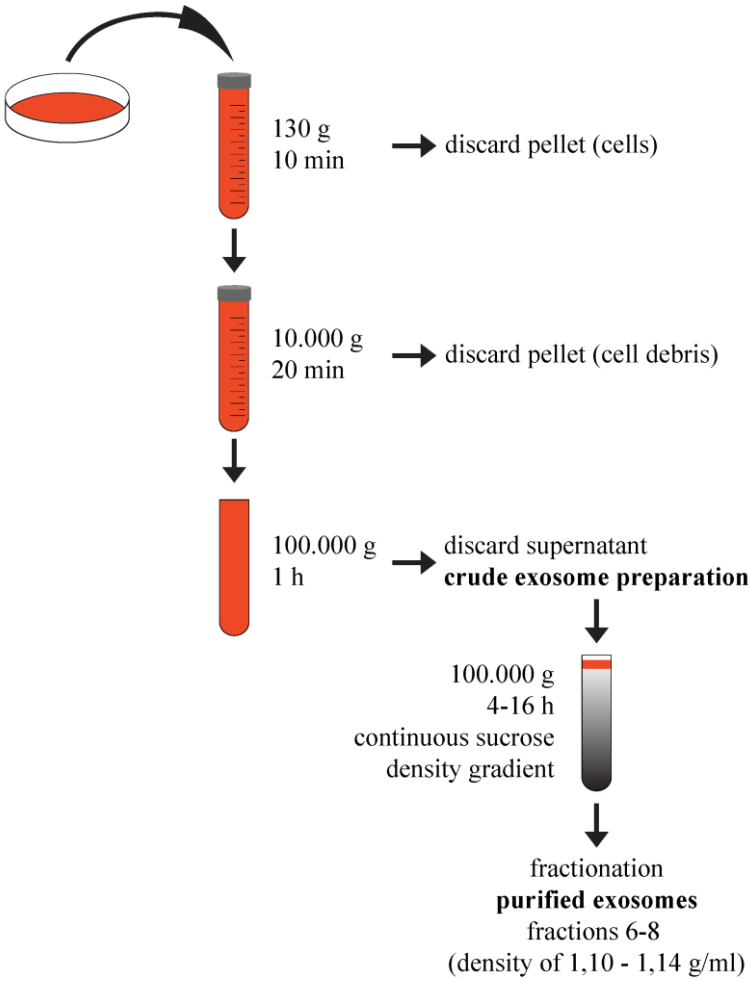

Figure 17: Flow chart for the exosome purification procedure. Culture supernatants of primary oligodendrocytes or of oligodendroglial cell lines were centrifuged for 10 min at 130 g. The supernatant was centrifuged at 10.000 g for 20 min. The resulting supernatant was centrifuged for 1 h at 100.000 g. The pellet contains the exosomes (crude exosome preparation). The exosomes can be further purified by sucrose density gradient centrifugation. Oligodendroglial exosomes due to their characteristic density of 1,10 - 1,14 g/ml can be recovered from fractions 6-8 of 12 (purified exosomes). All steps were carried out at 4° C.

2.12 Quantification of exosome release upon siRNA-mediated silencing of VAMP7

OPCs were siRNA-transfected and cultured for 3-4 days. Exosome release was stimulated by application of glutamate to study the role of VAMP7 in regulated exocytosis of MVBs. The medium was exchanged to fresh SATO/B27 medium containing glutamate (100 µM) and the supernatants were collected after 4 h of exosome release. The exosomes present in the supernatants were pelleted and analyzed by SDS-PAGE and western blotting, together with the corresponding lysates. Antibodies directed against PLP

(aa3) were used as a marker for oligodendroglial exosomes. The western blot signals were subjected to densitometric quantification and the values for PLP associated with exosomes were normalized to total expression of PLP obtained from the corresponding lysates.

2.13 MTT assay

The MTT assays were performed according to a modified protocol after (Behl, *et al.*, 1994). The yellow tetrazole MTT (3-(4,5-Di**M**ethyl**T**hiazol-2-yl)-2,5-diphenyl**T**etrazolium bromide) is reduced to purple formazan in living cells due to activity of mitochondrial dehydrogenases. The insoluble formazan product can be dissolved by addition of a solubilization solution leading to a yellow solution with a single absorption maximum at 570 nm. Therefore, the amount of transformed MTT serves as a measure for the metabolic activity of cells. To study the influence of oligodendroglial exosomes on neuronal metabolism, two different approaches were used. First, primary cortical neurons were incubated with supernatants of cultured primary oligodendrocytes. The oligodendrocytes were cocultured with primary cortical neurons utilizing the transwell system to stimulate oligodendroglial exosome release by glutamate released into the culture medium by the neurons. Primary cortical neurons obtained from an independent preparation were cultured in transwell plates for 7 d and 14 d, respectively, before they were incubated with oligodendroglial supernatants deprived of exosomes by 100.000 g centrifugation or exosome-containing supernatants. MTT assays were performed after 2 d of incubation. In the second approach, we utilized the transwell system to achieve a constant supply with oligodendroglial exosomes. Primary cortical neurons were cultured for 7 d and 14 d, respectively, before adding inserts carrying primary oligodendrocytes cultured for 5-8 d before (Figure 18). When the inserts were added the medium of both, the neurons and the oligodendrocytes, was exchanged to fresh SATO/B27 medium. The inserts exhibit pores, allowing factors smaller than 1 µm to pass. Exosomes as well as soluble factors released by the oligodendrocytes can pass the membrane and enter the bottom chamber, where they can be received by the neurons. The added oligodendrocytes were treated with glutamate (100 µM) to stimulate exosome release or with GW4869 (5 µM), an inhibitor of the neutral sphingomyelinase, to block it. The enzyme neutral sphingomyelinase is required for the transformation of the lipid sphingomyelin to ceramide and its inhibition by GW4869 was shown to block exosome release (Frühbeis, *et al.*, 2011). In the MTT assays using neurons after 7 DIV, glutamate was added each day to the oligodendrocytes, starting with the day of coculture. In case of neurons cultured for 14 DIV, glutamate was added only once on the first day of coculture. GW4869 was added once on the first day of coculture. Neurons and oligodendrocytes were cocultured for different time periods before the neurons were incubated with phenol red-free SATO/B27 medium containing 0,5 mg/ml MTT for 2 h.

The same volume of solubilization solution was added and incubated overnight to allow complete dissolution of the MTT precipitate. Finally, absorption at 570 nm was measured in a spectrophotometer.

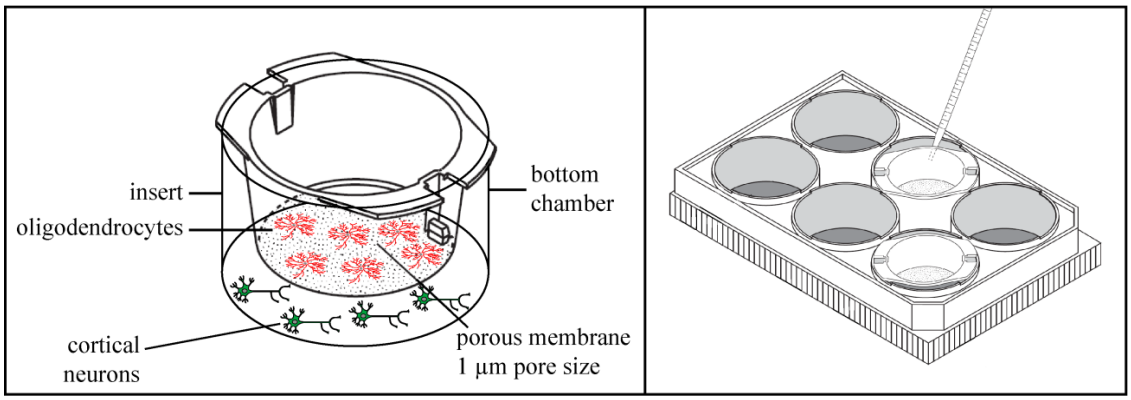

Figure 18: Cocultures of neurons and oligodendrocytes utilizing Boyden chambers. Oligodendrocytes were grown in inserts on a porous membrane with pores of 1 µm in diameter. These pores allow exosomes as well as soluble substances to pass and enter the bottom chamber, where they can be received by primary cortical neurons. **Left**, Design of the Boyden chamber. **Right**, transwell plate providing six bottom chambers.

2.14 Analysis of the phosphorylation state of the neurofilament heavy subunit

To analyze the phosphorylation levels of the heavy subunit of NFs upon influence of oligodendroglial exosomes, two different approaches were utilized. In the first approach we used isolated exosomes of the oligodendroglial cell line Oli-*neu* PLP-eGFP. Exosomes of the supernatants of 40 x 15 cm-culture dishes were collected using differential centrifugation and united. The protein content was determined by a mini Bradford protein assay (chapter 2.5.2.) Primary cortical neurons (7 DIV) were incubated for 3 h with exosomes containing 4,6 µg protein and lysed. In the second approach we utilized the transwell system. Primary cortical neurons were cultured in transwell plates before adding inserts carrying primary oligodendrocytes which previously have been cultured for 5 d before (Figure 18). Neurons and oligodendrocytes were cocultured for 2 d and 4 d, respectively, before preparing neuronal lysates (11 DIV). Lysates were prepared by scraping the cells into RIPA buffer containing protease and phosphatase inhibitors. After incubation for ½ h on a rotor the lysate was centrifuged for 10 min at 13.000 g and the supernatant was collected. All steps were carried out at 4° C. The lysates were analyzed by SDS-PAGE and western blotting. Western blots using antibodies recognizing the phosphorylated form of the heavy subunit of NFs (antibody SMI31) were subjected to densitometric quantification using the ImageJ software and were normalized either to signals for neuron-specific γ-enolase or for the medium subunit of NFs (antibody RMO44).

2.15 Phospho-MAPK array

We aimed to identify kinases that could be activated in neurons upon influence of oligodendroglial exosomes. Therefore, primary cortical neurons were cultured for 5 days in transwell plates before adding primary oligodendrocytes that have been cultured for 5 days before. Cells were cocultured for 3 days before preparing neuronal lysates. Control cells were cultured in the absence of oligodendrocytes. The protein content of the lysates was determined utilizing a Bradford protein assay. 200 µg of protein were used for the phospho-MAPK (**M**itogen-**A**ctivated **P**rotein **K**inase) array while 30 µg were analyzed by SDS-PAGE and western blotting. The phospho-MAPK array was performed using the kit from R&D systems according to the manufacturer´s instructions. The signals were subjected to densitometric quantification using the ImageJ software.

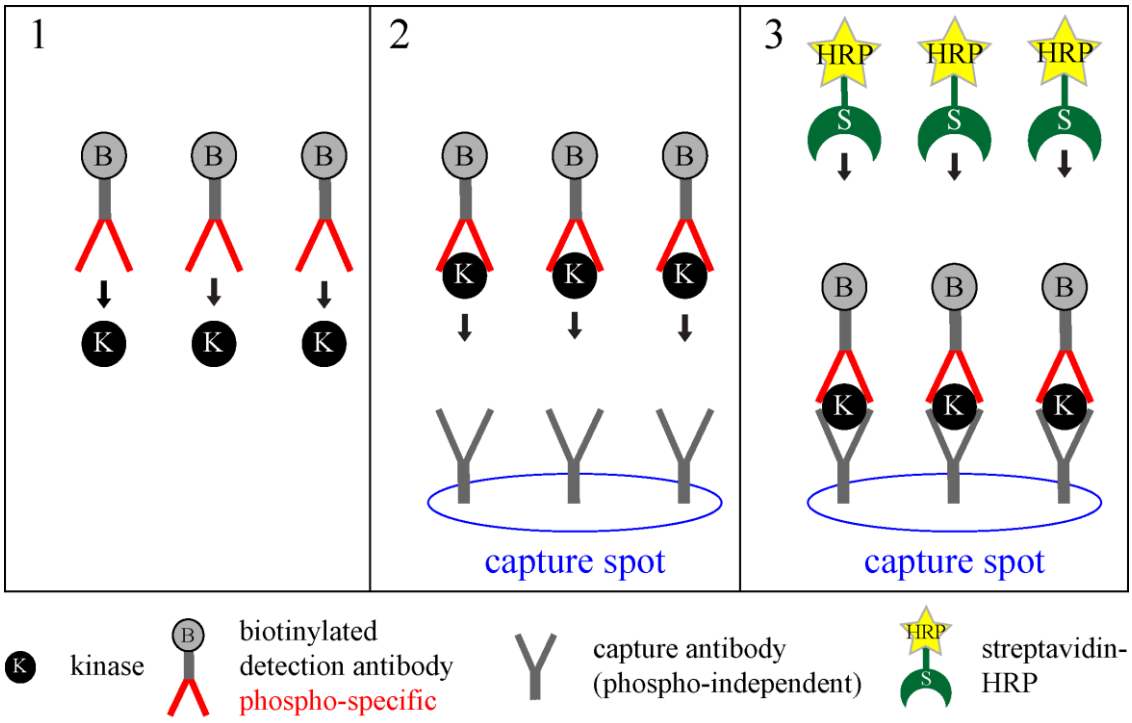

Figure 19: Principle of the assay. 1, Biotinylated detection antibodies (B, coupled biotin) are mixed with the lysate and bind to the kinases (K). The biotinylated detection antibodies are phospho-specific and recognize distinct phosphorylation sites of the corresponding kinases. **2**, The capture antibodies are spotted on a nitrocellulose membrane and recognize the kinases, regardless of whether they are phosphorylated or not, thereby linking them to the nitrocellulose membrane. **3**, Streptavidin-HRP binds to biotin and chemiluminescent detection reagents are applied to produce a signal at each capture spot corresponding to the amount of phosphorylated kinases bound.

3 Results

3.1 Establishment of neuron-oligodendrocyte cocultures

A major goal of this thesis was to initially establish a neuron-oligodendrocyte coculture system that allows analysis of the cellular basis of myelin formation *in vitro*. The most frequently utilized system in the field includes DRGs (**D**orsal **R**oot **G**anglion cells) and oligodendrocytes which does not reflect a realistic *in vivo* partnership. We thus chose to establish a myelinating culture system involving cortical neurons and oligodendrocytes. The precedent establishment of cortical neuronal cultures was a prerequisite.

3.1.1 Characterization of the neuronal cultures

The time course of neuronal differentiation was analyzed and the optimal time point of coculture was determined.

3.1.1.1 Coating and plating density

The optimal conditions for the primary cortical neurons were determined by varying coating of the culture dishes and coverslips as well as plating densities.

Neurons grown on coverslips sometimes built big neurospheres indicating an insufficient attachment of the cells to the underlying surface. We tried to improve the surface properties by using laminin for coating. Coverslips either were coated first with PLL and thereafter with laminin at concentrations of 2 µg/ml or 10 µg/ml or with laminin alone (at the same concentrations). But attachment of the cells could not be improved by laminin-coating.

To determine the optimal plating densities for the neuronal cultures, cells were plated in different densities. Cell suspensions were either directly applied to coverslips or the whole culture dish containing coverslips was flooded. The second variant turned out to be more suitable, resulting in a more even distribution of the cells. We tested plating densities of 1 x 10^6, 1,5 x 10^6, 2 x 10^6, 3 x 10^6 and 4 x 10^6 cells per 6 cm culture dish. We determined 1,5 x 10^6 - 2 x 10^6 cells (corresponding to 55.000 – 70.000 cells/cm^2) as the best concerning evenness of distribution and degree of neurite outgrowth. For 24 well plates and 96 well plates the optimal densities were determined to be 80.000 neurons/well and 10.000 neurons/well, respectively (corresponding to 45.000 cells/cm^2 and 35.000 cells/cm^2). We found that also an appropriate plating density could improve the attachment of the cells to the underlying surface.

3.1.1.2 Purity and expression of marker proteins

Cortical neurons were prepared from E15 mice and cultured for 3 d, 5 d, 7 d, 14 d and 21 d, respectively. Neuronal cultures were analyzed by immuno-stainings (Figure 20) and SDS-PAGE and western blotting of cell lysates (Figure 21).

NeuN (**Neu**ronal **N**uclei) is a neuron-specific nuclear protein which can be detected when neurons leave the cell cycle and/or initiate terminal differentiation and therefore was suggested to be important for the determination of the neuronal phenotype. Recently, it was identified as the splicing factor Fox-3 and as such could be a regulator of neural cell differentiation and development of the nervous system (Mullen, *et al.*, 1992, Kim, *et al.*, 2009). NeuN demonstrates the relative purity of the neuronal cultures until 7 DIV as nearly all cells show expression of NeuN (Figure 20 A-F). It is still weak after 3 DIV but constantly increases thereafter. GFAP serves as a marker for astrocytes whereas Olig2 labels OPCs as well as motor neurons. After 14 DIV astrocytes expanded in the culture and also Olig2-positive cells were observed (Figure 20 G, H). After 21 DIV we could see large areas of astrocytes spanning a few hundred µm. In these areas neurons were present in lower numbers (Figure 20 I). Olig2 was originally intended to be used as a marker for the oligodendroglial lineage but it also labels motor neurons. Olig2-positive cells arise after 14 DIV and their number further increases thereafter. Some of them are also NeuN-positive, indicating that they might be neurons. Cells expressing only Olig2 might be neurons, too, which have not turned on expression of NeuN yet or OPCs (Figure 20 J). In general, the cultures show increasing neurite extension with days in culture. Western blot analysis showed that the expression levels of oligodendroglial CNP and GFAP rise after 14 DIV which confirms the findings of the immuno-stainings and indicates the increased emergence of glial cells in the cultures (Figure 21). L1 belongs to the immunoglobulin superfamily. It is expressed on axons of the CNS and PNS. L1 is believed to be involved in axonal fasciculation and the initiation of myelination (Martini, 1994). In the CNS, L1 is diffusely expressed on non-myelinated axons but is downregulated with the onset of myelination. In the PNS, L1 additionally is expressed on Schwann cells, but is downregulated when they have made ca. 1½ turns around the axon. It remains expressed on non-myelinating Schwann cells and axons. Thus, L1 was suggested to play a positive role in the early stages of myelination. Later on, with F3/contactin one oligodendroglial partner for L1 was identified. It was found that the binding of L1 to F3/contactin activates Fyn kinase and this finally leads to localized synthesis of MBP protein from the MBP mRNA at the axon-glial contact site (Martini, 1994, Coman, *et al.*, 2005, White, *et al.*, 2008). PSD-95 is a specialized scaffold protein forming the backbone of the postsynaptic protein complex. The function of this extremely large disk-shaped complex appears to be the anchorage and organization of postsynaptic neurotransmitter receptors and corresponding signaling molecules at the active zone (Dosemeci, *et al.*, 2007).

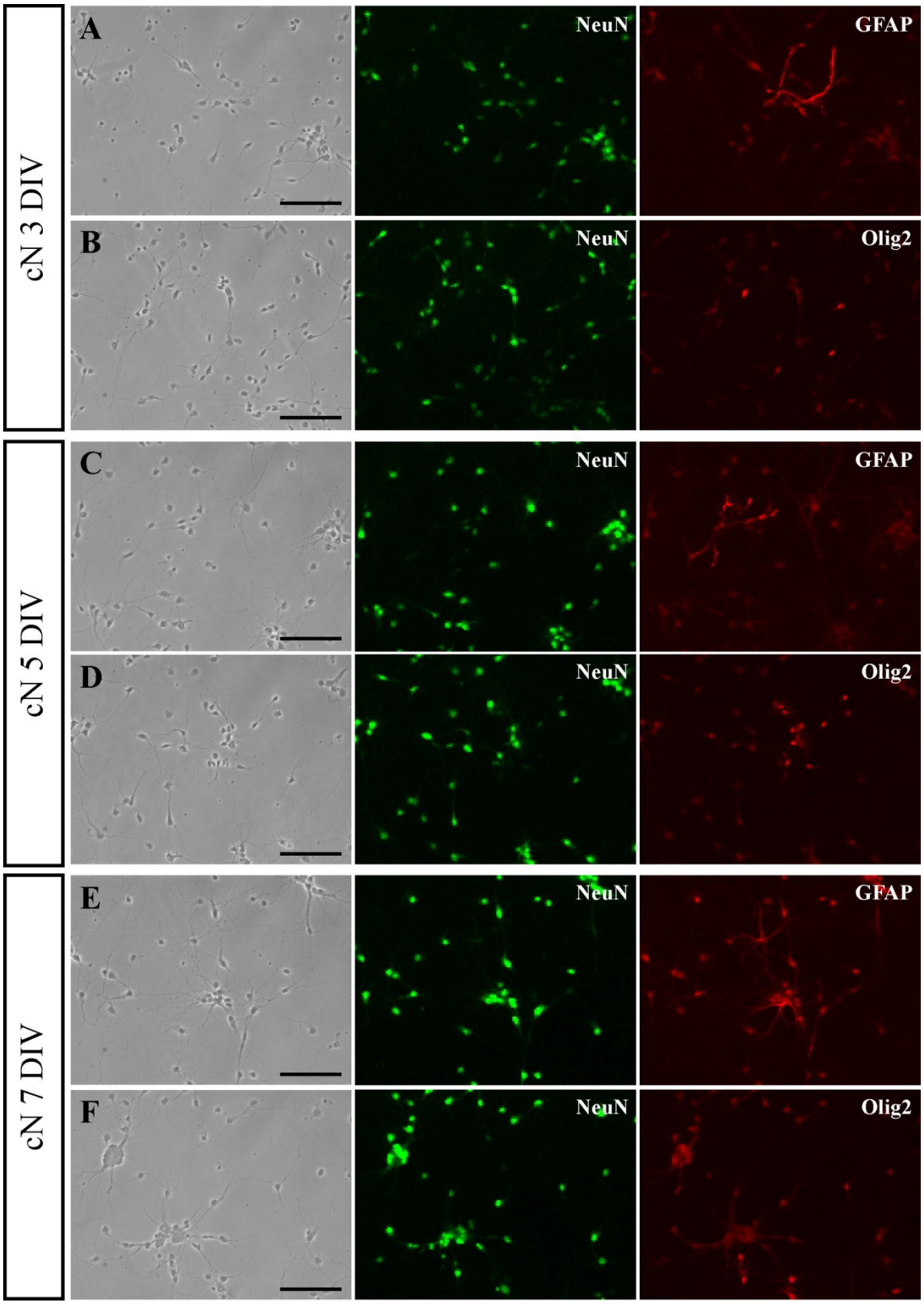
cN 3 DIV
A
NeuN
GFAP
B
NeuN
Olig2
cN 5 DIV
C
NeuN
GFAP
D
NeuN
Olig2
cN 7 DIV
E
NeuN
GFAP
F
NeuN
Olig2

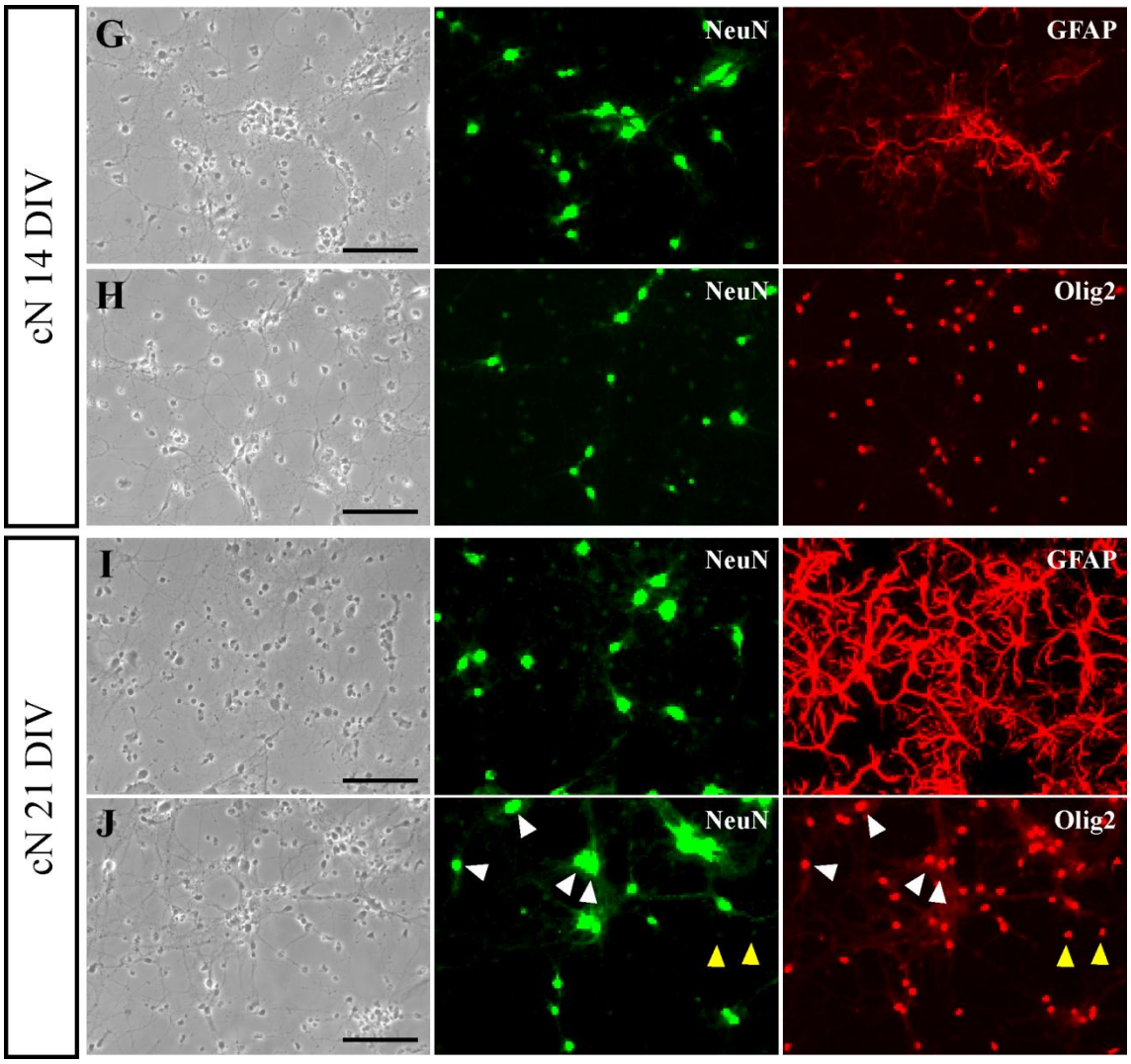

Figure 20: Characterization of cortical neuronal cultures by immunocytochemical analysis. Neurons were prepared from E15 mouse cortices and cultured for 3 d, 5 d, 7 d, 14 d and 21 d, respectively. Cultures were analyzed by immuno-staining using antibodies directed against NeuN as neuronal and GFAP as astrocytic markers. Olig2 was originally intended to label oligodendrocytes. The cells were recorded with same instrumental settings to ensure comparability. The neuronal marker NeuN demonstrates the relative purity of the neuronal cultures as nearly all cells are labeled until 7 DIV. Only few cells show GFAP expression, demonstrating that only a small percentage of the cells are astrocytes (A-F). After 14 DIV small areas of proliferating astrocytes with diameters of approximately 300 µm were observed (G). Olig2-positive cells also increasingly arise after 14 DIV. Some of them show expression of NeuN while others do not (J, white and yellow arrowheads, respectively). After 21 DIV large astrocytic areas have developed in which neurons are present in lower numbers (I). Scale bars, 100 µm.

VAMP2 in neurons together with Syntaxin1 and SNAP25 facilitates the fusion of synaptic vesicles with the plasma membrane within the presynaptic terminal and thus neurotransmitter release. γ-enolase is a neuron-specific isoform of the glycolytic enzyme enolase which catalyzes the conversion of 2-phosphoglycerate to phosphoenolpyruvate (and thus is also called **N**euron-**S**pecific **E**nolase, NSE). This special isoform was proved to be markedly more stable towards chloride-induced inactivation than the two non-neuronal isoforms (called non-neuronal enolase and muscle-specific enolase, re-

spectively). It was suggested that the resistance towards chloride evolved to accommodate to rising levels of this ion in depolarized neurons. There seems to be a developmental switch from non-neuronal enolase to γ-enolase during neural maturation which also depends on neural activity (Marangos & Schmechel, 1987). Doublecortin is a developmentally regulated, neuron-specific phosphoprotein which is expressed in young and migrating neurons and is associated with microtubules. It seems to be specifically required for neuronal migration and neocortical development (Francis, *et al.*, 1999, Gleeson, *et al.*, 1999, Bai, *et al.*, 2003). Doublecortin expression has already been strongly downregulated after 14 DIV whereas L1, the synaptic markers PSD 95 and VAMP2, and γ-enolase are upregulated. Taken together, the data show that glial cells do not come up until 14 DIV and that the transition to mature neurons is located between 7 and 14 DIV.

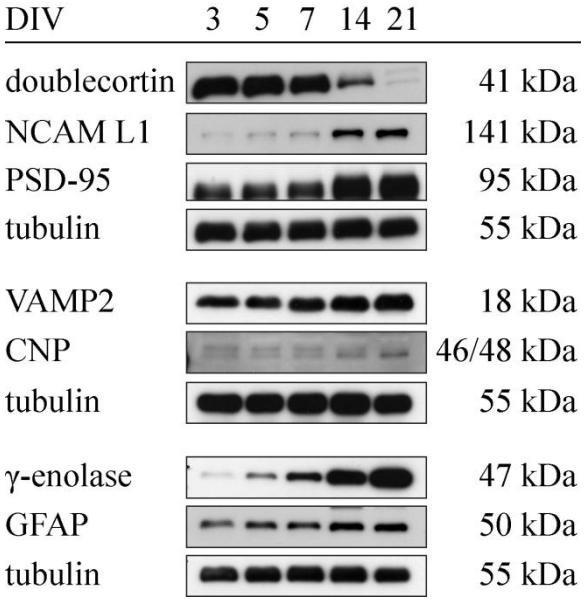

Figure 21: Expression of marker proteins in the neuronal cultures. Neurons were prepared from E15 mouse cortices and cultured for 3 d, 5 d, 7 d, 14 d and 21 d, respectively. Cells were lysed and lysates were analyzed by SDS-PAGE and western blotting. Tubulin serves as loading control. NCAM L1, **N**eural **C**ell **A**dhesion **M**olecule **L1**; PSD-95, **P**ost **S**ynaptic **D**ensity protein **95**; VAMP2, **V**esicle-**A**ssociated **M**embrane **P**rotein 2; CNP, **C**yclic **N**ucleotide **P**hosphodiesterase; GFAP, **G**lial **F**ibrillary **A**cidic **P**rotein.

3.1.2 Establishment of myelinating cocultures

To mimic myelination *in vitro*, OPCs were plated on cortical neuronal cultures and cells were cocultured for up to 3 weeks. The cocultures were characterized at distinct time points by immuno-stainings using different markers directed against neuronal and myelin epitopes. Among the neuronal markers were the antibodies 324, 555, SMI31, γ-enolase, NeuN, MAP-2 and TUJ1. 324 and 555 recognize the epitope L1, an adhesion molecule expressed on the axonal surface. Because L1 is downregulated with onset of myelination it was not suitable for the immunocytochemical analysis of our cocultures (Coman, *et al.*, 2005). Neuronal processes were labeled only weakly and unevenly.

SMI31 is directed against heavily phosphorylated NF-H and to a lesser extent also recognizes phosphorylated NF-M. Unfortunately, SMI31 often exhibited strong staining also of neuronal nuclei. Neither modification of the permeabilization procedure (0,01% Triton X-100 for 30 sec, 0,02% Triton X-100 for 1 min, 0,05% Triton X-100 for 1 min, 50% methanol for 10 min), of the blocking reagent (10% HS, 10% FCS, 0,1% gelatin, 10% NGS), nor of secondary antibody concentration were successful in removing the nuclear background staining of SMI31. The antibody directed against γ-enolase turned out to work only in western blots but not in immuno-stainings. Of the tested antibodies, NeuN, MAP-2 and TUJ1 turned out to be the best suited neuronal markers in the cocultures. NeuN is a widely used marker for neurons and was used to visualize neuronal cell bodies (Figure 20). The MAP-2 antibody recognizes the neuron-specific microtubule-associated protein 2 and labeled the cell bodies and the neurites of some, but not all neurons (not depicted). MAP-2 is able to bind and stabilize MTs, and it was identified as a component of crossbridges between MTs and NFs (Hirokawa, *et al.*, 1988). It was demonstrated that MAP-2 can bind F-actin and bundle actin filaments *in vitro* (Roger, *et al.*, 2004). TUJ1 is directed against neuron-specific tubulin β class III and is a widely used marker of differentiated neurons. In the cocultures, it was shown to nicely label all neuronal processes (Figure 22). Antibodies directed against PLP (antibody aa3) and against MBP (not depicted) showed nice labeling of the oligodendrocytes in our cocultures.

The optimal plating densities of neurons and oligodendroglial cells were assessed for the cocultures. For the neurons this were 1×10^6 cells per 6 cm culture dish, corresponding to 35.000 cells/cm^2 and below the density of genuine cortical neuronal cultures. Oligodendrocytes do not myelinate neuronal processes if these exceed a certain density. To determine the optimal plating density of OPCs, 1×10^6, 2×10^6, 3×10^6 and 4×10^6 OPCs were plated on top and analyzed after 7 d of coculture. 2×10^6 OPCs (corresponding to 70.000 cells/cm^2) turned out to be the appropriate cell number. At this density, oligodendrocytes exhibited optimal spacing and performed the best myelination result, as evidenced by neurite segments covered by oligodendroglial membranes.

The neuronal cultures showed a constantly increasing degree of differentiation with changes in protein expression. Myelination requires an intimate contact between the axon and the myelinating glial cell and interaction of neuronal and glial cell adhesion molecules. Therefore, the time point of adding the OPCs is critical for myelination, too. Because the previous analysis of the neuronal cultures revealed their transition to a mature stage between 7 and 14 DIV, we decided to plate OPCs on top of the neurons after having kept them in vitro for 6 d, 7 d and 8 d, respectively, and analyzed the cells after 7 d of coculture.

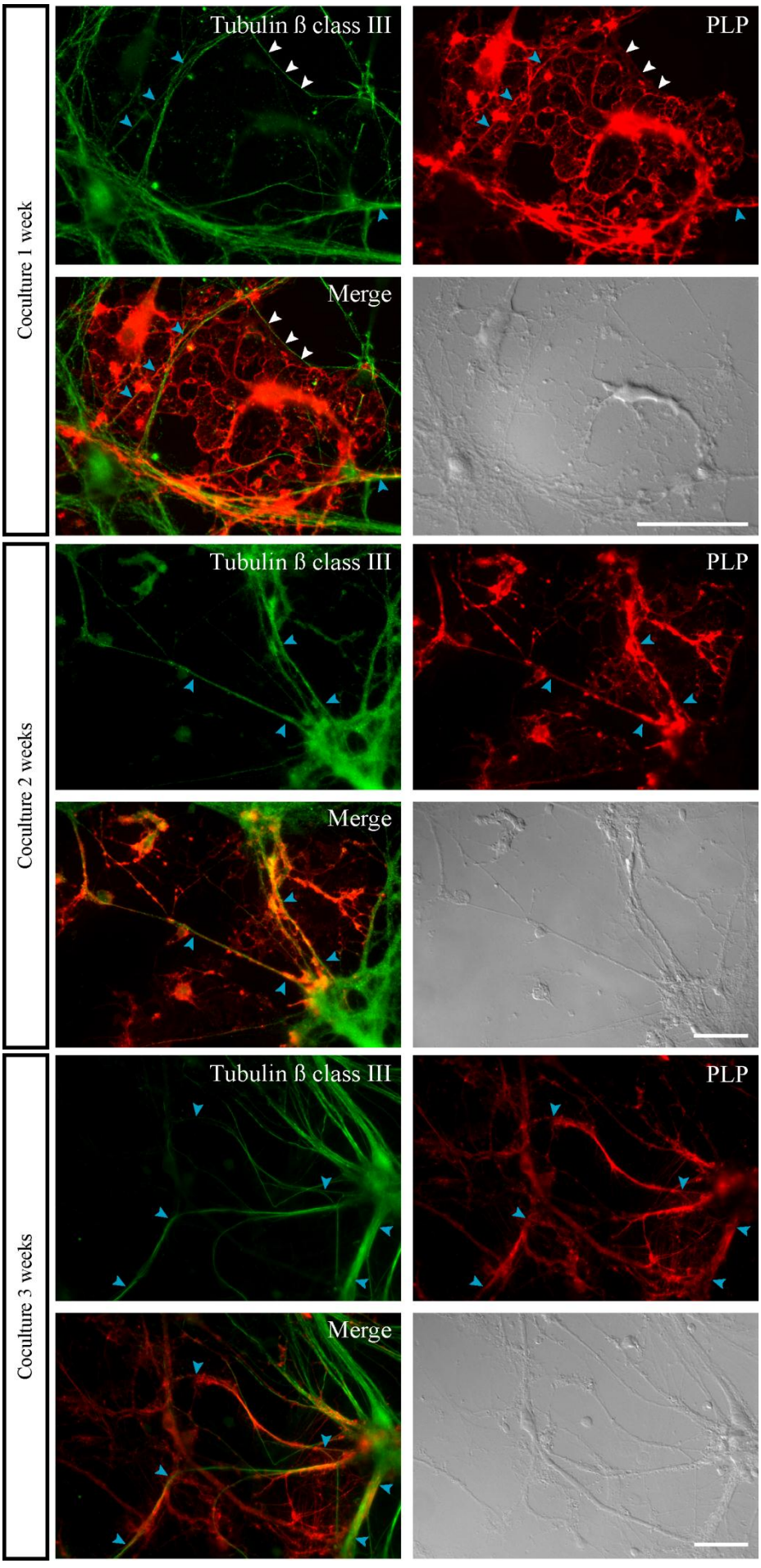
Coculture 1 week
Tubulin ß class III
PLP
Merge
Coculture 2 weeks
Tubulin ß class III
PLP
Merge
Coculture 3 weeks
Tubulin ß class III
PLP
Merge

Figure 22: Characterization of myelinating cocultures by immunocytochemistry. Primary cortical neurons were cultured for 1 week before seeding OPCs on top. Cells were analyzed by immuno-staining after 1 week, 2 weeks and 3 weeks of coculture, respectively. Aa3 antibodies directed against PLP were used to visualize oligodendrocytes, whereas TUJ1 antibodies directed against tubulin β class III were used as neuronal markers. Neuronal segments of overlapping immuno-staining have been enwrapped by oligodendroglial processes. These regions resemble myelination *in vivo* and are called myelinlike membranes (MLM). The white arrowheads mark contact sites between the MLM of the oligodendrocyte and neuronal processes. The blue arrowheads mark areas in which the MLM have already built tubular structures of myelin by wrapping up neuronal processes. Scale bars, 50 µm.

We observed no differences concerning morphology and degree of myelination. Thus, the process of myelination was not changed decisively when OPCs were added within the investigated time window.

The cocultures were analyzed after 1 week, 2 weeks and 3 weeks, respectively (Figure 22). After 1 week of coculture most of the oligodendrocytes have established neuronal contacts with some of them having already enwrapped neuronal processes, thereby building tubular structures around them. These structures show the biochemical and biophysical characteristics of myelin *in vivo* and thus are called myelinlike membranes (MLM). After 2 weeks the degree of myelination has increased and most of the oligodendrocytes not only have built contacts to neuronal processes but also have enwrapped them and tubular structures of ensheathment could be found more frequently. After 3 weeks the tubular structures became even more prominent and even very thin neuronal processes have been heavily enwrapped. Taken together, the cocultures showed an increasing degree of myelination with formation of tubular structures of myelin around neuronal processes.

3.2 Surface PLP is significantly reduced upon VAMP3/VAMP7 cosilencing

To investigate the role of VAMP3 and VAMP7 in transport of myelin components, the major myelin protein PLP was chosen as a model protein of the myelin membrane. OPCs were transfected with siRNAs and differentiated for 3-4 days to allow endogenous PLP expression. Surface localized and total PLP were determined by immunostaining using O10 (recognizing surface PLP) and aa3 (recognizing total PLP) antibodies, respectively. Total expression of PLP was not affected while surface-localized PLP was decreased (Figure 23 A, B). The decrease of surface-localized PLP was quantified utilizing the in-cell multiplex detection assay. Relative surface expression of PLP was calculated by assessing the ratios of epifluorescence values of surface and total PLP. Upon silencing of VAMP3, we observed decreases of surface PLP by 23% (+/- 15%) and for silencing of VAMP7 of 18% (+/- 12%) with p-values near significance of 0,059 and 0,060, respectively. The cosilencing of VAMP3/VAMP7 led to a significant de-

crease of surface PLP by 34% (+/- 11,7%) compared to control and there was a significant difference between single- and cosilencing experiments (VAMP3-silencing and VAMP7-silencing compared to VAMP3/VAMP7-cosilencing, respectively), indicating that VAMP3 and VAMP7 act synergistically and that two different pathways are involved in surface transport of PLP (Figure 23 C).

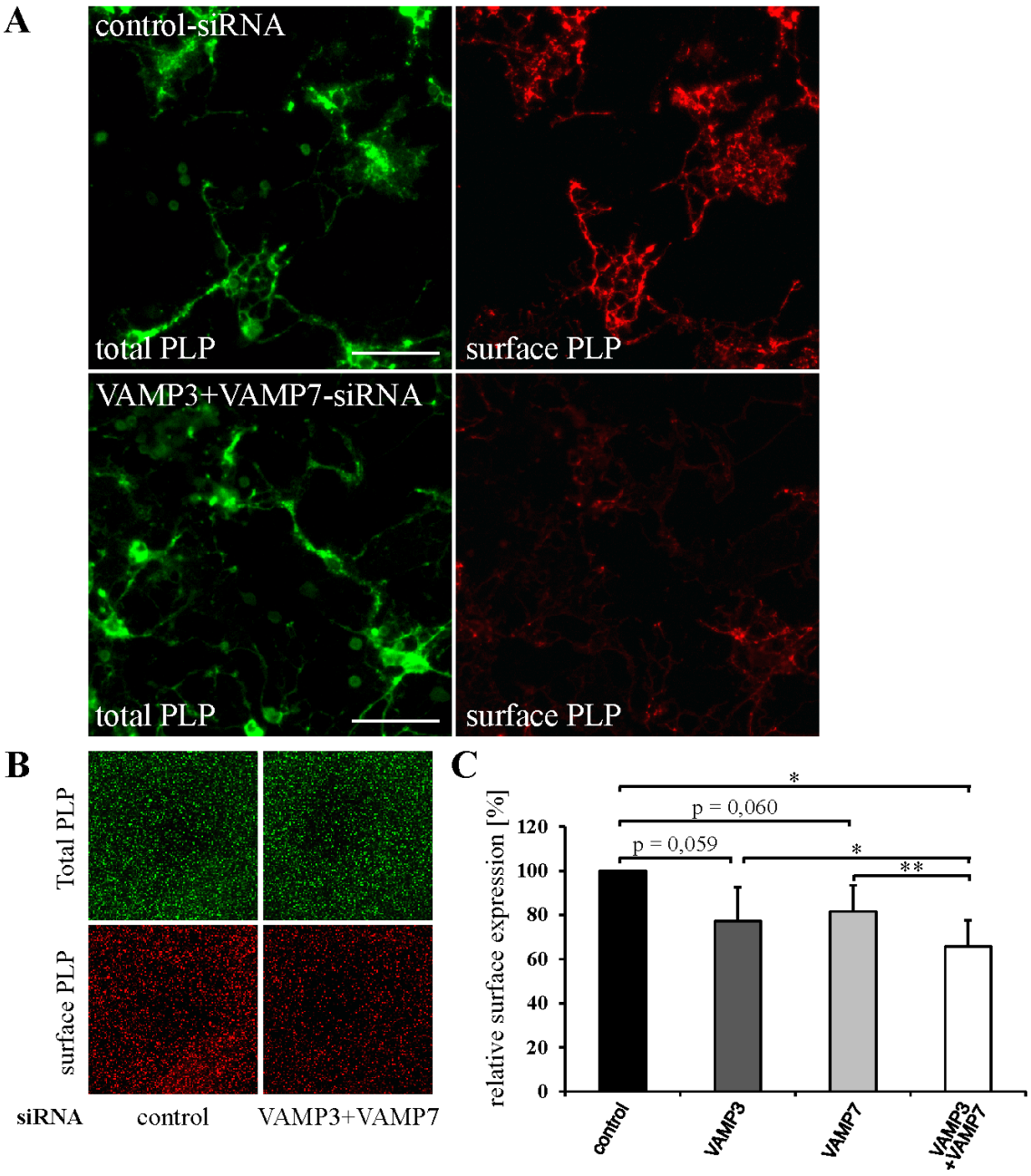

Figure 23: In-cell multiplex detection assay. OPCs were siRNA-transfected and differentiated for 3-4 days before analysis by immuno-staining and performance of the in-cell multiplex detection assay**. A**, Immuno-stainings using aa3 (total PLP, green) and O10 (surface PLP, red) antibodies, respectively. Scale bars, 50 µm. **B**, Odyssey infrared scan depicting total PLP (green) and surface PLP (red) of control- siRNA-transfected and VAMP3/VAMP7-cosilenced oligodendrocytes. A detail showing an identical field of the scan is shown. **C**, Surface PLP normalized to total PLP calculated from Odyssey scans of siRNA-treated cells (n=5 for single and n=4 for cosilencing experiments). Bars depict mean deviation, paired t-test, * p<0,05, ** p<0,01.

3.3 Association of PLP with myelinlike membranes is significantly reduced upon VAMP7-silencing and VAMP3/VAMP7-cosilencing in myelinating cocultures

The neuron-oligodendrocyte cocultures were used to study the involvement of VAMP3 and VAMP7 in myelination *in vitro*. Primary cortical neurons were cultured for one week before seeding siRNA-transfected OPCs on top. Since knockdown efficiency is limited due to half-life of the siRNAs, neuron-oligodendrocyte cocultures were analyzed after 5 days of coculture. At this time point MLM have already been established and the siRNA is still effective. Like myelin *in vivo*, MLM are enriched in lipids and exhibit a low density, facilitating their isolation by density gradient fractionation. Cocultures were analyzed by immuno-staining and the association of PLP with MLM fractions was determined.

3.3.1 VAMP3/VAMP7 cosilencing does not affect neuron-glia interaction

Immuno-stainings of the neuron-oligodendrocyte cocultures using tubulin β class III as neuronal and aa3 as oligodendroglial marker were analyzed concerning morphology of oligodendrocytes and number and extent of neuronal contacts. Neuronal interactions were quantified by subdividing the oligodendrocytes into 3 groups. The first included cells not only having contact to neuronal processes but having enwrapped axonal segments, thereby forming tubular structures around them ("myelinating"). The second included cells which have established neuronal contacts, but have not enwrapped them yet ("contacting"). The third were oligodendrocytes without any neuronal contacts ("no contact"). The analysis revealed no differences between the control-cultures and cultures upon VAMP3/VAMP7-cosilencing (Figure 24 A and B).

3.3.2 Association of PLP with MLM is significantly reduced after VAMP7-silencing and VAMP3/VAMP7-cosilencing

Neuron-oligodendrocyte cocultures were analyzed biochemically by subjecting them to density gradient centrifugation to isolate membranes of low, medium and high density (light, medium and heavy fraction). The light fraction contains MLM sharing characteristics with myelin *in vivo*. Fractions were analyzed by immuno-blotting using the antibody aa3 (Figure 25 A) and the relative association of PLP (B) and DM20 (C) with MLM was determined. The relative amount of PLP present in MLM was significantly reduced upon VAMP7-silencing (reduced to 70 +/- 19,6%) and further decreased upon VAMP3/VAMP7-cosilencing (reduced to 48,6 +/- 13,9%), indicating that VAMP3 and VAMP7 act synergistically. Analysis of DM20 revealed similar results (reduced to 52,2 +/- 22,16% upon VAMP3/VAMP7-cosilencing), confirming the notion that both isoforms, PLP and DM20, are delivered by the same transport pathway.

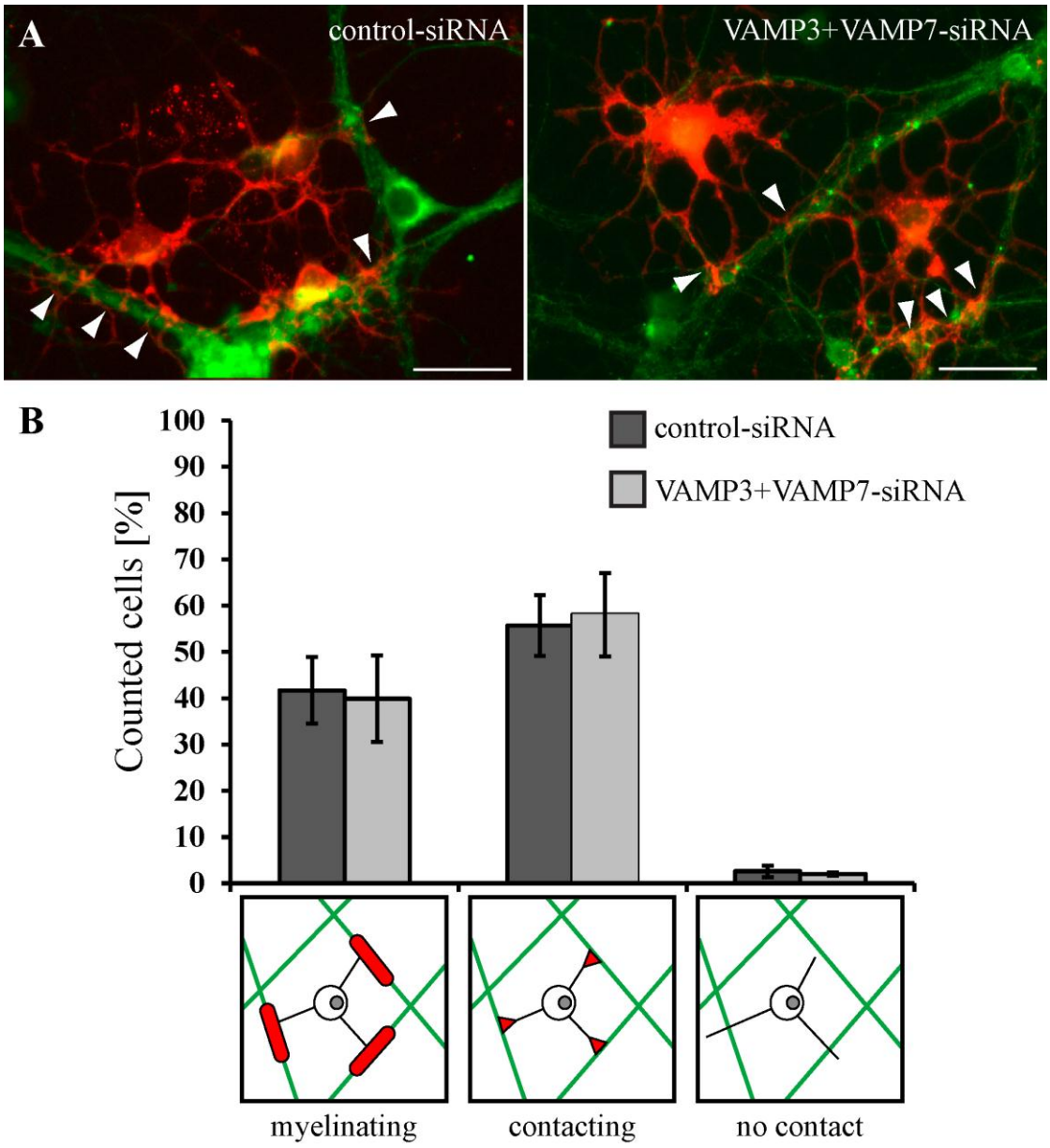

Figure 24: Quantification of oligodendroglial interactions with axons. Primary cortical neurons were cultured for one week before seeding siRNA-transfected OPCs on top. Neuron-oligodendrocyte cocultures were analyzed after 5 days of coculture. **A**, Immuno-stainings using tubulin β class III as neuronal (green) and aa3 as oligodendroglial marker (red). Arrowheads mark sites of glial ensheathment. Scale bars, 25 µm. **B**, Quantification of oligodendroglial interactions with neuronal processes. Oligodendrocytes were subdivided into 3 groups concerning interaction with neuronal processes, which were "myelinating", "contacting" and "no contact". Three independent experiments were evaluated. In one experiment at least 80 cells for each condition were included. Bars depict mean deviation; paired t-test.

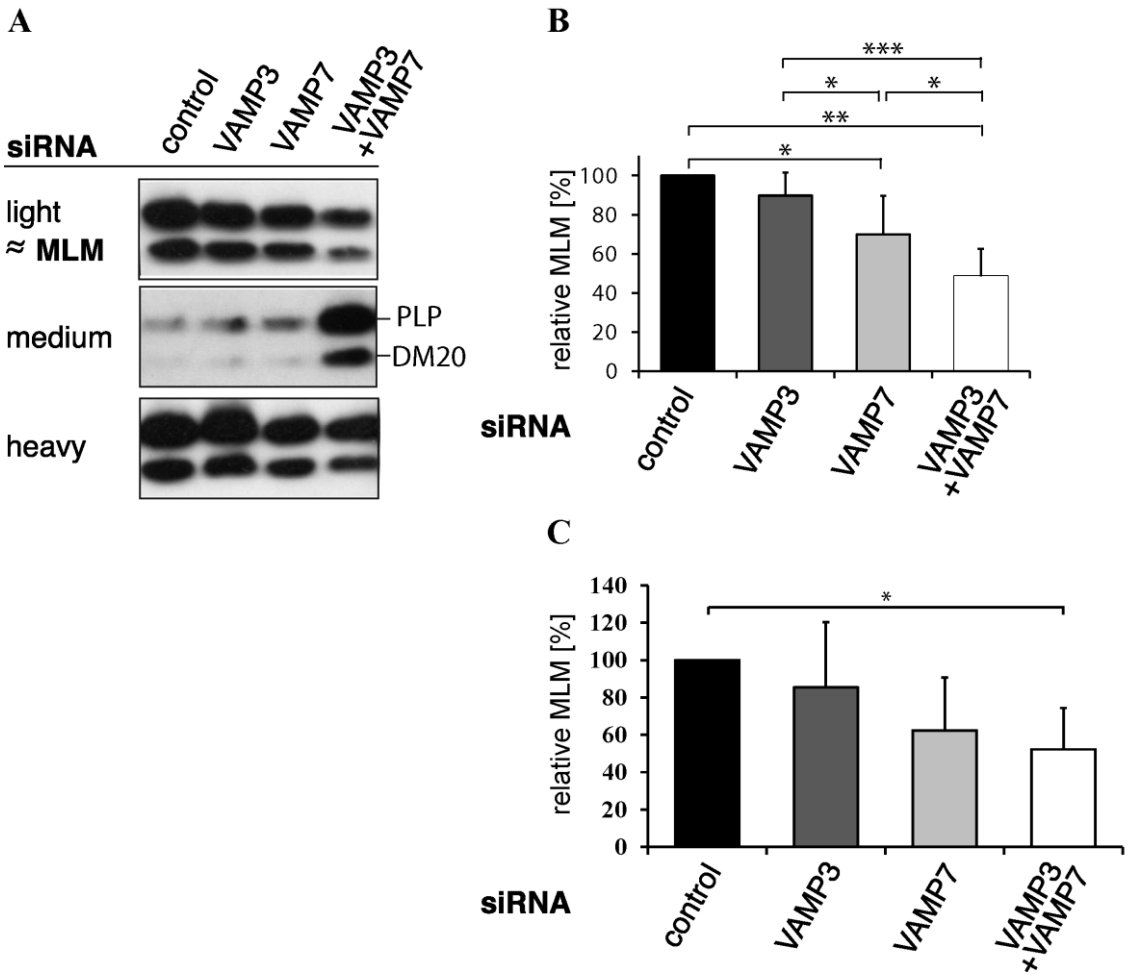

Figure 25: Density gradient fractionation of myelinating cocultures. Primary cortical neurons were cultured for one week before seeding siRNA-transfected OPCs on top. Neuron-oligodendrocyte cocultures were analyzed after 5 days of coculture by density gradient isolation of light, medium and heavy fractions. **A**, Western blot using aa3 antibodies showing the distribution of PLP and its isoform DM20 between light (corresponding to MLM), medium and heavy fractions in the different siRNA conditions. **B**, Densitometric quantification depicting association of PLP with MLM (n=5). **C**, Densitometric quantification depicting association of DM20 with MLM (n=5). PLP present in MLM is significantly reduced upon VAMP7-silencing and VAMP3/VAMP7-cosilencing. DM20 shows the same tendency and is significantly reduced upon VAMP3/VAMP7-cosilencing. Bars depict mean deviation, paired t-test, * $p<0,05$, ** $p<0,01$, *** $p<0,001$.

3.4 Does VAMP7 mediate the fusion of MVBs and exosome release?

To test whether VAMP7 is involved in the release of oligodendroglial exosomes, OPCs were transfected with control- and VAMP7-siRNA, respectively. Cells were stimulated with glutamate which has been demonstrated to trigger the regulated exocytosis of MVBs in oligodendrocytes (Frühbeis, *et al.*, 2011). Exosomes were recovered from the supernatants of siRNA-treated primary oligodendrocytes and isolated by differential centrifugation. The exosome-containing 100.000 g pellets of the supernatants and the corresponding lysates were analyzed by SDS-PAGE and western blotting. SiRNA-

mediated silencing resulted in a decrease of 53% of VAMP7 expression levels (reduced to 47% +/- 19%) compared to control (Figure 26 A, B). PLP antibodies were used to detect oligodendroglial exosomes in the 100.000 g pellets (Figure 26 C) and exosome release was normalized to total expression of PLP determined in western blots of the corresponding lysates. As a summary result of all experiments, we observed no significant differences in exosome release upon VAMP7-silencing compared to control (Figure 26 D). As indicated by the large mean deviation, the values showed strong variations, with the lowest showing a reduction of 71% and the highest showing an increase of exosome release of 227%.

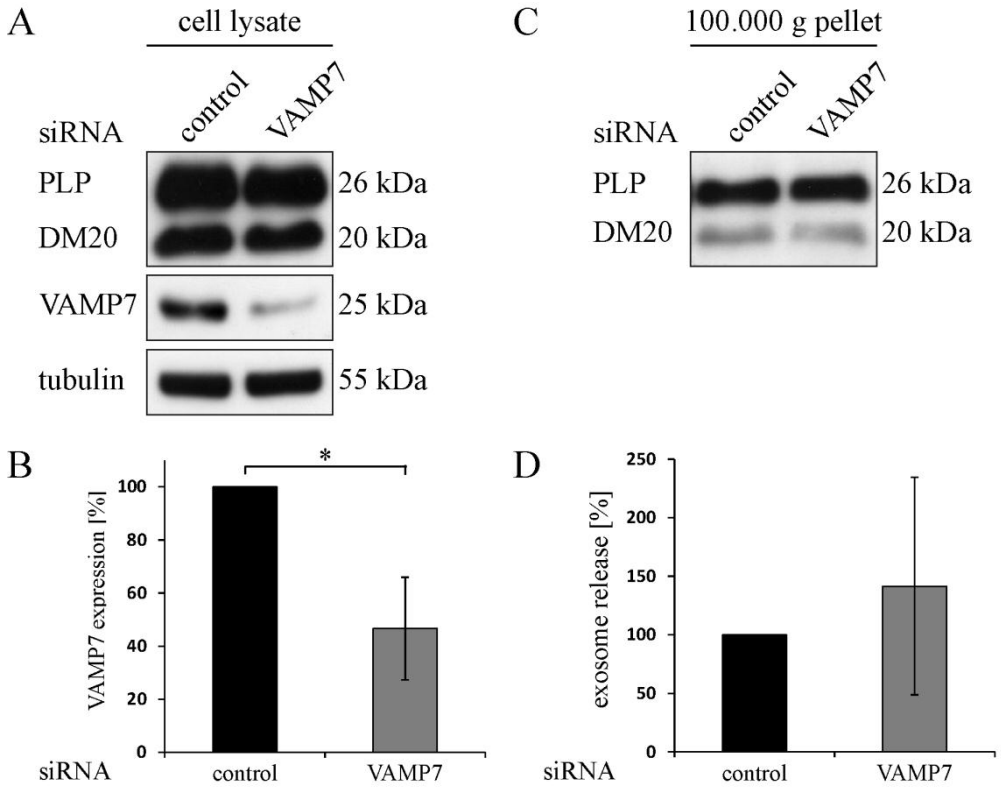

Figure 26: Quantification of oligodendroglial exosome release upon siRNA-mediated silencing of VAMP7. OPCs were transfected with control- and VAMP7-siRNA, respectively. 3-4 d after transfection the cells were treated with glutamate (100 µM) for 4 h to stimulate release of exosomes. The supernatants were collected and the exosomes were pelleted at 100.000 g. Lysates and 100.000 g pellets were analyzed by SDS-PAGE and western blotting. **A**, Western blots of cell lysates with antibodies directed against PLP (aa3) and VAMP7. Tubulin serves as loading control. **B**, Densitometric quantification of expression levels of VAMP7 upon siRNA-mediated silencing. **C**, Western blot of 100.000 g pellets with antibodies directed against PLP (aa3). **D**, Densitometric quantification of exosome release based on the western blot signals for PLP in the 100.000 g pellets (n=4). Exosome release was normalized by assessing the ratios of exosomal and total PLP obtained from western blots of the corresponding lysates. Bars depict mean deviation, paired t-test, * $p<0,05$.

3.5 Tamoxifen-induced translocation of Cre-ERT2 to the nucleus and cre-mediated reporter gene expression

A major goal of this thesis was to analyze the transfer of oligodendroglial exosomes to neurons and their physiological impact on the neuronal target cells. Cre-ERT2 is a fusion protein of cre recombinase and a genetically modified version of the human estrogen receptor ligand binding domain (ERT2). Steroid receptors were shown to convey ligand-dependent regulation to proteins which they are fused to. Due to the specific mutations in ERT2, the synthetic estrogen-like agonist tamoxifen is able to bind and activate cre, whereas binding of the natural ligand of the receptor 17β-estradiol is prevented. ERT2 in cells was shown to be associated with HSP90. We proposed that a sorting of HSP90 into exosomes would result also in inclusion of cre-ERT2. If cre-ERT2-containing exosomes are internalized by transgenic neurons carrying a cre reporter construct, cre-ERT2-mediated recombination would result in expression of the reporter (Figure 27).

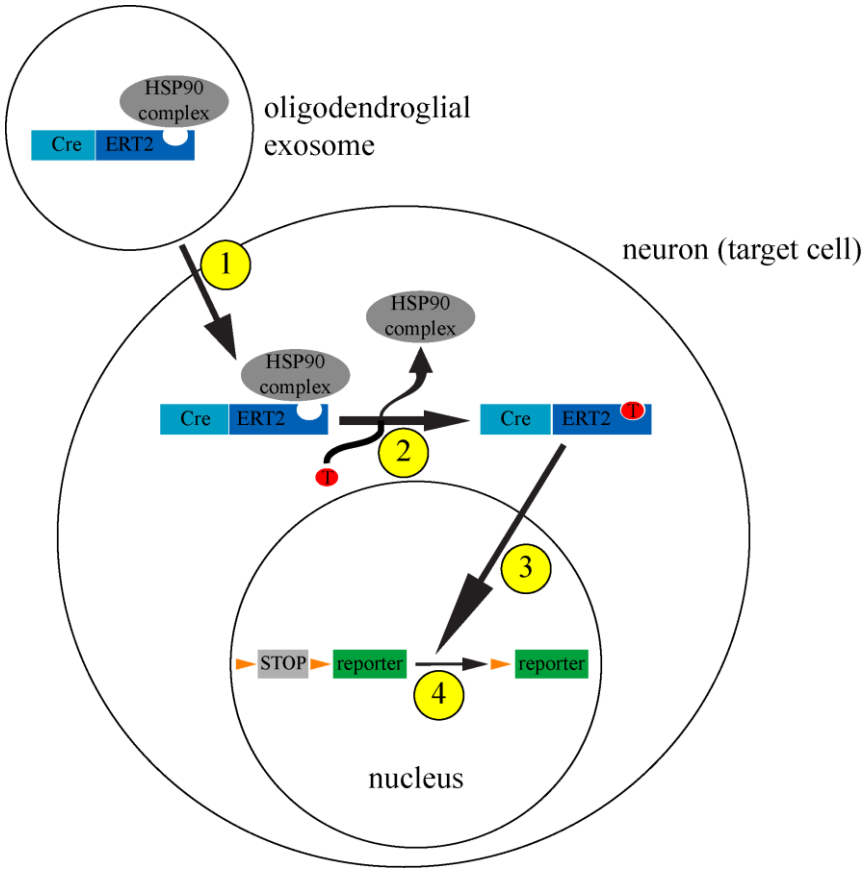

Figure 27: Model of cre-ERT2-mediated recombination upon uptake of oligodendroglial exosomes by neurons. (1) An oligodendroglial exosome containing Cre-ERT2 associated with the HSP90 complex is internalized by a neuron. **(2)** Application of tamoxifen leads to dissociation of the HSP90 complex. **(3)** The activated cre-ERT2 is able to enter the nucleus and **(4)** cre-mediated recombination leads to excision of the stop codon and expression of the reporter downstream the stop codon.

We generated two expression vectors carrying cre-ERT2. In the first one, cre-ERT2 is under control of a modified chicken β-actin (CBA)-promoter, which is a ubiquitous promoter that should allow expression of cre-ERT2 in most, if not all cell types. The second contains an MBP promoter and allows cell type-specific expression in oligodendroglial cells. The functionality of the former was tested by transfection into Oli-*neu* cells (Figure 28). The vector was cotransfected together with another vector carrying the sequence for GFP preceded by a floxed stop codon, providing a target for cre-ERT2. Cells were treated twice with tamoxifen before analysis by immuno-staining 2 d after transfection. In untreated cells, cre-ERT2 could be detected in the cytoplasm distributed in the whole cell whereas in cells treated with tamoxifen cre-ERT2 exclusively was found in the nucleus. However, cre-mediated recombination occurred in treated as well as untreated cells, indicating that cre-ERT2-mediated recombination can also occur on plasmids in the cytoplasm independent of tamoxifen. This is probably due to the overexpression of cre-ERT2. The endogenous HSP90 protein likely is not sufficient to block the enzymatic activity of all of the cre-ERT2 molecules present in a cell.

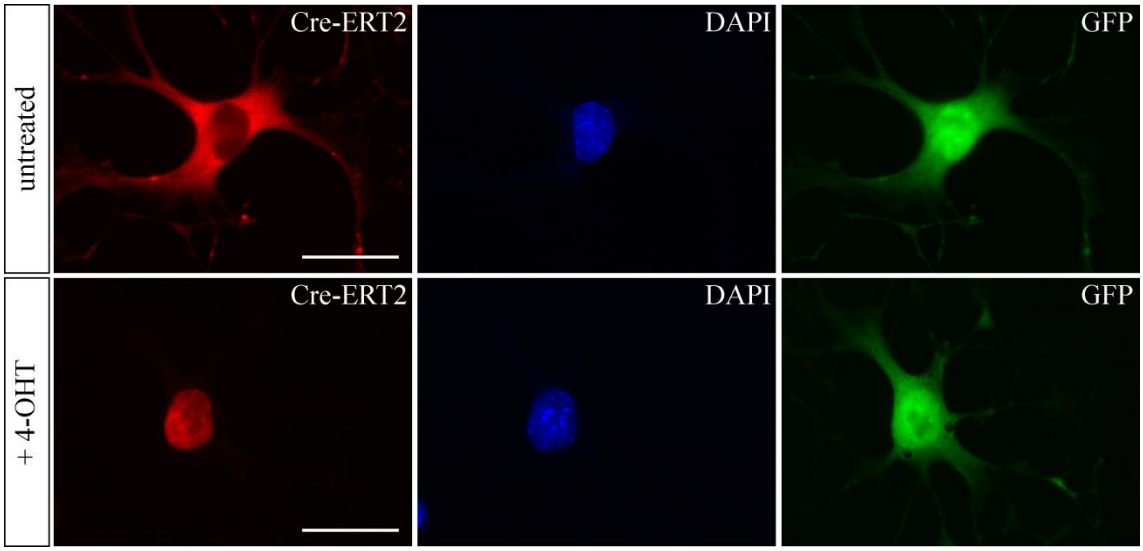

Figure 28: Tamoxifen-induced translocation of cre-ERT2 and cre-mediated reporter gene expression. Oli-*neu* cells were transfected with the pAM/CBA-cre-ERT2 expression vector and an expression vector, in which a floxed stop codon precedes the GFP sequence under control of the CBA promoter. DBcAMP (1 mM) was applied two times to prevent further proliferation and induce differentiation of the cells. Tamoxifen (4-OHT, 1 µM) was applied two times before cells were immuno-stained with antibodies directed against cre on the second day after transfection. DAPI was used to stain the nuclei. Tamoxifen leads to a clear translocation of cre-ERT2 to the nucleus (lower panel) whereas in untreated cells cre-ERT2 is distributed across the whole cell body (upper panel). Cre-mediated recombination occurred in both cases, since treated as well as untreated cells showed expression of GFP. Scale bars, 25 µm.

Next, we tested whether cre and cre-ERT2 are sorted into exosomes and whether sorting of cre-ERT2 indeed is more efficient compared to cre. Since there were hints that also cre could be sorted into exosomes, Oli-*neu* cells were transfected to achieve expression of cre and cre-ERT2, respectively. The cell line Oli-*neu* shows only low expression levels of endogenous PLP, thus we cotransfected another vector carrying the gene for the

fusion protein PLP-eGFP. The supernatants were collected and subjected to density gradient centrifugation. The exosomal fractions and the corresponding lysates were analyzed by SDS-PAGE and western blotting (Figure 29). TSG101 served as a marker for exosomes in general, whereas PLP-eGFP was used to detect oligodendroglial exosomes. Unfortunately, the cre antibody recognizes an unspecific band in the cell lysate of control cells which have not been transfected to express cre or cre-ERT2. This unspecific band exhibits a similar molecular weight like cre-ERT2. However, this unspecific band was only found in non-exosomal fractions of control cells (1,053 g/ml – 1,097 g/ml, not depicted), indicating that the signal obtained in the exosomal fractions of cre-ERT2-transfected cells indeed is associated with exosomes. In summary, cre as well as cre-ERT2 were found to be present in the exosomal fractions.

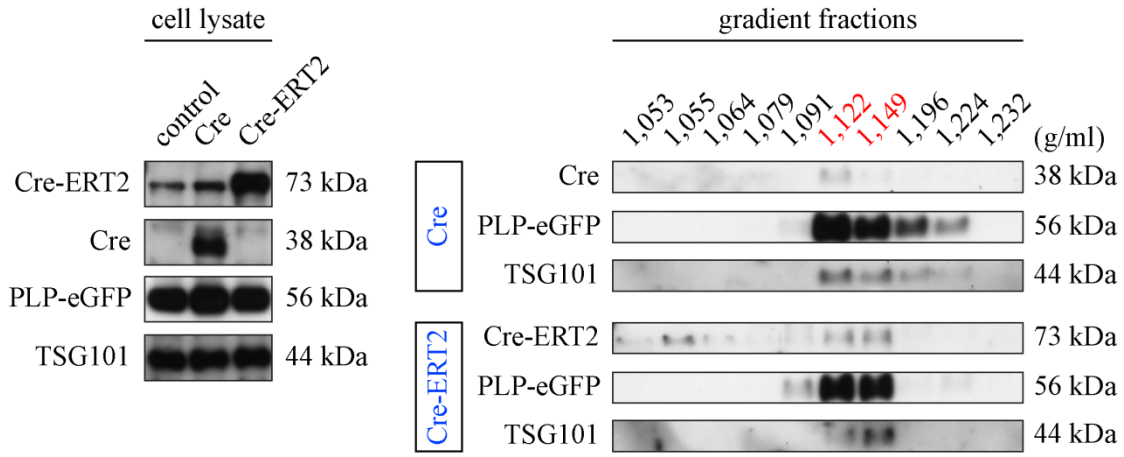

Figure 29: Association of cre and cre-ERT2 with exosomal fractions. Oli-*neu* cells were cotransfected with PLP-eGFP and Cre or cre-ERT2 expression vectors. The supernatants were collected 2 days after transfection and centrifuged at 100.000 g. The resulting membrane pellet was fractionated using a continuous sucrose gradient. The lysates and the corresponding fractions were analyzed by SDS-PAGE and western blotting. PLP-eGFP is used as a marker for oligodendroglial exosomes, whereas TSG101 serves as a marker for exosomes in general. Cre as well as cre-ERT2 are present in the exosomal fractions obtained from supernatants of transfected Oli-*neu* cells (1,122 g/ml and 1,149 g/ml, highlighted in red).

Oli-*neu* cells were transfected to express cre-ERT2 and either were seeded directly on cortical neurons or cocultured with these utilizing the transwell system. In the transwell system, the oligodendrocytes and the neurons are cultured in different chambers which are separated by a porous membrane allowing factors smaller than 1 µm, such as exosomes, to pass. The neurons were obtained from transgenic mice in which the RFP gene is under control of the ubiquitous ROSA26 promoter, preceded by a floxed stop codon (the ROSA26-floxstop-RFP mouse strain) (Luche, *et al.*, 2007). The cells were cocultured for several days and tamoxifen was added twice to activate cre. In both cases, we could not observe any RFP fluorescence in the neurons.

Because cre was shown to be sorted into exosomes, too, we prepared OPCs from transgenic CNP-Cre mice, in which cre is under control of the oligodendrocyte-specific CNP

promoter (CNCE mouse line). The OPCs were either seeded directly onto cortical neurons obtained from ROSA26-floxstop-RFP mice or cocultured with these in the transwell system. No recombination of target neurons was observed. We suppose that cre is only sorted into exosomes when it is present in high abundance in the cell, which is the case upon plasmid transfection into cells. The CNCE mouse line was generated using a knockin approach which means that the entire coding region for CNP was replaced by the cre-cassette. Thus, mice homozygous for the transgene carry only two copies of the cre-transgene. We assume that the resulting expression could be insufficient for cre being sorted into exosomes.

As a positive control the neurons obtained from the ROSA26-floxstop-RFP mice were infected with an adeno-associated virus (AAV) which carries an expression construct for cre. The neurons showed RFP fluorescence which confirms that cre basically can induce RFP expression in these neurons. However, RFP was expressed only weakly and was detectable only after several days after infection although the virus infection resulted in strong overexpression of cre, as verified by immuno-staining with cre antibodies (not depicted).

3.6 Influence of oligodendroglial exosomes on neuronal metabolic activity

To study whether oligodendroglial exosomes can influence neuronal metabolic activity we performed MTT assays. Because the degree of neuronal differentiation could be critical for their susceptibility to exosomal influence we used neurons of different differentiation stages. We utilized two different approaches. In the first approach, neurons were incubated with supernatants collected from cultured primary oligodendrocytes (Figure 30 A, B). The oligodendrocytes previously had been cocultured with primary cortical neurons using the transwell system to allow the stimulation of oligodendroglial exosome release by glutamate released into the culture medium by the neurons. Cortical neurons obtained from an independent preparation were incubated either with supernatants deprived of exosomes by 100.000 g centrifugation or supernatants containing exosomes (SN pOL –E and SN pOL +E, respectively). The exosome-deprived samples served as controls for the influence of factors other than exosomes that may be contained in the supernatants. In addition, neurons cultured in the absence of oligodendroglial supernatants were included (untreated). We observed no differences in metabolic activity when exposing neurons after 7 DIV (Figure 30 A). When neurons cultured for 14 DIV were incubated with oligodendroglial supernatants we observed a slightly higher metabolic activity after treatment with exosome-containing compared to exosome-deprived supernatants (Figure 30 B) but also a general decrease in the presence of oligodendroglial supernatants.

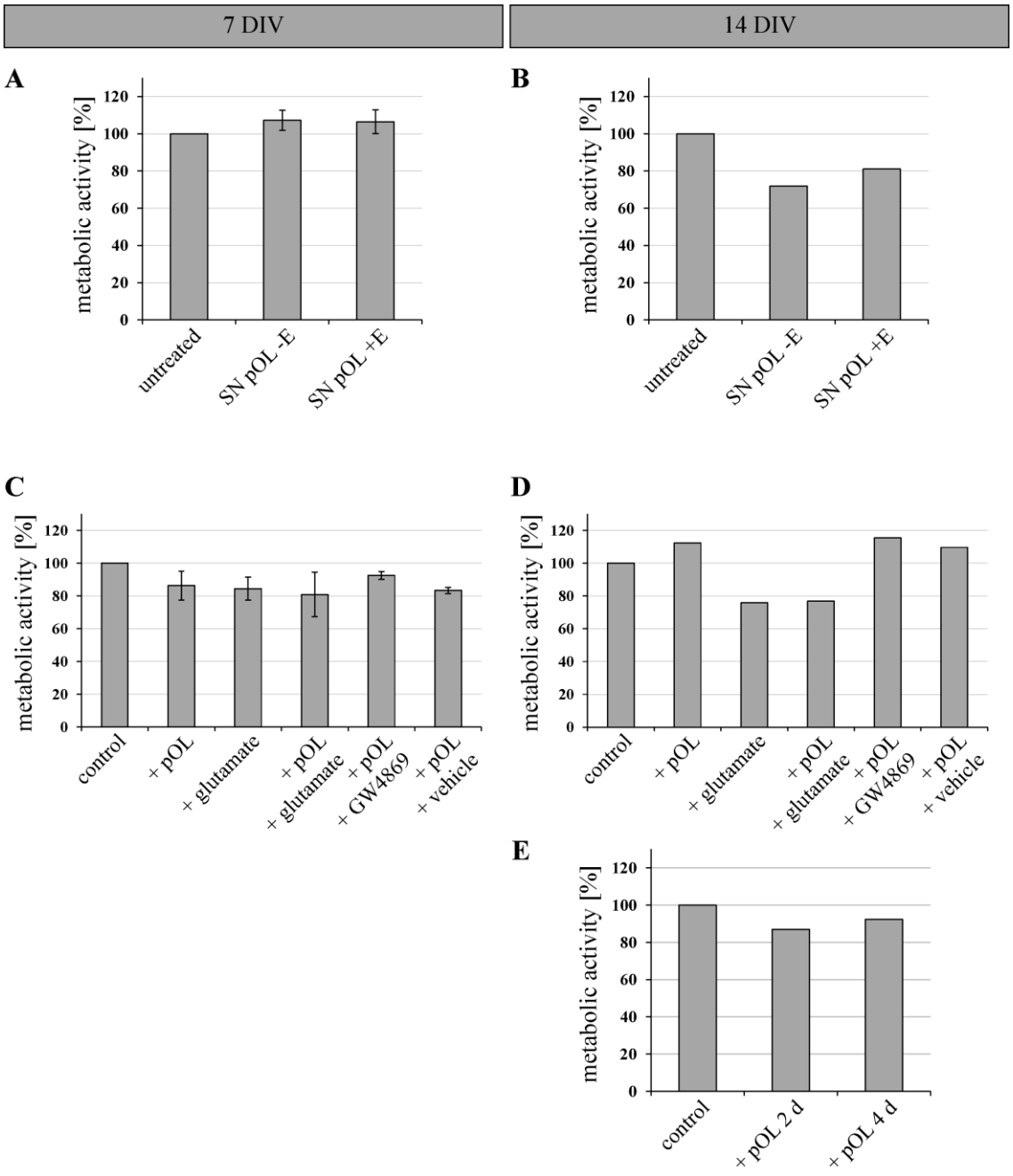

Figure 30: Influence of oligodendroglial exosomes on neuronal metabolism. Primary cortical neurons were cultured 7 d and 14 d, respectively. **A, B**, Primary cortical neurons were incubated for 2 d with oligodendroglial supernatants either deprived of exosomes by 100.000 g centrifugation (SN pOL –E) or supernatants containing exosomes (SN pOL +E) before performing the MTT assays. In addition, neurons were included which were cultured in the absence of oligodendroglial supernatants (untreated). **C, D**, Primary cortical neurons were grown in transwell plates. Inserts carrying primary oligodendrocytes were added and cells were cocultured for 2 d before performing the MTT assay. Glutamate was applied to the oligodendrocytes to enhance exosome release, whereas GW4869 was used to inhibit it. Control cells were cultured in the absence of oligodendrocytes. **E**, Primary cortical neurons were grown in transwell plates. Inserts carrying primary oligodendrocytes were added and cells were cocultured for 2 d and 4 d, respectively, before performing the MTT assay. Control cells were cultured in the absence of oligodendrocytes. Bars depict mean deviation. A, n=3; B, n=1; C, n=2; D, n=1; E, n=1.

In the second approach we utilized the transwell system to achieve a constant delivery of exosomes. Glutamate treatment of the oligodendrocytes was used to increase exosome release whereas the inhibitor GW4869 was used to block it. GW4869 is an inhibitor of the neutral sphingomyelinase the action of which is required for the transformation of the lipid sphingomyelin to ceramide and was shown to inhibit exosome release (Frühbeis, *et al.*, 2011). When we used neurons after 7 DIV the metabolic activity of target neurons was decreased in all instances, regardless of whether they were cultured in the presence or absence of oligodendrocytes (Figure 30 C). When we used the same approach for neurons cultured for 14 DIV, glutamate treatment turned out to be toxic for highly differentiated neurons, resulting in decreases of metabolic activity of more than 20%. Neurotoxic effects of glutamate have already been reported. Glutamate seems to be toxic for neurons in cultures as young as 4 DIV. Greater death was produced in older cultures which is in accordance with our findings (Dawson, *et al.*, 1991, Regan & Choi, 1991). Interestingly, we also observed an increase in all other cases in which oligodendrocytes were present (Figure 30 D). To follow up this, we cocultured neurons after 14 DIV with oligodendrocytes for 2 d and 4 d, respectively. In this case, neurons cocultured with oligodendrocytes showed decreased metabolic activity and nearly no difference was detected between neurons cocultured for 2 d compared to 4 d (Figure 30 E). Taken together, no clear effects of exosome-containing oligodendroglial culture supernatants were observed using the MTT assay and thus these experiments were not repeated.

3.7 Influence of oligodendroglial exosomes on phosphorylation levels of the neurofilament heavy subunit

To address the question whether oligodendroglial exosomes can influence the phosphorylation levels of the neurofilament heavy subunit (NF-H), we followed two different approaches. First, we incubated primary cortical neurons with exosomes obtained from the oligodendroglial cell line Oli-*neu* PLP-eGFP which were isolated by 100.000 g centrifugation of culture supernatants. Neuronal lysates were analyzed by SDS-PAGE and western blotting. The results showed strong variations. In half of the experiments we could observe an increase and in the other half a decrease. Two examples are depicted to demonstrate the variation of phosphorylation levels between single experiments (Figure 31 A (1)). No significant effects on phosphorylation levels of NF-H were observed (Figure 31 A (2)). Phosphorylated NF-H here was normalized to neuron-specific γ-enolase. Since isolated exosomes might have lost bioactivity, a more physiological approach of exosome transfer was chosen. We utilized the transwell system to ensure a permanent supply with oligodendroglial exosomes. The uptake of oligodendroglial exosomes was verified by performing PLP western blots on neuronal lysates (Figure 31 B (1)).

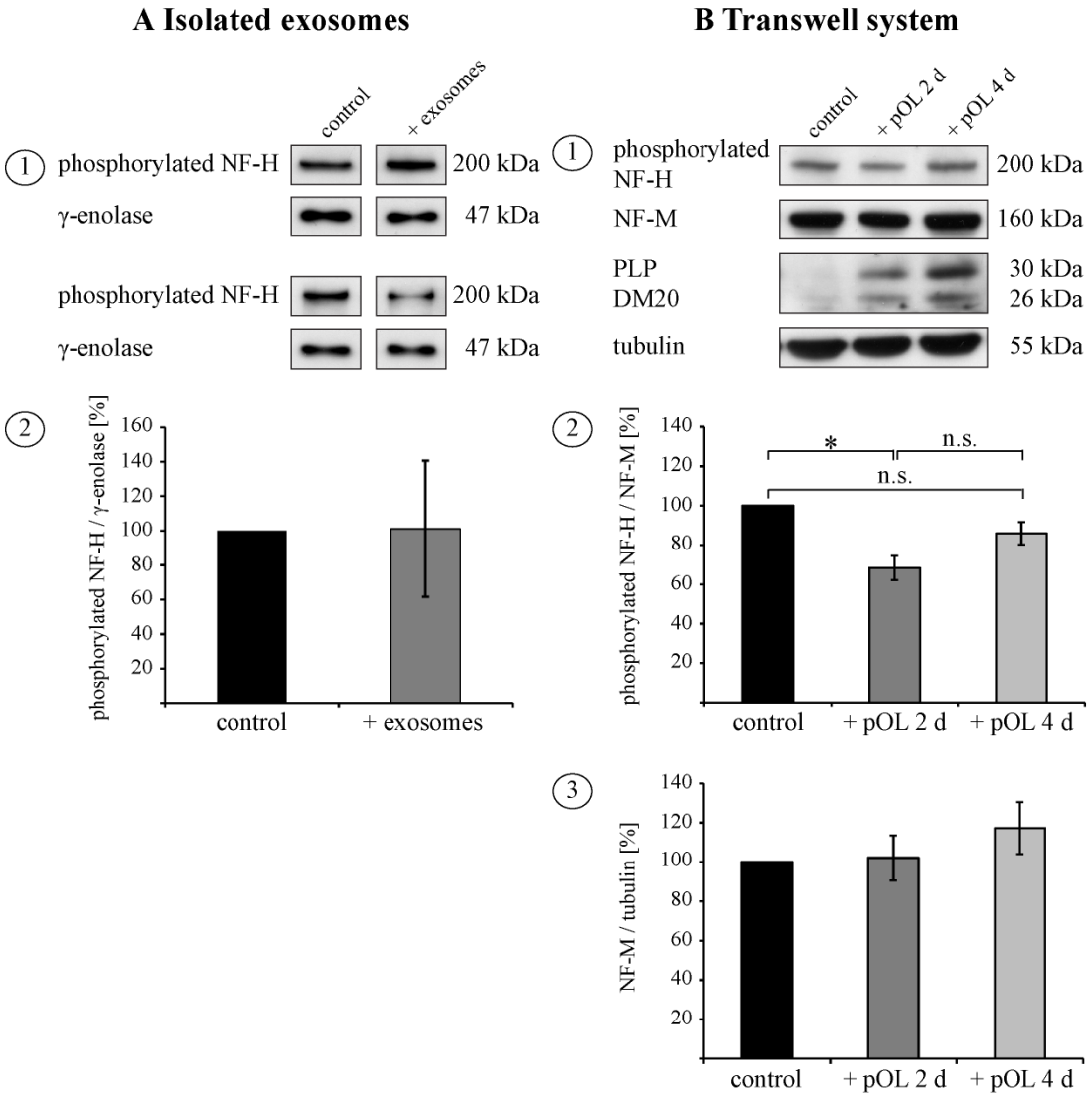

Figure 31: Relative phosphorylation levels of cortical neurons upon influence of oligodendroglial exosomes. In the first approach isolated exosomes of the oligodendroglial cell line Oli-*neu* PLP-eGFP were used (**A**). They were added to primary cortical neurons after 8 DIV. The neurons were lysed after 4 h incubation. Lysates were analyzed by SDS-PAGE and western blotting. **(1)**, Western blots with antibodies directed against the phosphorylated form of NF-H. Neuron-specific γ-enolase serves as loading control. The upper panel shows an increase of phosphorylated NF-H and the lower panel a decrease**. (2)**, Densitometric quantification of the phosphorylation level of NF-H normalized to γ-enolase (n=6). Bars depict mean deviation and illustrate the strong variations in this experimental setup. In the second approach we utilized the transwell system (**B**). Primary cortical neurons were cultured on their own for 7 d and 9 d, respectively. Inserts carrying primary oligodendrocytes were added and cells were cocultured for 2 d and 4 d, respectively. Control cells were cultured without oligodendrocytes. **(1)**, Western blots showing phosphorylated NF-H, NF-M and PLP/DM20. Tubulin serves as loading control. **(2)**, Densitometric quantification of phosphorylated NF-H normalized to NF-M (n=3). The phosphorylation level of NF-H is significantly decreased after 2 d of coculture. **(3)** Densitometric quantification of NF-M normalized to tubulin (n=3). Bars depict mean deviation; * $p<0,05$; n.s., not significant.

Levels of phosphorylated NF-H were normalized to the neurofilament medium subunit (NF-M), taking into account that NFs are obligate heteropolymers in rodents (Figure 31 B (1), (2)). We observed a significant decrease in phosphorylated NF-H after 2 d of co-

culture of 32% (reduced to 68% +/- 6%). Surprisingly, the decrease was lower after 4 d of coculture (86%, +/- 6%). In order to exclude a change in expression of NF-M itself, we determined expression levels of NF-M normalized to tubulin and observed a slight but not significant increase of NF-M after 4 d of coculture (Figure 31 B (3)). In summary, an oligodendroglial effect on the phosphorylation levels of NF-H could be demonstrated. Further studies are required to prove that the observed effects are indeed due to oligodendroglial exosomes.

3.8 Activation of kinases in neurons upon influence of oligodendroglial exosomes

We were interested in which kinases are possibly activated in the neurons upon influence of oligodendroglial exosomes. Primary cortical neurons were cocultured with primary oligodendrocytes in transwell plates before neurons were lysed. Lysates were analyzed in respect of the relative phosphorylation levels of 24 different kinases using a phospho-MAPK (**M**itogen-**A**ctivated **P**rotein **K**inase) array kit. Concurrently, the neuronal lysates were analyzed by SDS-PAGE and western blotting. Western blots using aa3 antibodies confirmed the uptake of exosomal PLP by the neurons (Figure 32 A). The phospho-MAPK array on each capture spot produces a signal which depends on the amount of phosphorylated kinase bound (Figure 32 B). Due to the strong variation of the measured values we were not able to clearly identify individual kinases that are regulated in response to exosome incubation. In the first experiment Akt2, GSK-3α/β and JNK3 were strongly activated (increase of more than 50%). However, in the second experiment ERK1, p38δ and p70 S6 kinase were activated most strongly. Akt1 phosphorylation was elevated by 26% in the first experiment and ERK1 phosphorylation was increased by 123% in the second experiment. The elevated phosphorylation levels of these two kinases in the phospho-MAPK array were validated in western blots, demonstrating the reliability of the array (not depicted). If the two experiments are summarized, the variation in the obtained values is striking. It is particular notable for ERK1 and p38δ. ERK1 was reduced to 70 % in the first experiment, whereas it was increased to 223% in the second experiment. P38δ was reduced to 91% in the first experiment, but increased to 166% in the second experiment. Kinases showing similar values and an increase of at least 10% in both experiments were CREB, the JNKs (c-Jun N-terminal kinases) JNK1, JNK2 and JNK3, p38α and p70 S6 kinase (Figure 32 C).

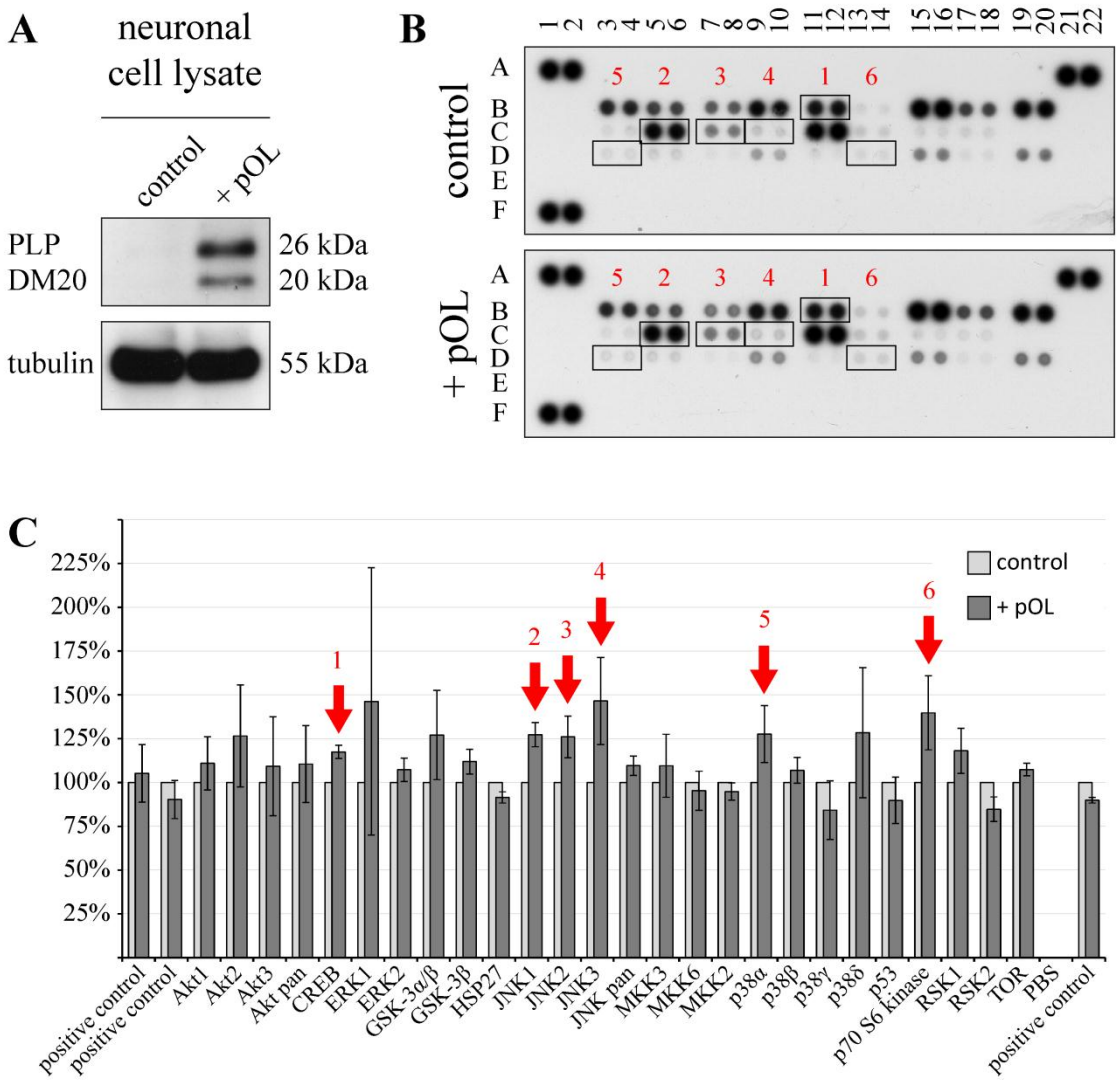

Figure 32: Relative phosphorylation levels of kinases in cortical neurons upon coculturing with primary oligodendrocytes. Primary cortical neurons were cultured for 5 d in transwell plates before adding primary oligodendrocytes in inserts. Cells were cocultured for 3 d. The neurons were lysed and phosphorylation levels of 24 kinases were analyzed using a phospho-MAPK array kit. **A**, PLP western blot using aa3 antibodies demonstrating the uptake of oligodendroglial exosomes by the neurons at the time of performing the assay. Tubulin serves as loading control. **B**, Phospho-MAPK array showing the spots on the nitrocellulose membrane corresponding to different phosphorylated kinases. Capture spots corresponding to kinases which show increased phosphorylation upon coculture with primary oligodendrocytes are encircled. **C**, Densitometric quantification of the relative phosphorylation levels obtained in two independent experiments. Kinases showing an increase of at least 10% in both experiments are indicated by red arrows. Control cells were cultured in the absence of oligodendrocytes and set to 100%. Bars depict mean deviation.

4 Discussion

During myelination, oligodendrocytes synthesize huge amounts of membrane components which are incorporated into the developing myelin sheath. SNARE proteins mediate the fusion of vesicular cargoes with the plasma membrane. The major myelin protein PLP was chosen as a model protein to study the transport of myelin components. A neuron-oligodendrocyte coculture system was established to mimic myelination *in vitro*. The functional inactivation of the v-SNAREs VAMP3 and VAMP7 in primary oligodendrocytes and in the myelinating cocultures confirmed their involvement in transport of PLP. Functional inactivation of VAMP7 in primary oligodendrocytes was performed to clarify whether VAMP7 also mediates the exocytosis of LEs of multivesicular appearance and thus release of exosomes. The cre-loxP system was utilized to demonstrate the neuronal uptake of oligodendroglial exosomes. Cre as well as cre-ERT2 were shown to be present in exosomes, but recombination events in transgenic target neurons could not be detected. In addition, the thesis was focused on possible effects of oligodendroglial exosomes in the target neurons. Three aspects of neuronal metabolism, including metabolic activity, phosphorylation levels of the neurofilament heavy subunit and the activation of kinases, were analyzed.

4.1 Neuron-oligodendrocyte cocultures are a valuable tool for studying myelination *in vitro*

To study the role of VAMP3 and VAMP7 in myelination *in vitro*, myelinating cocultures were established. The establishment and characterization of the neuronal cultures was a precondition. First, the optimal plating densities for the neuronal cultures were identified. Analysis including several marker proteins showed a relative purity until 7 DIV, with glial cells coming up after 14 DIV. The transition to mature neurons was determined to be between 7 and 14 DIV. Based on these findings, the optimal time point of coculture was assumed to be around 7 DIV. OPCs added at this time point face a pure neuronal culture and thus influences of other glial cell types are excluded. Varying time points of adding the OPCs between 6 DIV and 8 DIV had no influence on morphology or degree of myelination. In the next step the optimal proportions of neurons and oligodendrocytes in the cocultures were determined. Immuno-stainings with antibodies directed against different neuronal and oligodendroglial epitopes revealed that the antibodies NeuN, MAP-2 and TUJ1 are the best suited neuronal markers, whereas the PLP antibody aa3 and the MBP antibody showed the best labeling of oligodendrocytes and MLM. This was the basis for the immunocytochemical analysis of the cocultures which were subsequently analyzed after distinct timespans. The oligodendrocytes first estab-

lished contacts to neuronal processes. This was followed by the ensheathment of the processes. This process continued and finally, also thin neuronal processes showed relatively strong ensheathment. The neuron-oligodendrocyte cocultures could be cultured up to 3 weeks and during this time span showed a constantly increasing degree of myelination. Thus, they turned out to be a suitable tool to study myelination *in vitro*. The currently used myelinating culture systems can be divided in three types, including slice cultures, mixed cultures and cocultures of DRGs and oligodendrocytes. In each of these systems, myelination requires several weeks. Due to the involvement of several cell types, slice cultures and mixed cultures are of high complexity and this can confound interpretation of the obtained results. Cocultures of purified neurons and glia allow the analysis of myelination in a more defined system. The usually utilized cocultures include DRGs. But these are neurons of the PNS and in addition remain largely unmyelinated *in vivo* (Watkins, *et al.*, 2008). Thus, our coculture system combines advantages such as rapidity of myelination, the involvement of CNS neurons and easy manipulation. The oligodendrocytes can be manipulated before seeding them onto the neurons, for example by siRNA-mediated silencing of distinct proteins, which are thought to play a role in myelination. One could also investigate the role of neuronal proteins, which have putative roles in myelination, by manipulating the neurons before adding the oligodendrocytes.

4.2 PLP is transported to the cell surface by two different pathways which are mediated by VAMP3 and VAMP7

In Oli-*neu* cells, the functional inactivation of VAMP3 or VAMP7 and the siRNA-mediated cosilencing of both led to a significant decrease of surface PLP, as determined by analysis of immuno-stainings and cell ELISAs (**E**nzyme-**L**inked **I**mmuno**S**orbent **A**ssays). However, the cell line Oli-*neu* shows characteristics of precursor cells, therefore it was important to show the involvement of VAMP3 and VAMP7 in PLP surface transport also in primary cells. Besides, the time-consuming analysis of immunostainings allowed the inclusion of only a relatively low number of cells and the cell ELISAs had the disadvantage that only the absolute surface levels of PLP could be determined and total expression levels of PLP were not taken into account.

To study the involvement of VAMP3 and VAMP7 in surface transport of PLP in primary oligodendrocytes we utilized the in-cell multiplex detection assay which allows the laser-based detection of surface PLP and total PLP across the whole cell population. The siRNA-mediated cosilencing of VAMP3/VAMP7 led to a significant decrease of surface PLP. Furthermore, the observed effect was stronger compared to the single silencing experiments, indicating that VAMP3 and VAMP7 act synergistically and that two different transport pathways might be utilized in the cells. The observed decreases

were relatively low with reductions to approximately 70% upon VAMP3/VAMP7-cosilencing and approximately 80% upon single silencing of VAMP3 or VAMP7. This is probably due to the low knockdown efficiencies of siRNA-mediated silencing in primary oligodendrocytes.

4.3 Silencing of VAMP3 and VAMP7 affects formation of myelin-like membranes *in vitro*

We utilized the established neuron-oligodendrocyte cocultures to study VAMP3- and VAMP7-dependent transport of PLP in myelination *in vitro*. OPCs transfected with siRNAs against VAMP3 and VAMP7 were seeded on top of the neurons. Analysis of immuno-stainings concerning interaction with neuronal processes revealed no differences between control cells and oligodendrocytes in which VAMP3 and VAMP7 have been functionally inactivated. This indicates that initiation of myelination per se is not affected. We performed density gradient isolation of MLM to investigate a role of VAMP3 and VAMP7 in formation of myelin membranes *in vitro*. Association of PLP with MLM was significantly reduced upon VAMP7-silencing and VAMP3/VAMP7-cosilencing. The decrease upon cosilencing was higher compared to silencing of VAMP3 and VAMP7 alone. This indicates that VAMP3 and VAMP7 act synergistically and that two different pathways might be involved. The decrease upon silencing of VAMP7 was significantly higher than that upon VAMP3 silencing, pointing to a dominance of the VAMP7-mediated pathway in transport of PLP particularly to MLM. This is in accordance with observations made concerning the *mocha* mouse strain. In these mice VAMP7 is mislocalized due to a mutation in the *AP3δ1* gene, encoding the δ1 subunit of the adaptor protein 3 (AP-3δ1). This subunit was shown to interact with the N-terminal Longin-domain of VAMP7 which mediates the localization of VAMP7 to Ly/LEs. The lack of functional AP-3 results in mislocalization of VAMP7 to early endosomes and impairment of lysosomal secretion (Proux-Gillardeaux, *et al.*, 2007). In these mice a reduction of PLP in myelin was observed, whereas VAMP3-deficient mice exhibited no myelination defects (Feldmann, *et al.*, 2011). Therefore, we suggest that VAMP7, but not VAMP3, contributes to myelin formation *in vivo*. Since AP-3 certainly is involved in other transport processes, the observed effects on myelination also could be due to influences on other proteins. Another possibility could be that in these mice the mislocalization of VAMP7 has an effect on the neurons and the disturbance on myelination therefore could be an indirect effect which is primarily caused by the mutant neurons. For example, VAMP7 was supposed to be involved in neurite outgrowth (Coco, *et al.*, 1999). Recently, VAMP7 knockout mice have been generated. They were indistinguishable from control mice. Lysosomal exocytosis was not affected in the mutant fibroblasts, but a reduction of neurite outgrowth was confirmed (Sato, *et al.*, 2011). A possible disturbance of myelination has not been investigated yet. The myelination

defects observed in the mice with the mutated *AP-3δ1* gene were only subtle and thus the VAMP7 knockout mice have to be analyzed in greater detail before myelin defects can be excluded. However, ablation of many genes can be compensated *in vivo*, and this could also be the case for VAMP3 and VAMP7 knockout mice. Studies on mice with an oligodendrocyte-specific knockout of VAMP3 and VAMP7 and on VAMP3/VAMP7 double-knockout mice could help to further elucidate the roles of VAMP3 and VAMP7 in PLP transport *in vivo*.

4.4 A model of VAMP3- and VAMP7-dependent surface transport of PLP

Based on these data we propose a model, in which PLP is transported to the plasma membrane on two independent pathways mediated by VAMP3 and VAMP7, respectively (Figure 33). First, PLP is delivered on a VAMP3-dependent pathway from the TGN (***T**rans*-**G**olgi **N**etwork) via recycling endosomes to the plasma membrane. From there, it is internalized again and stored in Ly/LE. Finally, PLP is redistributed to the plasma membrane to sites of myelin formation on a VAMP7-dependent pathway. In Oli-*neu* cells, we observed a dependency on DBcAMP. A decrease of surface PLP only was observed when VAMP3 was functionally inactivated in the presence of DBcAMP whereas for VAMP7 we could only detect an effect in the absence of DBcAMP (Feldmann, *et al.*, 2011). The functional inactivation of both, VAMP3 and VAMP7, was not able to completely block the transport of PLP. First, this again could be due to the relatively low knockdown efficiencies. The remaining levels of VAMP3 and VAMP7 could facilitate that some of the vesicles carrying PLP still reach the plasma membrane. Second, there could be other SNARE proteins which take on the task. For many SNARE proteins it has been shown that they can functionally replace each other and thus the loss of one SNARE can be compensated by another. A promising candidate for the replacement of VAMP3 could be VAMP2. At first, VAMP2 was identified in connection with tetanus and botulism. It was shown that the two zinc endopeptidases tetanus and botulinum neurotoxin cleave VAMP2, thereby blocking neurotransmitter release. The cognate t-SNAREs involved in this process were identified as Syntaxin1 and SNAP25. VAMP2 shows remarkable sequence homologies to VAMP3. Like VAMP3, it was shown to interact with the t-SNARE Syntaxin 4. In adipocytes, VAMP2 and VAMP3 are involved in the transport of GLUT4 (**GLU**cose **T**ransporter) to the plasma membrane. VAMP2 was found on GLUT4-containing vesicles together with VAMP3 (Schiavo, *et al.*, 1992, Martin, *et al.*, 1996, Mollinedo, *et al.*, 2003, Zhao, *et al.*, 2009). Studies on the localization of VAMP2 in oligodendrocytes confirmed that, like VAMP3, it is associated also with recycling endosomes. Some evidence was found that VAMP2 could play a subordinate role in PLP surface transport and support VAMP3 in its function (Diploma thesis (Kuo, 2011)). Third, it cannot be excluded that other

transport routes for PLP exist. One candidate could be VAMP4. VAMP4 in other cell types was found to be localized to the TGN, vesicles, endosomes and the plasma membrane and a role in transport between the cell surface and the TGN was suggested (Steegmaier, *et al.*, 1999, Tran, *et al.*, 2007). Thus, it could function to deliver PLP along a direct transport route from the Golgi to the plasma membrane. Studies on VAMP4 in oligodendrocytes demonstrated its localization in the Golgi and in recycling endosomes. A role in transport of PLP could not been proved yet. It was suggested that VAMP4 plays only a minor role in PLP transport (Diploma thesis (Schmunk, 2009)).

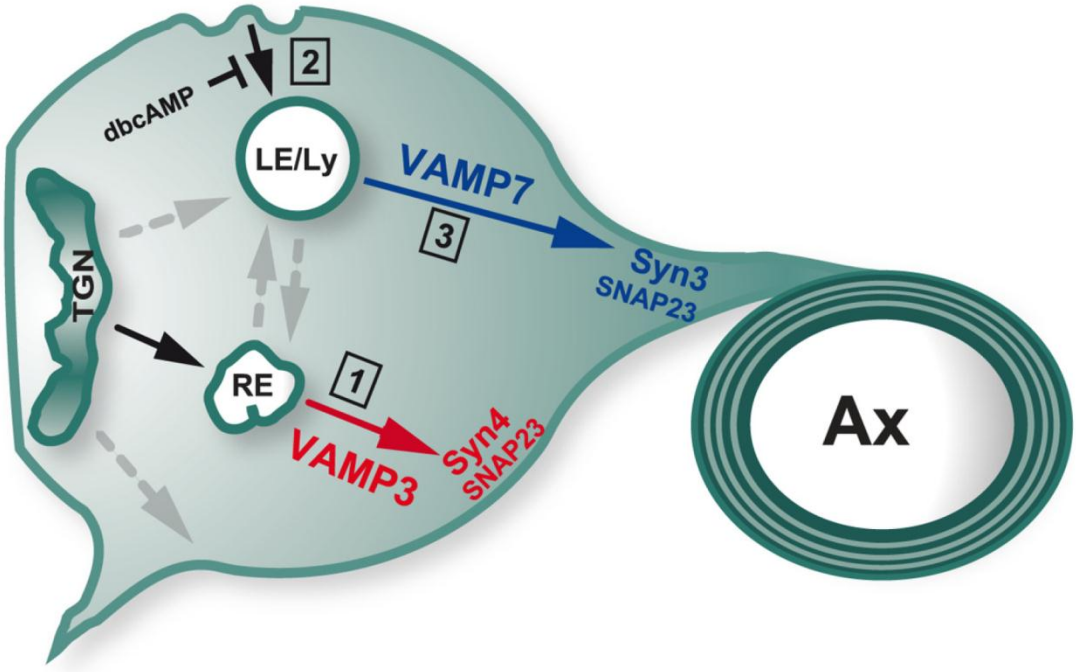

Figure 33: Model of VAMP3- and VAMP7-dependent surface transport of PLP. PLP is transported to the plasma membrane on two independent pathways. First, PLP is delivered from the TGN via recycling endosomes to the plasma membrane on a VAMP3-dependent pathway **(1)**. Upon endocytosis, PLP is stored in LE/Lys **(2)** and then follows a VAMP7-dependent pathway to the plasma membrane at sites of myelin formation **(3)**. DBcAMP blocks endocytosis and reinforces the VAMP3-dependent pathway. A decrease of surface PLP upon functional inactivation of VAMP3 thus can only be observed under these conditions. In absence of DBcAMP, interruption of the VAMP7-dependent delivery of LE/Ly to the plasma membrane leads to decrease of surface PLP. The cognate t-SNAREs were determined in co-immunoprecipitation studies. Syntaxin4 and SNAP23 were found to be the putative t-SNAREs interacting with VAMP3, whereas Syntaxin 3 and SNAP23 are likely to interact with VAMP7. Other possible transport routes are indicated by pale grey dashed arrows. TGN, **T**rans-**G**olgi **N**etwork; RE, **R**ecycling **E**ndosome; LE/Ly, **L**ate **E**ndosome/**Ly**sosome.

4.5 Is VAMP7 involved in regulated exocytosis of exosomes?

Studies of our group showed that the release of oligodendroglial exosomes is triggered by the neurotransmitter glutamate. The release appeared to be dose-dependent with an increase until a concentration of 100 µM. At this concentration the maximum of exo-

some release was reached and further dosage increase was not able to enhance it. Addition of the calcium-chelator EDTA (**E**thylene**D**iamine **T**etraacetic **A**cid) blocked the release of exosomes, pointing to a calcium-dependency also of oligodendroglial exosome release (Frühbeis, *et al.*, 2011).

The R-SNARE VAMP7 has been demonstrated to mediate the fusion of LE/Lys in several cell types such as kidney cells, melanocytes and immune cells (Rao, *et al.*, 2004, Stinchcombe, *et al.*, 2004, Idone, *et al.*, 2008, Sander, *et al.*, 2008). The N-terminal Longin-domain of VAMP7 has been shown to dominant-negatively interfere with VAMP7-mediated fusion reactions by preventing SNARE complex formation. Overexpression of this domain leads to a decrease in exosome release of MDCK (**M**adin-**D**arby **C**anine **K**idney epithelial cell line) cells (Proux-Gillardeaux, *et al.*, 2007). In K562 cells, it furthermore involves an accumulation of MVBs at the cell periphery, indicating a blocking of the final fusion step with the plasma membrane (Fader, *et al.*, 2009). Taking into account that exocytic MVBs are of LE/Ly origin, VAMP7 seems to be a good candidate for being the SNARE protein involved in the release of exosomes. In surface transport of PLP, VAMP7 mediates transport from LE to the plasma membrane (Feldmann, *et al.*, 2009). Moreover, soluble factors which are released by neurons trigger exocytosis of PLP from LEs (Trajkovic, *et al.*, 2006). We thus hypothesize that VAMP7 also mediates the regulated release of exosomes. Using siRNA, VAMP7 was functionally inactivated in primary oligodendrocytes and exosome release was triggered by adding glutamate. Unfortunately, the knockdown was not equally efficient among experiments. Most likely due to this fact, exosome release also exhibited strong variations between single experiments. Thus, the question whether VAMP7 mediates exosome release could not yet been definitely resolved. To follow this question, an independent inactivation of VAMP7 function, such as a dominant-negative approach, should be utilized.

4.6 Are oligodendroglial exosomes internalized by neurons?

To follow this question, we utilized the cre-ERT2-loxP system. We chose the modified version cre-ERT2 because it was known that in cells it is associated with a complex containing HSP90. Mass spectrometry revealed that HSP90 is part of the oligodendroglial exosome (Kramer-Albers, *et al.*, 2007). We therefore proposed that cre-ERT2 would have a greater chance to be sorted to exosomes compared to unmodified cre. Moreover, it was shown that cre is one of only a few prokaryotic proteins which contain a nuclear localization signal (NLS), allowing them the active access to the eukaryotic nucleus (Le, *et al.*, 1999). In immuno-stainings of Oli-*neu* cells which have been transfected to express cre, it was exclusively localized within the nucleus. To achieve cell type-specific expression of cre, we generated expression vectors for cre-ERT2. It turned

out that cre as well as cre-ERT2 are present in oligodendroglial exosomes. Exosomes were also shown to contain mRNAs which are functional in the target cells (Valadi, *et al.*, 2007). A group in Frankfurt analyzed fusion events between hematopoietic cells and Purkinje neurons. Mice carrying cre under control of the hematopoietic-specific promoter *vav* were crossbred with floxed ROSA26 reporter mice. They found mononucleated Purkinje neurons expressing the reporter which was in contrast to previous studies showing that such fusion events result in fused cells containing two nuclei. They proposed this could be due to a vesicular transport between hematopoietic and non-hematopoietic cells allowing the transfer of cre protein and/or nucleic acid (Nern, *et al.*, 2009). Indeed, cre mRNA could be found in exosomes released by cre-expressing oligodendroglial cells (Frühbeis, *et al.*, 2011), as well as the cre protein. Since tamoxifen treatment of neurons is associated with various side effects, it was chosen to utilize the wildtype cre isoform. The cre project was carried on by another person in the lab. In the course of these studies exosome transfer and cre-mediated recombination of target neurons indeed could be demonstrated, thus providing proof of principle that glial exosomes transfer bioactive molecules to neurons (Frühbeis, *et al.*, 2011). In these studies, also the reporter was overexpressed in the target neurons, thus resulting in a higher sensitivity of target cell recombination. The present thesis was focused on the specific metabolic influences of oligodendroglial exosomes on neurons.

4.7 Can oligodendroglial exosomes affect neuronal metabolism?

4.7.1 Influence on metabolic activity

In the PLP and the CNP knockout mice a primary oligodendroglial defect leads to late onset axonal degeneration. In these mice the myelin sheath shows normal compaction and formation of microdomains. Thus, oligodendrocytes seem to support axonal function and survival independent of myelin function (Griffiths, *et al.*, 1998, Lappe-Siefke, *et al.*, 2003). Because myelination of an axon also entails its isolation from the external milieu, it was suggested that oligodendrocytes provide trophic support to the neurons they have myelinated (Nave & Trapp, 2008, Edgar & Nave, 2009). We hypothesize that oligodendroglial exosomes can provide trophic support to axons and alter neuronal metabolism. Neurons of distinct differentiation stages were supplied with oligodendroglial exosomes and metabolic activity was measured utilizing the MTT assay. It has been demonstrated that the neurotransmitter glutamate stimulates exosome release whereas the neutral sphingomyelinase inhibitor GW4869 blocks it (Frühbeis, *et al.*, 2011). Therefore, these reagents were included in the experiments to demonstrate that effects are specifically related to exosome release and not to other secreted factors. We obtained very contradictory results and changes in metabolic activity were only subtle.

Glutamate was used to increase oligodendroglial exosome release but turned out to affect also the neurons. For the assays in which we utilized the transwell system, we changed media of both, the neurons and the added oligodendrocytes, to minimize effects of soluble substances which might have accumulated. For controls, neurons were cultured in the absence of oligodendrocytes. Thus, when neurons are cocultured with oligodendrocytes, more cells have to be supplied with nutrients and metabolic activity could be decreased due to an undersupply. In the first experiment using the transwell system for neurons after 14 DIV, we observed an increase of metabolic activity after coculture with oligodendrocytes. Thus, we repeated the experiment and cocultured neurons and oligodendrocytes for 2 d and 4 d, respectively. But in this case we detected a decrease. The variations between single experiments could be due to variations in the oligodendroglial cultures which always contain other cell types such as neurons and astrocytes. As mentioned previously, the PLP and CNP knockout mice develop a late onset axonal degeneration. An impairment of motor functions is not detectable until the age of 4 months in CNP knockout and even 16 months in the PLP knockout mice (Lappe-Siefke, *et al.*, 2003, Edgar & Nave, 2009), indicating that subtle alterations have to add up to cause to the symptoms. Mass spectrometry analysis of oligodendroglial exosomes revealed that they carry a striking group of proteins with putative functions in the relief of stress (Kramer-Albers, *et al.*, 2007). Therefore, differences between neurons, that receive support and those which do not receive it, are perhaps subtle and only detectable under stress conditions.

4.7.2 Phosphorylation levels of the neurofilament heavy subunit are altered upon influence of oligodendrocytes

Abnormal localization, composition and modification of NFs are hallmarks of many neurodegenerative diseases, such as ALS, AD, PD, CMT, and diabetes. In the PLP knockout mice, axonal swellings and an impairment of the transport machinery including anterograde and retrograde transport were detected (Edgar, *et al.*, 2004). We thus were interested in whether oligodendroglial exosomes can affect the neuronal cytoskeleton and analyzed phosphorylation levels of the NF heavy subunit. In the first approach, in which we incubated the neurons with isolated exosomes, we observed no overall changes of phosphorylation levels after several experiments, although individual experiments appeared promising. However, the isolated exosomes were obtained from an oligodendroglial cell line which shows characteristics of precursor cells. Therefore, their exosomes might lack characteristics which are present in exosomes released from differentiated cells. Moreover, the procedure used to isolate the exosomes could have affected their bioactive properties. In the second approach we utilized the transwell system to achieve a constant supply with exosomes. Here, we observed a low but significant decrease of phosphorylation after 2 d of coculture. However, longer periods of co-

culture did not result in a further decrease. This could perhaps be explained by the action of mechanisms for compensation. An effect on NF phosphorylation was only achieved utilizing the transwell system whereas the incubation with isolated exosomes was inefficient. It may be possible that effects of exosomes on the neuronal cytoskeleton are only subtle and small but constantly supplied amounts of exosomes are required. The PLP knockout mice show swellings containing highly phosphorylated NFs. The phosphorylation state of NFs is considered to be a dynamic balance between the action of kinases and phosphatases. Exosomes could contribute to the maintenance of this balance. Some studies demonstrate that dephosphorylated NFs exhibit better attachment to motor proteins such as kinesin and dynein/dynactin and thus undergo faster transport in the axon (Shah, *et al.*, 2000, Yabe, *et al.*, 2000). Dephosphorylation of NF-H also seems to induce the binding of NFs to MTs (Hisanaga & Hirokawa, 1990). Thus, dephosphorylation of NFs could play a role during axonal outgrowth, when the system needs to be highly dynamic. In our transwell system the neurons are supplied with oligodendroglial exosomes but interaction between neurons and oligodendrocytes by adhesion molecules is not possible which represents an unphysiological situation. It seems likely that both, trophic support and the interaction by cell adhesion molecules are needed for the maintenance of axonal integrity. We also have to clarify where the dephosphorylated NF-H subunits are located in the cell. It was shown that phosphorylation of NFs is topologically regulated. Under normal conditions, dephosphorylated NFs are found in cell bodies, neurites and nodes of Ranvier. Furthermore, there is a proximo-distal gradient with most intense phosphorylation in the axon and little or no expression in cell bodies and dendrites (Nixon, *et al.*, 1994, Brown, 1998).

Control cells were cultured in the absence of oligodendrocytes, but the optimal control would have been the coculturing with oligodendrocytes, which produce no or at least less exosomes. This could be achieved by siRNA-mediated silencing of Rab35, which in Oli-*neu* cells was shown to reduce exosome release by approximately 50% (Hsu, *et al.*, 2010). However, this might not be sufficient to affect target cell functions. Perhaps it is possible to further decrease exosome release by silencing of Rab35 together with other Rab proteins such as Rab11, Rab27a and Rab27b, which also were shown to be involved in exosome biogenesis (Savina, *et al.*, 2005, Ostrowski, *et al.*, 2009). Since the inserts which carry the oligodendrocytes in the transwell system exhibit pores of 1 µm in diameter, which also allow soluble substances, such as growth factors, to pass, it cannot be totally excluded that these contribute to the observed effects. Furthermore, exosomes and soluble substances could act together to modify the neuronal cytoskeleton. In summary, we could show that oligodendrocytes affect the phosphorylation levels of the NF heavy subunit. Further studies are required to answer the question whether these effects are due to oligodendroglial exosomes or other secreted factors.

4.7.3 Which kinases are activated upon the influence of oligodendroglial exosomes?

Oligodendrocytes are able to modify NF phosphorylation and perhaps also other aspects of neuronal metabolism. The cellular pathways are regulated by a plethora of kinases. We tried to identify kinases which are activated upon oligodendroglial exosome influence. Most of the analyzed kinases varied in their activity between single experiments. However, a number of kinases appeared to act consistently. Among these were CREB, the JNKs JNK1, JNK2 and JNK3, p38α and p70 S6 kinase. CREB (**C**AMP-**R**esponse-**E**lement-**B**inding protein) functions as a transcription factor and is present in all cells in the brain. The key steps involved in CREB-mediated gene transcription include dimerization, binding to CREB response elements (CRE) in the DNA and phosphorylation. Phosphorylated CREB activates a cascade of events including the recruitment of CREB-binding protein (CBP) and assembly of a transcriptional complex. CREB can be activated by various factors. These include neurotrophins such as brain-derived neurotrophic factor (BDNF) which was shown to promote neuronal survival (Finkbeiner, *et al.*, 1997, Carlezon, *et al.*, 2005). CREB can be phosphorylated by p70 S6 kinase which also was found to be activated in the presence of oligodendrocytes. P70 S6 kinase has a prominent role in mitogenesis. Phosphorylation of the ribosomal subunit S6 by p70 S6 kinase correlates with increased translation and several studies indicate that it plays a role in progression through the G_1 phase of the cell cycle (Chou & Blenis, 1995, Jefferies, *et al.*, 1997). C-Jun N-terminal kinases (JNKs) are strongly activated during cellular stress and thus are also known as stress-activated protein kinases (SAPKs). For many years, the JNKs were thought to have pro-apoptotic effects. But in the recent years it emerged that the outcome of JNK signaling is cell- and context-dependent (Basu & Kolesnick, 1998). They were also shown to have positive effects, e.g. they seem to play a role in axon formation. Phosphorylated JNK is enriched in the axon and forms a proximo-distal gradient in young axons. JNK can phosphorylate the transcription factor ATF-2, a member of the ATF/CREB family, which was suggested to play a role in neuronal survival (Robinson, 1996, Kreutz, *et al.*, 1999, Oliva, *et al.*, 2006). JNK1 and JNK3 were shown to target multiple phosphorylation sites in NF-H side arms, leading to aberrant phosphorylation of NF-H in the neuronal cell body under stress conditions (Giasson & Mushynski, 1996, Giasson & Mushynski, 1997, Brownlees, *et al.*, 2000). The activation of JNKs would lead to an increase of NF-H phosphorylation and thus is in contrast to our findings that NF-H phosphorylation was decreased upon oligodendroglial influence. A possible explanation would be the concurrent activation of phosphatases. The phosphorylation state of NFs in a cell likely is the result of a balance between the activity of kinases and phosphatases and a dominance of the activity of phosphatases could overlay the effects of operating kinases. P38α seems to be involved in phosphorylation under stress conditions and like JNK can activate ATF-2 (Livingstone, *et al.*, 1995). The con-

sequences of p38 downstream signaling and its role in neuronal survival are still unknown.

In summary, results of the present thesis suggest that oligodendroglial exosomes affect neurofilament phosphorylation. Kinases showing the tendency of being upregulated in the presence of oligodendrocytes have putative roles in neuronal survival. Further experiments are required to confirm these results and to specify the involved exosomal factors as well as kinases acting in the target cells.

Publications

Transport of the major myelin protein is directed by VAMP3 and VAMP7

Anke Feldmann, Jesa Amphornrat, Madeleine Schönherr, Christine Winterstein, Wiebke Möbius, Torben Ruhwedel, Lydia Danglot, Klaus-Armin Nave, Thierry Galli, Dieter Bruns, Jacqueline Trotter, and Eva-Maria Krämer-Albers

The Journal of Neuroscience, April 13, 2011; 31(15):5659-5672

Exosomes mediate oligodendrocyte-neuron communication

Carsten Frühbeis, Dominik Fröhlich, Jesa Amphornrat, Sebastian Thilemann, Aiman S. Saab, Frank Kirchhoff, Wiebke Möbius, Klaus-Armin Nave, Anja Schneider, Mikael Simons, Matthias Klugmann, Jacqueline Trotter and Eva-Maria Krämer-Albers

(Submitted, Nature Neuroscience)

Table of figures

List of tables

Abbreviations

4-OHT	**4**-Hydroxy (**OH**)-**T**amoxifen
aa	**a**mino **a**cid
AAA+	**A**TPase **A**ssociated with various cellular **A**ctivities
AAV	**A**deno-**A**ssociated **V**irus
AD	**A**lzheimer´s **D**isease
ALG-2	**A**poptosis-**L**inked-**G**ene **2**
Alix	**AL**G-2-**i**nteracting protein **X**
ALS	**A**myotrophic **L**ateral **S**clerosis
AmpR	**Amp**icillin **R**esistance gene
ATP	**A**denosine **T**ri**P**hosphate
bGHpA	**b**ovine **G**rowth **H**ormone **p**oly**A**denylation signal
BSA	**B**ovine **S**erum **A**lbumin
cAMP	**c**yclic-**A**denosine-**M**ono**P**hosphate
Caspr	**C**ontactin-**a**ssociated **pr**otein
CMT	**C**harcot-**M**arie-**T**ooth disease
CMV	**C**yto**M**egalo**V**irus
CNP	**C**yclic **N**ucleotide **P**hosphodiesterase
CNS	**C**entral **N**ervous **S**ystem
Cntn	**Cont**acti**n**
Cre	**Cre** recombinase
CREB	**C**yclic AMP-**R**esponsive **E**lement-**B**inding protein
Cre-ERT2	**Cre** recombinase-**E**strogen **R**eceptor **T**amoxifen-inducible **2**
CSF	**C**erebro**S**pinal **F**luid
Cx	**C**onne**x**in
DBcAMP	**D**i**B**utyryl-**c**yclic-**A**denosine-**M**ono**P**hosphate
DC	**D**endritic **C**ell
DIV	**D**ays ***In Vitro***
DMSO	**D**i**M**ethyl **S**ulf**O**xide
DNA	**D**eoxyribo**N**ucleic **A**cid
dNTP	**d**eoxy**N**ucleotide **T**ri**P**hosphate
DRG	**D**orsal **R**oot **G**anglion cell
DTT	**D**i**T**hio**T**hreitol
E	**E**mbryonic day

EDTA	**E**thylene**D**iamine **T**etraacetic **A**cid
eGFP	**e**nhanced **G**reen **F**luorescent **P**rotein
ELISA	**E**nzyme-**L**inked **I**mmuno**S**orbent **A**ssay
ERK	**E**xtracellular signal-**R**egulated **K**inase
ESCRT	**E**ndosomal **S**orting **C**omplex **R**equired for **T**ransport
FGF	**F**ibroblast **G**rowth **F**actor
floxed	**f**lanked by **lox**P sites
GABA	**G**amma-**A**mino**B**utyric **A**cid
GAP	**G**TPase-**A**ctivating **P**rotein
GFAP	**G**lial **F**ibrillary **A**cidic **P**rotein
GFP	**G**reen **F**luorescent **P**rotein
GSK	**G**lycogen **S**ynthase **K**inase
GTP	**G**uanosine **T**ri**P**hosphate
HBSS	**H**ank´s **B**alanced **S**alt **S**olution
HEK cells	**H**uman **E**mbryonic **K**idney cell line
hrGFP	**h**umanized **r**enilla **G**reen **F**luorescent **P**rotein
HRP	**H**orse **R**adish **P**eroxidase
HSP	**H**eat **S**hock **P**rotein
IC	**I**mmuno**C**ytochemistry
IF	**I**ntermediate **F**ilament
ILV	**I**ntra**L**uminal **V**esicle
ITR	**I**nverted **T**erminal **R**epeats
JNK	c-**J**un **N**-terminal **K**inase
K562 cells	myelogenous leukemia cell line
KCh	fast potassium (**K**) **Ch**annels
LB	**L**ysogeny **B**roth
LE/Ly	**L**ate Endosome/**Ly**sosome
loxP	**l**ocus **o**f crossover [**X**] in **P**1
MAG	**M**yelin-**A**ssociated **G**lycoprotein
MAL	**M**yelin **A**nd **L**ymphocyte protein
MAPK	**M**itogen-**A**ctivated **P**rotein **K**inase
MBP	**M**yelin **B**asic **P**rotein
MDCK cells	**M**adin-**D**arby **C**anine **K**idney epithelial cell line
MF	**M**icro**F**ilament
MHC	**M**ajor **H**istocompatibility **C**omplex
miRNA	**mi**cro**RNA**

MLM	**M**yelin**L**ike **M**embrane
MOBP	**M**yelin-associated **O**ligodendrocytic **B**asic **P**rotein
MOG	**M**yelin/**O**ligodendrocyte **G**lycoprotein
mRNA	**m**essenger**RNA**
MT	**M**icro**T**ubule
MTT	Di**M**ethyl**T**hiazol-diphenyl**T**etrazolium bromide
MVB	**M**ulti**V**esicular **B**ody
NaCh	voltage-gated sodium (**Na**) **Ch**annels
NCAM	**N**eural **C**ell **A**dhesion **M**olecule
NECL	**NEC**tin-**L**ike protein
NF155/186	**N**euro**F**ascin 155 kDa/186 kDa
NF-H	**NF H**eavy subunit
NF-L	**NF L**ight subunit
NF-M	**NF M**edium subunit
NSE	**N**euron-**S**pecific **E**nolase
NSF	**N**-ethylmaleimide-**S**ensitive **F**actor
OPC	**O**ligodendroglial **P**recursor **C**ell
OSP	**O**ligodendrocyte-**S**pecific **P**rotein
P	**P**ostnatal day
PBS	**P**hosphate-**B**uffered **S**aline
PD	**P**arkinson´s **D**isease
PDGF	**P**latelet-**D**erived **G**rowth **F**actor
PFA	**P**ara**F**orm**A**ldehyde
PLL	**P**oly-**L**-**L**ysine
PLP	**P**roteo**L**ipid **P**rotein
PNS	**P**eripheral **N**ervous **S**ystem
pOL	**p**rimary **OL**igodendrocytes
PSD	**P**ost**s**ynaptic **D**ensity
PVDF	**P**oly**V**inyli**D**ene **F**luoride
RE	**R**ecycling **E**ndosome
RFP	**R**ed **F**luorescent **P**rotein
RIPA	**R**adio**I**mmuno**P**recipitation **A**ssay buffer
RNA	**R**ibo**N**ucleic **A**cid
RT	**R**oom **T**emperature
SCa	**S**low **C**omponent **a**
SCb	**S**low **C**omponent **b**

SDS-PAGE	**S**odium **D**odecyl **S**ulfate **P**oly**A**crylamide **G**el **E**lectrophoresis
siRNA	**s**mall **i**nterfering **RNA**
SM proteins	**S**ec/**M**unc18-related proteins
SNAP	**S**oluble **N**-ethylmaleimide-sensitive factor **A**ttachment **P**rotein
SNARE	**S**oluble **N**-ethylmaleimide-sensitive factor **A**ttachment protein **RE**-ceptor
SPG2/HSP	**S**pastic **P**araple**G**ia **2**/**H**ereditary **S**pastic **P**araplegia
TAE	**T**ris base/**A**cetic acid/**E**DTA buffer
TBS	**T**ris-**B**uffered **S**aline
TGN	***T****rans*-**G**olgi **N**etwork
t-SNARE	**t**arget membrane **SNARE**
VAMP3	**V**esicle-**A**ssociated **M**embrane **P**rotein **3**
VAMP7	**V**esicle-**A**ssociated **M**embrane **P**rotein **7**
v-SNARE	**v**esicle membrane **SNARE**
WB	**W**estern **B**lotting
WPRE	**W**oodchuck hepatitis virus (WHP) **P**osttranscriptional **R**egulatory **E**lement

Bibliography

Abremski K, Wierzbicki A, Frommer B & Hoess RH (1986) Bacteriophage P1 Cre-loxP site-specific recombination. Site-specific DNA topoisomerase activity of the Cre recombination protein. *J Biol Chem* **261**: 391-396.

Aguayo AJ, Attiwell M, Trecarten J, Perkins S & Bray GM (1977) Abnormal myelination in transplanted Trembler mouse Schwann cells. *Nature* **265**: 73-75.

Alvarez-Erviti L, Seow Y, Yin H, Betts C, Lakhal S & Wood MJ (2011) Delivery of siRNA to the mouse brain by systemic injection of targeted exosomes. *Nat Biotechnol* **29**: 341-345.

Arroyo EJ & Scherer SS (2000) On the molecular architecture of myelinated fibers. *Histochemistry and cell biology* **113**: 1-18.

Bacaj T, Pang ZP & Sudhof TC (2010) Testing the SNARE/SM protein model of membrane fusion. *Proc Natl Acad Sci U S A* **107**: 22365-22366.

Bai J, Ramos RL, Ackman JB, Thomas AM, Lee RV & LoTurco JJ (2003) RNAi reveals doublecortin is required for radial migration in rat neocortex. *Nat Neurosci* **6**: 1277-1283.

Baron W & Hoekstra D (2010) On the biogenesis of myelin membranes: sorting, trafficking and cell polarity. *FEBS Lett* **584**: 1760-1770.

Basu S & Kolesnick R (1998) Stress signals for apoptosis: ceramide and c-Jun kinase. *Oncogene* **17**: 3277-3285.

Baumann N & Pham-Dinh D (2001) Biology of oligodendrocyte and myelin in the mammalian central nervous system. *Physiol Rev* **81**: 871-927.

Beaulieu JM, Robertson J & Julien JP (1999) Interactions between peripherin and neurofilaments in cultured cells: disruption of peripherin assembly by the NF-M and NF-H subunits. *Biochemistry and cell biology = Biochimie et biologie cellulaire* **77**: 41-45.

Behl C, Davis JB, Lesley R & Schubert D (1994) Hydrogen peroxide mediates amyloid beta protein toxicity. *Cell* **77**: 817-827.

Blanc L, De Gassart A, Geminard C, Bette-Bobillo P & Vidal M (2005) Exosome release by reticulocytes--an integral part of the red blood cell differentiation system. *Blood Cells Mol Dis* **35**: 21-26.

Boison D & Stoffel W (1994) Disruption of the compacted myelin sheath of axons of the central nervous system in proteolipid protein-deficient mice. *Proceedings of the National Academy of Sciences of the United States of America* **91**: 11709-11713.

Brady ST (1993) Motor neurons and neurofilaments in sickness and in health. *Cell* **73**: 1-3.

Brady ST (2000) Neurofilaments run sprints not marathons. *Nat Cell Biol* **2**: E43-45.

Brady ST, Witt AS, Kirkpatrick LL, de Waegh SM, Readhead C, Tu PH & Lee VM (1999) Formation of compact myelin is required for maturation of the axonal cytoskeleton. *J Neurosci* **19**: 7278-7288.

Brown A (1998) Contiguous phosphorylated and non-phosphorylated domains along axonal neurofilaments. *J Cell Sci* **111 (Pt 4)**: 455-467.

Brownlees J, Yates A, Bajaj NP, *et al.* (2000) Phosphorylation of neurofilament heavy chain side-arms by stress activated protein kinase-1b/Jun N-terminal kinase-3. *J Cell Sci* **113 (Pt 3)**: 401-407.

Bruni JE (1998) Ependymal development, proliferation, and functions: a review. *Microsc Res Tech* **41**: 2-13.

Buser AM, Schmid D, Kern F, Erne B, Lazzati T & Schaeren-Wiemers N (2009) The myelin protein MAL affects peripheral nerve myelination: a new player influencing p75 neurotrophin receptor expression. *Eur J Neurosci* **29**: 2276-2290.

Carlezon WA, Jr., Duman RS & Nestler EJ (2005) The many faces of CREB. *Trends in neurosciences* **28**: 436-445.

Chairoungdua A, Smith DL, Pochard P, Hull M & Caplan MJ (2010) Exosome release of beta-catenin: a novel mechanism that antagonizes Wnt signaling. *J Cell Biol* **190**: 1079-1091.

Ching GY & Liem RK (1993) Assembly of type IV neuronal intermediate filaments in nonneuronal cells in the absence of preexisting cytoplasmic intermediate filaments. *The Journal of cell biology* **122**: 1323-1335.

Chou MM & Blenis J (1995) The 70 kDa S6 kinase: regulation of a kinase with multiple roles in mitogenic signalling. *Current opinion in cell biology* **7**: 806-814.

Coco S, Raposo G, Martinez S, *et al.* (1999) Subcellular localization of tetanus neurotoxin-insensitive vesicle-associated membrane protein (VAMP)/VAMP7 in neuronal cells: evidence for a novel membrane compartment. *The Journal of neuroscience : the official journal of the Society for Neuroscience* **19**: 9803-9812.

Cocucci E, Racchetti G & Meldolesi J (2009) Shedding microvesicles: artefacts no more. *Trends Cell Biol* **19**: 43-51.

Coman I, Barbin G, Charles P, Zalc B & Lubetzki C (2005) Axonal signals in central nervous system myelination, demyelination and remyelination. *J Neurol Sci* **233**: 67-71.

Dawson VL, Dawson TM, London ED, Bredt DS & Snyder SH (1991) Nitric oxide mediates glutamate neurotoxicity in primary cortical cultures. *Proceedings of the National Academy of Sciences of the United States of America* **88**: 6368-6371.

De Vos KJ, Grierson AJ, Ackerley S & Miller CC (2008) Role of Axonal Transport in Neurodegenerative Diseases *. *Annu Rev Neurosci* **31**: 151-173.

de Waegh S & Brady ST (1990) Altered slow axonal transport and regeneration in a myelin-deficient mutant mouse: the trembler as an in vivo model for Schwann cell-axon interactions. *J Neurosci* **10**: 1855-1865.

de Waegh SM & Brady ST (1991) Local control of axonal properties by Schwann cells: neurofilaments and axonal transport in homologous and heterologous nerve grafts. *Journal of neuroscience research* **30**: 201-212.

de Waegh SM, Lee VM & Brady ST (1992) Local modulation of neurofilament phosphorylation, axonal caliber, and slow axonal transport by myelinating Schwann cells. *Cell* **68**: 451-463.

Debruin LS & Harauz G (2007) White matter rafting--membrane microdomains in myelin. *Neurochem Res* **32**: 213-228.

Del Bigio MR (2010) Ependymal cells: biology and pathology. *Acta neuropathologica* **119**: 55-73.

Demerens C, Stankoff B, Logak M, *et al.* (1996) Induction of myelination in the central nervous system by electrical activity. *Proc Natl Acad Sci U S A* **93**: 9887-9892.

Dosemeci A, Makusky AJ, Jankowska-Stephens E, Yang X, Slotta DJ & Markey SP (2007) Composition of the synaptic PSD-95 complex. *Mol Cell Proteomics* **6**: 1749-1760.

Edgar JM & Nave KA (2009) The role of CNS glia in preserving axon function. *Curr Opin Neurobiol* **19**: 498-504.

Edgar JM, McLaughlin M, Werner HB, *et al.* (2009) Early ultrastructural defects of axons and axon-glia junctions in mice lacking expression of Cnp1. *Glia* **57**: 1815-1824.

Edgar JM, McLaughlin M, Yool D, *et al.* (2004) Oligodendroglial modulation of fast axonal transport in a mouse model of hereditary spastic paraplegia. *J Cell Biol* **166**: 121-131.

Fader CM, Sanchez DG, Mestre MB & Colombo MI (2009) TI-VAMP/VAMP7 and VAMP3/cellubrevin: two v-SNARE proteins involved in specific steps of the autophagy/multivesicular body pathways. *Biochim Biophys Acta* **1793**: 1901-1916.

Faure J, Lachenal G, Court M, *et al.* (2006) Exosomes are released by cultured cortical neurones. *Molecular and cellular neurosciences* **31**: 642-648.

Feil R, Wagner J, Metzger D & Chambon P (1997) Regulation of Cre recombinase activity by mutated estrogen receptor ligand-binding domains. *Biochem Biophys Res Commun* **237**: 752-757.

Feldmann A, Winterstein C, White R, Trotter J & Kramer-Albers EM (2009) Comprehensive analysis of expression, subcellular localization, and cognate pairing of SNARE proteins in oligodendrocytes. *J Neurosci Res* **87**: 1760-1772.

Feldmann A, Amphornrat J, Schonherr M, *et al.* (2011) Transport of the Major Myelin Proteolipid Protein Is Directed by VAMP3 and VAMP7. *J Neurosci* **31**: 5659-5672.

Fevrier B & Raposo G (2004) Exosomes: endosomal-derived vesicles shipping extracellular messages. *Curr Opin Cell Biol* **16**: 415-421.

Fields RD & Burnstock G (2006) Purinergic signalling in neuron-glia interactions. *Nat Rev Neurosci* **7**: 423-436.

Finkbeiner S, Tavazoie SF, Maloratsky A, Jacobs KM, Harris KM & Greenberg ME (1997) CREB: a major mediator of neuronal neurotrophin responses. *Neuron* **19**: 1031-1047.

Francis F, Koulakoff A, Boucher D, *et al.* (1999) Doublecortin is a developmentally regulated, microtubule-associated protein expressed in migrating and differentiating neurons. *Neuron* **23**: 247-256.

Friede RL (1972) Control of myelin formation by axon caliber (with a model of the control mechanism). *The Journal of comparative neurology* **144**: 233-252.

Friedrich G & Soriano P (1991) Promoter traps in embryonic stem cells: a genetic screen to identify and mutate developmental genes in mice. *Genes Dev* **5**: 1513-1523.

Frühbeis C, Fröhlich F, Amphornrat J, *et al.* (2011) Exosomes mediate oligodendrocyte-neuron communication. *submitted*.

Giasson BI & Mushynski WE (1996) Aberrant stress-induced phosphorylation of perikaryal neurofilaments. *The Journal of biological chemistry* **271**: 30404-30409.

Giasson BI & Mushynski WE (1997) Study of proline-directed protein kinases involved in phosphorylation of the heavy neurofilament subunit. *The Journal of neuroscience : the official journal of the Society for Neuroscience* **17**: 9466-9472.

Gleeson JG, Lin PT, Flanagan LA & Walsh CA (1999) Doublecortin is a microtubule-associated protein and is expressed widely by migrating neurons. *Neuron* **23**: 257-271.

Glick BS & Rothman JE (1987) Possible role for fatty acyl-coenzyme A in intracellular protein transport. *Nature* **326**: 309-312.

Gotow T, Tanaka T, Nakamura Y & Takeda M (1994) Dephosphorylation of the largest neurofilament subunit protein influences the structure of crossbridges in reassembled neurofilaments. *J Cell Sci* **107 (Pt 7)**: 1949-1957.

Gow A, Southwood CM & Lazzarini RA (1998) Disrupted proteolipid protein trafficking results in oligodendrocyte apoptosis in an animal model of Pelizaeus-Merzbacher disease. *The Journal of cell biology* **140**: 925-934.

Graeber MB (2010) Changing face of microglia. *Science* **330**: 783-788.

Grant P & Pant HC (2000) Neurofilament protein synthesis and phosphorylation. *J Neurocytol* **29**: 843-872.

Griffiths I, Klugmann M, Anderson T, Thomson C, Vouyiouklis D & Nave KA (1998) Current concepts of PLP and its role in the nervous system. *Microsc Res Tech* **41**: 344-358.

Griffiths I, Klugmann M, Anderson T, *et al.* (1998) Axonal swellings and degeneration in mice lacking the major proteolipid of myelin. *Science* **280**: 1610-1613.

Griffiths IR, Scott I, McCulloch MC, Barrie JA, McPhilemy K & Cattanach BM (1990) Rumpshaker mouse: a new X-linked mutation affecting myelination: evidence for a defect in PLP expression. *Journal of neurocytology* **19**: 273-283.

Hartline DK & Colman DR (2007) Rapid conduction and the evolution of giant axons and myelinated fibers. *Curr Biol* **17**: R29-35.

Hirokawa N, Hisanaga S & Shiomura Y (1988) MAP2 is a component of crossbridges between microtubules and neurofilaments in the neuronal cytoskeleton: quick-freeze, deep-etch immunoelectron microscopy and reconstitution studies. *The Journal of neuroscience : the official journal of the Society for Neuroscience* **8**: 2769-2779.

Hisanaga S & Hirokawa N (1990) Dephosphorylation-induced interactions of neurofilaments with microtubules. *J Biol Chem* **265**: 21852-21858.

Hoogenraad CC, Popa I, Futai K, *et al.* (2010) Neuron specific Rab4 effector GRASP-1 coordinates membrane specialization and maturation of recycling endosomes. *PLoS Biol* **8**: e1000283.

Hsieh ST, Kidd GJ, Crawford TO, *et al.* (1994) Regional modulation of neurofilament organization by myelination in normal axons. *The Journal of neuroscience : the official journal of the Society for Neuroscience* **14**: 6392-6401.

Hsu C, Morohashi Y, Yoshimura S, *et al.* (2010) Regulation of exosome secretion by Rab35 and its GTPase-activating proteins TBC1D10A-C. *J Cell Biol* **189**: 223-232.

Hua Y & Scheller RH (2001) Three SNARE complexes cooperate to mediate membrane fusion. *Proc Natl Acad Sci U S A* **98**: 8065-8070.

Huang P, Chandra V & Rastinejad F (2010) Structural overview of the nuclear receptor superfamily: insights into physiology and therapeutics. *Annu Rev Physiol* **72**: 247-272.

Hunter MP, Ismail N, Zhang X, *et al.* (2008) Detection of microRNA expression in human peripheral blood microvesicles. *PLoS ONE* **3**: e3694.

Hurley JH (2008) ESCRT complexes and the biogenesis of multivesicular bodies. *Curr Opin Cell Biol* **20**: 4-11.

Idone V, Tam C & Andrews NW (2008) Two-way traffic on the road to plasma membrane repair. *Trends Cell Biol* **18**: 552-559.

Inoue K (2005) PLP1-related inherited dysmyelinating disorders: Pelizaeus-Merzbacher disease and spastic paraplegia type 2. *Neurogenetics* **6**: 1-16.

Jahn O, Tenzer S & Werner HB (2009) Myelin proteomics: molecular anatomy of an insulating sheath. *Mol Neurobiol* **40**: 55-72.

Jahn R & Scheller RH (2006) SNAREs--engines for membrane fusion. *Nat Rev Mol Cell Biol* **7**: 631-643.

Jahn R, Lang T & Sudhof TC (2003) Membrane fusion. *Cell* **112**: 519-533.

Jefferies HB, Fumagalli S, Dennis PB, Reinhard C, Pearson RB & Thomas G (1997) Rapamycin suppresses 5'TOP mRNA translation through inhibition of p70s6k. *The EMBO journal* **16**: 3693-3704.

Johnstone RM, Adam M, Hammond JR, Orr L & Turbide C (1987) Vesicle formation during reticulocyte maturation. Association of plasma membrane activities with released vesicles (exosomes). *J Biol Chem* **262**: 9412-9420.

Jung C, Chylinski TM, Pimenta A, Ortiz D & Shea TB (2004) Neurofilament transport is dependent on actin and myosin. *J Neurosci* **24**: 9486-9496.

Jung M, Sommer I, Schachner M & Nave KA (1996) Monoclonal antibody O10 defines a conformationally sensitive cell-surface epitope of proteolipid protein (PLP): evidence that PLP misfolding underlies dysmyelination in mutant mice. *J Neurosci* **16**: 7920-7929.

Jung M, Kramer E, Grzenkowski M, *et al.* (1995) Lines of murine oligodendroglial precursor cells immortalized by an activated neu tyrosine kinase show distinct degrees of interaction with axons in vitro and in vivo. *The European journal of neuroscience* **7**: 1245-1265.

Karim SA, Barrie JA, McCulloch MC, *et al.* (2007) PLP overexpression perturbs myelin protein composition and myelination in a mouse model of Pelizaeus-Merzbacher disease. *Glia* **55**: 341-351.

Kim KK, Adelstein RS & Kawamoto S (2009) Identification of neuronal nuclei (NeuN) as Fox-3, a new member of the Fox-1 gene family of splicing factors. *J Biol Chem* **284**: 31052-31061.

Kimelberg HK (2010) Functions of mature mammalian astrocytes: a current view. *Neuroscientist* **16**: 79-106.

Kirkpatrick LL, Witt AS, Payne HR, Shine HD & Brady ST (2001) Changes in microtubule stability and density in myelin-deficient shiverer mouse CNS axons. *J Neurosci* **21**: 2288-2297.

Klugmann M, Schwab MH, Puhlhofer A, Schneider A, Zimmermann F, Griffiths IR & Nave KA (1997) Assembly of CNS myelin in the absence of proteolipid protein. *Neuron* **18**: 59-70.

Kokubo H, Helms JB, Ohno-Iwashita Y, Shimada Y, Horikoshi Y & Yamaguchi H (2003) Ultrastructural localization of flotillin-1 to cholesterol-rich membrane microdomains, rafts, in rat brain tissue. *Brain Res* **965**: 83-90.

Kramer-Albers EM, Gehrig-Burger K, Thiele C, Trotter J & Nave KA (2006) Perturbed interactions of mutant proteolipid protein/DM20 with cholesterol and lipid rafts in oligodendroglia: implications for dysmyelination in spastic paraplegia. *J Neurosci* **26**: 11743-11752.

Kramer-Albers EM, Bretz N, Tenzer S, *et al.* (2007) Oligodendrocytes secrete exosomes containing major myelin and stress-protective proteins: Trophic support for axons? *Proteomics. Clinical applications* **1**: 1446-1461.

Kramer EM, Schardt A & Nave KA (2001) Membrane traffic in myelinating oligodendrocytes. *Microsc Res Tech* **52**: 656-671.

Kramer EM, Koch T, Niehaus A & Trotter J (1997) Oligodendrocytes direct glycosyl phosphatidylinositol-anchored proteins to the myelin sheath in glycosphingolipid-rich complexes. *J Biol Chem* **272**: 8937-8945.

Kreutz MR, Bien A, Vorwerk CK, Bockers TM, Seidenbecher CI, Tischmeyer W & Sabel BA (1999) Co-expression of c-Jun and ATF-2 characterizes the surviving retinal ganglion cells which maintain axonal connections after partial optic nerve injury. *Brain research. Molecular brain research* **69**: 232-241.

Kuo WP (2011) Charakterisierung des R-SNAREs VAMP2 und seine funktionelle Rolle im PLP-Transport. *Diploma thesis.*

Lachenal G, Pernet-Gallay K, Chivet M, *et al.* (2011) Release of exosomes from differentiated neurons and its regulation by synaptic glutamatergic activity. *Molecular and cellular neurosciences* **46**: 409-418.

Lakkaraju A & Rodriguez-Boulan E (2008) Itinerant exosomes: emerging roles in cell and tissue polarity. *Trends Cell Biol* **18**: 199-209.

Lappe-Siefke C, Goebbels S, Gravel M, *et al.* (2003) Disruption of Cnp1 uncouples oligodendroglial functions in axonal support and myelination. *Nat Genet* **33**: 366-374.

Le Y, Gagneten S, Tombaccini D, Bethke B & Sauer B (1999) Nuclear targeting determinants of the phage P1 cre DNA recombinase. *Nucleic Acids Res* **27**: 4703-4709.

Leblanc P, Alais S, Porto-Carreiro I, Lehmann S, Grassi J, Raposo G & Darlix JL (2006) Retrovirus infection strongly enhances scrapie infectivity release in cell culture. *Embo J* **25**: 2674-2685.

Lee A & Pow DV (2010) Astrocytes: Glutamate transport and alternate splicing of transporters. *Int J Biochem Cell Biol* **42**: 1901-1906.

Lee MT, Mishra A & Lambright DG (2009) Structural mechanisms for regulation of membrane traffic by rab GTPases. *Traffic* **10**: 1377-1389.

Liu Q, Xie F, Siedlak SL, *et al.* (2004) Neurofilament proteins in neurodegenerative diseases. *Cell Mol Life Sci* **61**: 3057-3075.

Livingstone C, Patel G & Jones N (1995) ATF-2 contains a phosphorylation-dependent transcriptional activation domain. *The EMBO journal* **14**: 1785-1797.

Luche H, Weber O, Nageswara Rao T, Blum C & Fehling HJ (2007) Faithful activation of an extra-bright red fluorescent protein in "knock-in" Cre-reporter mice ideally suited for lineage tracing studies. *Eur J Immunol* **37**: 43-53.

Maier O, Hoekstra D & Baron W (2008) Polarity development in oligodendrocytes: sorting and trafficking of myelin components. *J Mol Neurosci* **35**: 35-53.

Maire JC, Medilanski J & Straub RW (1982) Uptake of adenosine and release of adenine derivatives in mammalian non-myelinated nerve fibres at rest and during activity. *The Journal of physiology* **323**: 589-602.

Maragakis NJ & Rothstein JD (2006) Mechanisms of Disease: astrocytes in neurodegenerative disease. *Nat Clin Pract Neurol* **2**: 679-689.

Marangos PJ & Schmechel DE (1987) Neuron specific enolase, a clinically useful marker for neurons and neuroendocrine cells. *Annu Rev Neurosci* **10**: 269-295.

Martin S, Tellam J, Livingstone C, Slot JW, Gould GW & James DE (1996) The glucose transporter (GLUT-4) and vesicle-associated membrane protein-2 (VAMP-2) are segregated from recycling endosomes in insulin-sensitive cells. *The Journal of cell biology* **134**: 625-635.

Martini R (1994) Expression and functional roles of neural cell surface molecules and extracellular matrix components during development and regeneration of peripheral nerves. *J Neurocytol* **23**: 1-28.

Mata M, Kupina N & Fink DJ (1992) Phosphorylation-dependent neurofilament epitopes are reduced at the node of Ranvier. *Journal of neurocytology* **21**: 199-210.

May AP, Whiteheart SW & Weis WI (2001) Unraveling the mechanism of the vesicle transport ATPase NSF, the N-ethylmaleimide-sensitive factor. *The Journal of biological chemistry* **276**: 21991-21994.

McLaughlin M, Hunter DJ, Thomson CE, Yool D, Kirkham D, Freer AA & Griffiths IR (2002) Evidence for possible interactions between PLP and DM20 within the myelin sheath. *Glia* **39**: 31-36.

Metzger D & Chambon P (2001) Site- and time-specific gene targeting in the mouse. *Methods* **24**: 71-80.

Miller CC, Ackerley S, Brownlees J, Grierson AJ, Jacobsen NJ & Thornhill P (2002) Axonal transport of neurofilaments in normal and disease states. *Cell Mol Life Sci* **59**: 323-330.

Mitchell LS, Gillespie SC, McAllister F, *et al.* (1992) Developmental expression of major myelin protein genes in the CNS of X-linked hypomyelinating mutant rumpshaker. *Journal of neuroscience research* **33**: 205-217.

Mittelbrunn M, Gutierrez-Vazquez C, Villarroya-Beltri C, *et al.* (2011) Unidirectional transfer of microRNA-loaded exosomes from T cells to antigen-presenting cells. *Nature communications* **2**: 282.

Mohrmann R, de Wit H, Verhage M, Neher E & Sorensen JB (2010) Fast vesicle fusion in living cells requires at least three SNARE complexes. *Science* **330**: 502-505.

Mollinedo F, Martin-Martin B, Calafat J, Nabokina SM & Lazo PA (2003) Role of vesicle-associated membrane protein-2, through Q-soluble N-ethylmaleimide-sensitive factor attachment protein receptor/R-soluble N-ethylmaleimide-sensitive factor attachment protein receptor interaction, in the exocytosis of specific and tertiary granules of human neutrophils. *Journal of immunology* **170**: 1034-1042.

Mullen RJ, Buck CR & Smith AM (1992) NeuN, a neuronal specific nuclear protein in vertebrates. *Development* **116**: 201-211.

Nave KA (2010) Myelination and support of axonal integrity by glia. *Nature* **468**: 244-252.

Nave KA & Salzer JL (2006) Axonal regulation of myelination by neuregulin 1. *Current opinion in neurobiology* **16**: 492-500.

Nave KA & Trapp BD (2008) Axon-glial signaling and the glial support of axon function. *Annu Rev Neurosci* **31**: 535-561.

Nave KA, Lai C, Bloom FE & Milner RJ (1987) Splice site selection in the proteolipid protein (PLP) gene transcript and primary structure of the DM-20 protein of central nervous system myelin. *Proc Natl Acad Sci U S A* **84**: 5665-5669.

Nern C, Wolff I, Macas J, von Randow J, Scharenberg C, Priller J & Momma S (2009) Fusion of hematopoietic cells with Purkinje neurons does not lead to stable heterokaryon formation under noninvasive conditions. *J Neurosci* **29**: 3799-3807.

Nixon RA, Paskevich PA, Sihag RK & Thayer CY (1994) Phosphorylation on carboxyl terminus domains of neurofilament proteins in retinal ganglion cell neurons in vivo: influences on regional neurofilament accumulation, interneurofilament spacing, and axon caliber. *J Cell Biol* **126**: 1031-1046.

Ohya T, Miaczynska M, Coskun U, *et al.* (2009) Reconstitution of Rab- and SNARE-dependent membrane fusion by synthetic endosomes. *Nature* **459**: 1091-1097.

Oliva AA, Jr., Atkins CM, Copenagle L & Banker GA (2006) Activated c-Jun N-terminal kinase is required for axon formation. *The Journal of neuroscience : the official journal of the Society for Neuroscience* **26**: 9462-9470.

Ostrowski M, Carmo NB, Krumeich S, *et al.* (2009) Rab27a and Rab27b control different steps of the exosome secretion pathway. *Nat Cell Biol* **12**: 19-30; sup pp 11-13.

Pedraza L, Huang JK & Colman DR (2001) Organizing principles of the axoglial apparatus. *Neuron* **30**: 335-344.

Pegtel DM, Cosmopoulos K, Thorley-Lawson DA, *et al.* (2010) Functional delivery of viral miRNAs via exosomes. *Proc Natl Acad Sci U S A* **107**: 6328-6333.

Pelham HR (2001) SNAREs and the specificity of membrane fusion. *Trends Cell Biol* **11**: 99-101.

Perrot R, Berges R, Bocquet A & Eyer J (2008) Review of the multiple aspects of neurofilament functions, and their possible contribution to neurodegeneration. *Mol Neurobiol* **38**: 27-65.

Pfeffer S & Aivazian D (2004) Targeting Rab GTPases to distinct membrane compartments. *Nat Rev Mol Cell Biol* **5**: 886-896.

Poliak S & Peles E (2003) The local differentiation of myelinated axons at nodes of Ranvier. *Nat Rev Neurosci* **4**: 968-980.

Popko B, Puckett C, Lai E, *et al.* (1987) Myelin deficient mice: expression of myelin basic protein and generation of mice with varying levels of myelin. *Cell* **48**: 713-721.

Proux-Gillardeaux V, Raposo G, Irinopoulou T & Galli T (2007) Expression of the Longin domain of TI-VAMP impairs lysosomal secretion and epithelial cell migration. *Biol Cell* **99**: 261-271.

Ransohoff RM & Perry VH (2009) Microglial physiology: unique stimuli, specialized responses. *Annu Rev Immunol* **27**: 119-145.

Rao MV, Garcia ML, Miyazaki Y, *et al.* (2002) Gene replacement in mice reveals that the heavily phosphorylated tail of neurofilament heavy subunit does not affect axonal caliber or the transit of cargoes in slow axonal transport. *J Cell Biol* **158**: 681-693.

Rao SK, Huynh C, Proux-Gillardeaux V, Galli T & Andrews NW (2004) Identification of SNAREs involved in synaptotagmin VII-regulated lysosomal exocytosis. *J Biol Chem* **279**: 20471-20479.

Readhead C & Hood L (1990) The dysmyelinating mouse mutations shiverer (shi) and myelin deficient (shimld). *Behavior genetics* **20**: 213-234.

Readhead C, Takasashi N, Shine HD, Saavedra R, Sidman R & Hood L (1990) Role of myelin basic protein in the formation of central nervous system myelin. *Annals of the New York Academy of Sciences* **605**: 280-285.

Readhead C, Popko B, Takahashi N, Shine HD, Saavedra RA, Sidman RL & Hood L (1987) Expression of a myelin basic protein gene in transgenic shiverer mice: correction of the dysmyelinating phenotype. *Cell* **48**: 703-712.

Regan RF & Choi DW (1991) Glutamate neurotoxicity in spinal cord cell culture. *Neuroscience* **43**: 585-591.

Rios JC, Melendez-Vasquez CV, Einheber S, *et al.* (2000) Contactin-associated protein (Caspr) and contactin form a complex that is targeted to the paranodal junctions during myelination. *J Neurosci* **20**: 8354-8364.

Robinson GA (1996) Changes in the expression of transcription factors ATF-2 and Fra-2 after axotomy and during regeneration in rat retinal ganglion cells. *Brain research. Molecular brain research* **41**: 57-64.

Roger B, Al-Bassam J, Dehmelt L, Milligan RA & Halpain S (2004) MAP2c, but not tau, binds and bundles F-actin via its microtubule binding domain. *Current biology : CB* **14**: 363-371.

Roitbak T, Surviladze Z, Tikkanen R & Wandinger-Ness A (2005) A polycystin multiprotein complex constitutes a cholesterol-containing signalling microdomain in human kidney epithelia. *Biochem J* **392**: 29-38.

Rosenbluth J, Nave KA, Mierzwa A & Schiff R (2006) Subtle myelin defects in PLP-null mice. *Glia* **54**: 172-182.

Rothman JE (1994) Mechanisms of intracellular protein transport. *Nature* **372**: 55-63.

Roy S, Coffee P, Smith G, Liem RK, Brady ST & Black MM (2000) Neurofilaments are transported rapidly but intermittently in axons: implications for slow axonal transport. *J Neurosci* **20**: 6849-6861.

Salzer JL (2003) Polarized domains of myelinated axons. *Neuron* **40**: 297-318.

Sander LE, Frank SP, Bolat S, *et al.* (2008) Vesicle associated membrane protein (VAMP)-7 and VAMP-8, but not VAMP-2 or VAMP-3, are required for activation-induced degranulation of mature human mast cells. *Eur J Immunol* **38**: 855-863.

Sato M, Yoshimura S, Hirai R, *et al.* (2011) The role of VAMP7/TI-VAMP in cell polarity and lysosomal exocytosis in vivo. *Traffic.*

Savina A, Fader CM, Damiani MT & Colombo MI (2005) Rab11 promotes docking and fusion of multivesicular bodies in a calcium-dependent manner. *Traffic* **6**: 131-143.

Schaeren-Wiemers N, Bonnet A, Erb M, *et al.* (2004) The raft-associated protein MAL is required for maintenance of proper axon--glia interactions in the central nervous system. *J Cell Biol* **166**: 731-742.

Schiavo G, Benfenati F, Poulain B, Rossetto O, Polverino de Laureto P, DasGupta BR & Montecucco C (1992) Tetanus and botulinum-B neurotoxins block neurotransmitter release by proteolytic cleavage of synaptobrevin. *Nature* **359**: 832-835.

Schmitz G, Leuthauser-Jaschinski K & Orso E (2009) Are circulating monocytes as microglia orthologues appropriate biomarker targets for neuronal diseases? *Cent Nerv Syst Agents Med Chem* **9**: 307-330.

Schmunk S (2009) The functional roles of the SNARE proteins VAMP3 and VAMP4 in myelination. *Diploma thesis*.

Schneider A, Montague P, Griffiths I, Fanarraga M, Kennedy P, Brophy P & Nave KA (1992) Uncoupling of hypomyelination and glial cell death by a mutation in the proteolipid protein gene. *Nature* **358**: 758-761.

Schneider AM, Griffiths IR, Readhead C & Nave KA (1995) Dominant-negative action of the jimpy mutation in mice complemented with an autosomal transgene for myelin proteolipid protein. *Proceedings of the National Academy of Sciences of the United States of America* **92**: 4447-4451.

Schorey JS & Bhatnagar S (2008) Exosome function: from tumor immunology to pathogen biology. *Traffic* **9**: 871-881.

Segura E, Amigorena S & Thery C (2005) Mature dendritic cells secrete exosomes with strong ability to induce antigen-specific effector immune responses. *Blood cells, molecules & diseases* **35**: 89-93.

Shah JV, Flanagan LA, Janmey PA & Leterrier JF (2000) Bidirectional translocation of neurofilaments along microtubules mediated in part by dynein/dynactin. *Mol Biol Cell* **11**: 3495-3508.

Shea TB & Chan WK (2008) Regulation of neurofilament dynamics by phosphorylation. *The European journal of neuroscience* **27**: 1893-1901.

Shen J, Tareste DC, Paumet F, Rothman JE & Melia TJ (2007) Selective activation of cognate SNAREpins by Sec1/Munc18 proteins. *Cell* **128**: 183-195.

Sherman DL & Brophy PJ (2005) Mechanisms of axon ensheathment and myelin growth. *Nat Rev Neurosci* **6**: 683-690.

Shine HD, Readhead C, Popko B, Hood L & Sidman RL (1992) Morphometric analysis of normal, mutant, and transgenic CNS: correlation of myelin basic protein expression to myelinogenesis. *Journal of neurochemistry* **58**: 342-349.

Simons M & Trotter J (2007) Wrapping it up: the cell biology of myelination. *Curr Opin Neurobiol* **17**: 533-540.

Simpson RJ, Jensen SS & Lim JW (2008) Proteomic profiling of exosomes: current perspectives. *Proteomics* **8**: 4083-4099.

Simpson RJ, Lim JW, Moritz RL & Mathivanan S (2009) Exosomes: proteomic insights and diagnostic potential. *Expert Rev Proteomics* **6**: 267-283.

Skog J, Wurdinger T, van Rijn S, *et al.* (2008) Glioblastoma microvesicles transport RNA and proteins that promote tumour growth and provide diagnostic biomarkers. *Nat Cell Biol* **10**: 1470-1476.

Sollner T, Bennett MK, Whiteheart SW, Scheller RH & Rothman JE (1993) A protein assembly-disassembly pathway in vitro that may correspond to sequential steps of synaptic vesicle docking, activation, and fusion. *Cell* **75**: 409-418.

Stecca B, Southwood CM, Gragerov A, Kelley KA, Friedrich VL, Jr. & Gow A (2000) The evolution of lipophilin genes from invertebrates to tetrapods: DM-20 cannot replace proteolipid protein in CNS myelin. *J Neurosci* **20**: 4002-4010.

Steegmaier M, Klumperman J, Foletti DL, Yoo JS & Scheller RH (1999) Vesicle-associated membrane protein 4 is implicated in trans-Golgi network vesicle trafficking. *Molecular biology of the cell* **10**: 1957-1972.

Stenmark H & Olkkonen VM (2001) The Rab GTPase family. *Genome Biol* **2**: REVIEWS3007.

Stevens B & Fields RD (2000) Response of Schwann cells to action potentials in development. *Science* **287**: 2267-2271.

Stevens B, Porta S, Haak LL, Gallo V & Fields RD (2002) Adenosine: a neuron-glial transmitter promoting myelination in the CNS in response to action potentials. *Neuron* **36**: 855-868.

Stevens MJ & Hoh JH (2011) Interactions between Planar Grafted Neurofilament Side-Arms. *J Phys Chem B*.

Stinchcombe J, Bossi G & Griffiths GM (2004) Linking albinism and immunity: the secrets of secretory lysosomes. *Science* **305**: 55-59.

Stoorvogel W, Kleijmeer MJ, Geuze HJ & Raposo G (2002) The biogenesis and functions of exosomes. *Traffic* **3**: 321-330.

Strauss K, Goebel C, Runz H, *et al.* (2010) Exosome secretion ameliorates lysosomal storage of cholesterol in Niemann-Pick type C disease. *J Biol Chem* **285**: 26279-26288.

Sudhof TC & Rothman JE (2009) Membrane fusion: grappling with SNARE and SM proteins. *Science* **323**: 474-477.

Susuki K & Rasband MN (2008) Molecular mechanisms of node of Ranvier formation. *Curr Opin Cell Biol*.

Suter U, Welcher AA, Ozcelik T, *et al.* (1992) Trembler mouse carries a point mutation in a myelin gene. *Nature* **356**: 241-244.

Suzuki M, Nelson AD, Eickstaedt JB, Wallace K, Wright LS & Svendsen CN (2006) Glutamate enhances proliferation and neurogenesis in human neural progenitor cell cultures derived from the fetal cortex. *Eur J Neurosci* **24**: 645-653.

Taveggia C, Zanazzi G, Petrylak A, *et al.* (2005) Neuregulin-1 type III determines the ensheathment fate of axons. *Neuron* **47**: 681-694.

Thery C, Ostrowski M & Segura E (2009) Membrane vesicles as conveyors of immune responses. *Nat Rev Immunol* **9**: 581-593.

Thery C, Amigorena S, Raposo G & Clayton A (2006) Isolation and characterization of exosomes from cell culture supernatants and biological fluids. *Curr Protoc Cell Biol* **Chapter 3**: Unit 3 22.

Timsit SG, Bally-Cuif L, Colman DR & Zalc B (1992) DM-20 mRNA is expressed during the embryonic development of the nervous system of the mouse. *J Neurochem* **58**: 1172-1175.

Trajkovic K, Dhaunchak AS, Goncalves JT, *et al.* (2006) Neuron to glia signaling triggers myelin membrane exocytosis from endosomal storage sites. *J Cell Biol* **172**: 937-948.

Trajkovic K, Hsu C, Chiantia S, *et al.* (2008) Ceramide triggers budding of exosome vesicles into multivesicular endosomes. *Science* **319**: 1244-1247.

Tran TH, Zeng Q & Hong W (2007) VAMP4 cycles from the cell surface to the trans-Golgi network via sorting and recycling endosomes. *Journal of cell science* **120**: 1028-1041.

Trapp BD, Quarles RH & Suzuki K (1984) Immunocytochemical studies of quaking mice support a role for the myelin-associated glycoprotein in forming and maintaining the periaxonal space and periaxonal cytoplasmic collar of myelinating Schwann cells. *The Journal of cell biology* **99**: 594-606.

Trioulier Y, Torch S, Blot B, Cristina N, Chatellard-Causse C, Verna JM & Sadoul R (2004) Alix, a protein regulating endosomal trafficking, is involved in neuronal death. *J Biol Chem* **279**: 2046-2052.

Tuason MC, Rastikerdar A, Kuhlmann T, *et al.* (2008) Separate proteolipid protein/DM20 enhancers serve different lineages and stages of development. *J Neurosci* **28**: 6895-6903.

Valadi H, Ekstrom K, Bossios A, Sjostrand M, Lee JJ & Lotvall JO (2007) Exosome-mediated transfer of mRNAs and microRNAs is a novel mechanism of genetic exchange between cells. *Nat Cell Biol* **9**: 654-659.

van den Bogaart G, Holt MG, Bunt G, Riedel D, Wouters FS & Jahn R (2010) One SNARE complex is sufficient for membrane fusion. *Nature structural & molecular biology* **17**: 358-364.

van Niel G, Porto-Carreiro I, Simoes S & Raposo G (2006) Exosomes: a common pathway for a specialized function. *J Biochem* **140**: 13-21.

Wagner OI, Lifshitz J, Janmey PA, Linden M, McIntosh TK & Leterrier JF (2003) Mechanisms of mitochondria-neurofilament interactions. *J Neurosci* **23**: 9046-9058.

Wang E, Dimova N & Cambi F (2007) PLP/DM20 ratio is regulated by hnRNPH and F and a novel G-rich enhancer in oligodendrocytes. *Nucleic Acids Res* **35**: 4164-4178.

Wang L & Brown A (2001) Rapid intermittent movement of axonal neurofilaments observed by fluorescence photobleaching. *Mol Biol Cell* **12**: 3257-3267.

Wang L, Ho CL, Sun D, Liem RK & Brown A (2000) Rapid movement of axonal neurofilaments interrupted by prolonged pauses. *Nat Cell Biol* **2**: 137-141.

Watkins TA, Emery B, Mulinyawe S & Barres BA (2008) Distinct stages of myelination regulated by gamma-secretase and astrocytes in a rapidly myelinating CNS coculture system. *Neuron* **60**: 555-569.

Weimbs T & Stoffel W (1992) Proteolipid protein (PLP) of CNS myelin: positions of free, disulfide-bonded, and fatty acid thioester-linked cysteine residues and implications for the membrane topology of PLP. *Biochemistry* **31**: 12289-12296.

White R, Gonsior C, Kramer-Albers EM, Stohr N, Huttelmaier S & Trotter J (2008) Activation of oligodendroglial Fyn kinase enhances translation of mRNAs transported in hnRNP A2-dependent RNA granules. *J Cell Biol* **181**: 579-586.

Winterstein C, Trotter J & Kramer-Albers EM (2008) Distinct endocytic recycling of myelin proteins promotes oligodendroglial membrane remodeling. *J Cell Sci* **121**: 834-842.

Witt A & Brady ST (2000) Unwrapping new layers of complexity in axon/glial relationships. *Glia* **29**: 112-117.

Yabe JT, Jung C, Chan WK & Shea TB (2000) Phospho-dependent association of neurofilament proteins with kinesin in situ. *Cell Motil Cytoskeleton* **45**: 249-262.

Yates DM, Manser C, De Vos KJ, Shaw CE, McLoughlin DM & Miller CC (2009) Neurofilament subunit (NFL) head domain phosphorylation regulates axonal transport of neurofilaments. *Eur J Cell Biol* **88**: 193-202.

Yin X, Crawford TO, Griffin JW, *et al.* (1998) Myelin-associated glycoprotein is a myelin signal that modulates the caliber of myelinated axons. *The Journal of neuroscience : the official journal of the Society for Neuroscience* **18**: 1953-1962.

Yin X, Baek RC, Kirschner DA, *et al.* (2006) Evolution of a neuroprotective function of central nervous system myelin. *J Cell Biol* **172**: 469-478.

Yool D, Klugmann M, Barrie JA, McCulloch MC, Nave KA & Griffiths IR (2002) Observations on the structure of myelin lacking the major proteolipid protein. *Neuropathology and applied neurobiology* **28**: 75-78.

Yu IM & Hughson FM (2010) Tethering factors as organizers of intracellular vesicular traffic. *Annu Rev Cell Dev Biol* **26**: 137-156.

Yuan A, Nixon RA & Rao MV (2006) Deleting the phosphorylated tail domain of the neurofilament heavy subunit does not alter neurofilament transport rate in vivo. *Neurosci Lett* **393**: 264-268.

Zambrowicz BP, Imamoto A, Fiering S, Herzenberg LA, Kerr WG & Soriano P (1997) Disruption of overlapping transcripts in the ROSA beta geo 26 gene trap strain leads to widespread expression of beta-galactosidase in mouse embryos and hematopoietic cells. *Proc Natl Acad Sci U S A* **94**: 3789-3794.

Zerial M & McBride H (2001) Rab proteins as membrane organizers. *Nat Rev Mol Cell Biol* **2**: 107-117.

Zhao J, Nassar MA, Gavazzi I & Wood JN (2006) Tamoxifen-inducible NaV1.8-CreERT2 recombinase activity in nociceptive neurons of dorsal root ganglia. *Genesis* **44**: 364-371.

Zhao P, Yang L, Lopez JA, *et al.* (2009) Variations in the requirement for v-SNAREs in GLUT4 trafficking in adipocytes. *Journal of cell science* **122**: 3472-3480.

Zheng YL, Li BS, Veeranna & Pant HC (2003) Phosphorylation of the head domain of neurofilament protein (NF-M): a factor regulating topographic phosphorylation of NF-M tail domain KSP sites in neurons. *J Biol Chem* **278**: 24026-24032.